INFORMATION TO USERS

This manuscript has been reproduced from the microfilm master. UMI films the text directly from the original or copy submitted. Thus, some thesis and dissertation copies are in typewriter face, while others may be from any type of computer printer.

The quality of this reproduction is dependent upon the quality of the copy submitted. Broken or indistinct print, colored or poor quality illustrations and photographs, print bleedthrough, substandard margins, and improper alignment can adversely affect reproduction.

In the unlikely event that the author did not send UMI a complete manuscript and there are missing pages, these will be noted. Also, if unauthorized copyright material had to be removed, a note will indicate the deletion.

Oversize materials (e.g., maps, drawings, charts) are reproduced by sectioning the original, beginning at the upper left-hand corner and continuing from left to right in equal sections with small overlaps.

Photographs included in the original manuscript have been reproduced xerographically in this copy. Higher quality 6" x 9" black and white photographic prints are available for any photographs or illustrations appearing in this copy for an additional charge. Contact UMI directly to order.

Bell & Howell Information and Learning
300 North Zeeb Road, Ann Arbor, MI 48106-1346 USA

UMI®
800-521-0600

Reproduced with permission of the copyright owner. Further reproduction prohibited without permission.

NOTE TO USERS

This reproduction is the best copy available.

UMI

Reproduced with permission of the copyright owner. Further reproduction prohibited without permission.

DISSERTATION

MULTRAN: A FINITE DIFFERENCE, MULTI-SPECIES, THREE-DIMENSIONAL CONTAMINANT TRANSPORT MODEL

Submitted by

Brian Anthony Waldron

Civil Engineering Department

In partial fulfillment of the requirements

For the Degree of Doctor of Philosophy

Colorado State University

Fort Collins, Colorado

Fall 1999

Reproduced with permission of the copyright owner. Further reproduction prohibited without permission.

UMI Number: 9950920

UMI®

UMI Microform 9950920
Copyright 2000 by Bell & Howell Information and Learning Company.
All rights reserved. This microform edition is protected against
unauthorized copying under Title 17, United States Code.

Bell & Howell Information and Learning Company
300 North Zeeb Road
P.O. Box 1346
Ann Arbor, MI 48106-1346

Reproduced with permission of the copyright owner. Further reproduction prohibited without permission.

COLORADO STATE UNIVERSITY

July 30, 1999

WE HEREBY RECOMMEND THAT THE DISSERTATION PREPARED UNDER OUR SUPERVISION BY BRIAN ANTHONY WALDRON ENTITLED, MULTRAN: A FINITE DIFFERENCE, MULTI-SPECIES, THREE-DIMENSIONAL CONTAMINANT TRANSPORT MODEL, BE ACCEPTED AS FULFILLING IN PART THE REQUIREMENTS FOR THE DEGREE OF DOCTOR OF PHILOSOPHY.

Committee on Graduate Work

Advisor

Co-Advisor

Department Head

Reproduced with permission of the copyright owner. Further reproduction prohibited without permission.

ABSTRACT OF DISSERTATION

MULTRAN: A FINITE DIFFERENCE, MULTI-SPECIES, THREE-DIMENSIONAL CONTAMINANT TRANSPORT MODEL

Ground water contamination occurs since nothing is perfectly sealed or always environmentally safe. To return ground water systems to their previous state before contamination, remediation is necessary. Tools to aid agencies and environmental contractors to determine contaminant migration and its fate are available in many different forms such as analytical solutions, numerical models, and laboratory experiments.

As there are a number of tools to study ground water contamination, so there are a number of numerical models for analyzing contaminant migration and its fate. Popular contaminant transport models, such as MT3D, are used widely for single species transport. However, ground water chemistry and/or multiple species can sometimes affect the transport of contaminants. Though models exist that can handle multi-species transport, an easy to understand model that also connects to the extremely popular ground water model, MODFLOW, does not exist.

Therefore, the multi-species, three-dimensional, contaminant transport model, MULTRAN, is developed to fill this need. MULTRAN is a finite difference model that can simulate the stress packages associated with MODFLOW, capable of handling single species transport akin to MT3D, and handle multi-species transport.

Verification of MULTRAN's numerical code and contaminant transport modeling capability is conducted for one-, two-, and three-dimensional systems. In all cases, MULTRAN matches the analytical solutions well. Though single species transport is

Reproduced with permission of the copyright owner. Further reproduction prohibited without permission.

possible with MULTRAN, the main thrust of this study is the modeling of multi-species transport.

To show this multi-species capability and its significance in contaminant transport, an example case study involving remediation of a contaminated site is conducted. Clearly, the adding of a competing species that can be used to drive off contaminants from the soil matrix will aid and expedite the cleanup process. MULTRAN's multi-species capability indicates this procedure to be true. Therefore, MULTRAN allows modelers a greater freedom in modeling contaminated ground water systems due to its multi-species capability.

Brian Anthony Waldron
Civil Engineering Department
Colorado State University
Fort Collins, CO 80523
Fall 1999

Reproduced with permission of the copyright owner. Further reproduction prohibited without permission.

ACKNOWLEDGEMENTS

To work for and acquire a doctor of philosophy degree, a number of people will play important roles in one's journey. Along my journey, I thank all those people who patted me on the back for encouragement, the individuals who so nicely asked about my dissertation and then sat there politely while I explained with excitement, and those friends who pushed me to my ultimate goal by continually stating, "You said three weeks ago you'd be done in three weeks!" Thank you.

There are, of course, those groups of individuals who I would like to give extra thanks. First and foremost is God whose will I followed and will continue to follow. Second are my parents who have encouraged me throughout all of my life to follow my dreams and supported me in all my works and accomplishments. I thank Suzy, my wife, who always had a smile on her face and joy in her praise. Special thanks also goes to Dr. Warner who taught me how to be self taught and for his advice without which my dissertation would be less. Last but not least, I thank all of my friends at John XXIII who supplied the breaks and play time.

This dissertation has a piece of you in it and to all of you, I thank you.

Reproduced with permission of the copyright owner. Further reproduction prohibited without permission.

Table of Contents

Reproduced with permission of the copyright owner. Further reproduction prohibited without permission.

Reproduced with permission of the copyright owner. Further reproduction prohibited without permission.

List of Tables

Reproduced with permission of the copyright owner. Further reproduction prohibited without permission.

List of Figures

Reproduced with permission of the copyright owner. Further reproduction prohibited without permission.

Reproduced with permission of the copyright owner. Further reproduction prohibited without permission.

Reproduced with permission of the copyright owner. Further reproduction prohibited without permission.

Chapter 1

Introduction

Purpose:

Groundwater contamination is a result of natural processes and human activities. Contamination of groundwater occurs when wastes are placed above or below the ground surface without proper leakage protection. Without adequate protection, contaminants enter the groundwater flowing to production wells or to downstream outlets such as rivers and wetlands. The transport of contaminants in groundwater is of major interest for the sake of health concerns.

For simplistic, ideal systems of contaminant transport, analytical solutions can provide an accurate solution to the migration patterns of contaminants in saturated systems. However, these analytical solutions are unable to model complexities such as heterogeneous soils and the effects of multiple aquifer stress (wells, river reaches, drains). Numerical models have become more popular and useful because of the limiting nature of the analytical solutions and the need to model these complex systems. One such numerical model is MODFLOW.

MODFLOW is an extremely popular numerical model developed by the USGS for modeling ground water flow systems; yet, MODFLOW cannot model contaminant transport. While taking advantage of MODFLOW's popularity, the contaminant transport model, MT3D, utilizes the flow rates determined by MODFLOW to solve contaminant transport problems. Although MT3D is used extensively in contaminant transport modeling, it can only model single species transport. The complex, non-static, chemical

Reproduced with permission of the copyright owner. Further reproduction prohibited without permission.

nature of ground water, however, has multiple effects on contaminant migration. Consequently, there is a need for a multi-species contaminant transport model that also utilizes the ground water modeling ability of MODFLOW.

Objective:

Therefore, the objective of this study is to develop a multi-species, contaminant transport model able to employ the results from MODFLOW. Because MODFLOW is a finite difference model, the proposed study incorporates the finite difference scheme to solve the contaminant transport equation. In order to develop this model, the tasks of this study include:

- handling the many stresses capable of being modeled by MODFLOW,
- expanding the contaminant transport equation using centered in space for the dispersion derivatives and upwinding for the time and advection terms,
- accounting for numerical dispersion,
- allowing for multiple chemical reactions including cation exchange,
- allowing for single species transport with limited chemical reactions such as radioactive decay and sorption via isotherms,
- developing the numerical code to model the aforementioned goals,
- verifying the code using analytical models and comparisons with MT3D, and
- showing the robustness of the numerical model by simulating remediation of a site using multi-species verses single species.

Reproduced with permission of the copyright owner. Further reproduction prohibited without permission.

Approach:

To achieve the objective of this study and to accomplish the individual tasks, the new multi-species transport model is systematically developed and varified using previously established ground water flow systems and contaminant transport procedures.

1. The three-dimensional, partial differential, contaminant transport equation is expanded using the finite difference scheme. At the same time, numerical dispersion is accounted for by subtracting this quantity from the longitudinal dispersivity coefficient.
2. A computer code is developed that can initially read the output flow rates from MODFLOW including those rates from the various sources MODFLOW simulates is developed.
3. Supplementary input files are designed to provide additional information to the model such as transport parameters, chemical species characteristics, and contaminant attributes.
4. The finite difference contaminant transport equation is transformed into code.
5. An iterative solver for asymmetric arrays is attached.

After these steps are accomplished, the model is developed as a single species model. Verifying the code via comparisons with analytical solutions and other contaminant transport codes, the model is then adapted to handling multi-species as well. This is accomplished by utilizing both Afifi's (Afifi, 1994) chemical reaction code and his methodology for attachment for its attachment to his transport code. Upon completion of attaching the chemical reaction code to this model, verification of the numerical model is performed. In addition an example case study of a site

Reproduced with permission of the copyright owner. Further reproduction prohibited without permission.

remediation is conducted to show the code's adaptability and diversification as a multi-species contaminant transport model. The following chapters detail the development and validation of the three-dimensional, multi-species contaminant transport code, MULTRAN.

Reproduced with permission of the copyright owner. Further reproduction prohibited without permission.

Chapter 2

Literature Review

Multi-species Contaminant Transport:

The modeling of contaminants through porous media has been extensively studied by a number of researchers. Though earlier models only simulate single species transport, an effort has been made in recent years to incorporate the hydraulic transport modeling of contaminants in the subsoil with the rigorous nature of batch, chemical reaction models. Modeling multi-species contaminant transport allows for better field representation.

As discussed by Westall *et al.* (1976) and reiterated by Yeh *et al.*(1989), the two most common terms in chemical transport are components and species. Components are chemical entities that can be combined with other components to form a species. Since these components are unique, they cannot be exchanged for or represented by other components.

Three mathematical strategies are reviewed by Yeh *et al.* (1989) which describe the connection between the transport of the contaminants and the chemical reactions regarding components and species with the groundwater, the porous media, and between themselves. The three strategies are the differential and algebraic equation approach, the direct substitution approach and the sequential iterative approach. A fourth strategy is the mixing cell approach, or reaction splitting. (Schultz, 1983; Narasimhan, 1986). It is important to properly select the primary and secondary variables when determining a strategy to use. The primary dependent variables (PDV's) are chosen from the transport

Reproduced with permission of the copyright owner. Further reproduction prohibited without permission.

equations and the SDV's computed analytically or numerically from the chemical equations (Yeh, *et al.*, 1989). Following is a review of the four strategies.

Differential and Algebraic Equations Approach:

In the differential and algebraic equation (DAE) approach, the transport and chemical equations are simultaneously mixed. The DAE approach can be solved in the two following ways: (1) allow the primary dependent variables (PDV's) to be written for the concentration of all species or (2) PDV's written for all component and precipitated species. The first possible scheme would require simultaneously solving a set of mixed DAE's. The mixed set of DAE's stems from substituting the total analytical concentrations, total dissolved, total sorbed, and total precipitated concentrations into the transport PDE's which in turn define the primary governing equations (PGE's). The primary differential equations (PDE's) for this scheme would be discretized over space producing ordinary differential equations (ODE's). These ODE's represent the concentrations of species at each node. The ODE's and the algebraic equations are then also applied to the spatial nodes. Hence, the set of mixed DAE's are created from these manipulations (Yeh, *et al.*, 1989).

The second scheme simulating the differential and algebraic equation approach is to iterate between two subsets of equations. The primary governing equaitons are developed by substituting the algebraic equations describing aqueous complexation, sorption via ion exchange, and sorption via surface complexation into the PGE's of the first scheme. The precipitation/dissolution algebraic equation is also included in this set of PGE's. The PGE's are solved for the PDV's and the SGE's for the SDV's.

Reproduced with permission of the copyright owner. Further reproduction prohibited without permission.

Yeh *et al.* (1989) conducted studies on each approach for one-, two-, and three-dimensional systems using a CRAY-XMP mainframe computer. Allowing a small three-dimensional model to be the crux of each approach, the DAE model would certainly not be used for three-dimensional systems. The CPU storage area for the coefficient matrix for a 30x20x10 discretized model with 10 aqueous components and 2 sorbent components would require approximately 1164.40 MB for the first scheme and 291.60 MB for the second utilizing an iteration method. Other mathematical strategies (full matrix, band matrix, sparse matrix, frontal method) aside from the iteration method were employed, but resulted in higher CPU storage with the full matrix strategy the highest as one would expect. The CPU time in seconds for one-time step computation using the iteration method on the CRAY-XMP was about 750 seconds for the first scheme and 180 seconds for the second scheme. In general, the DAE approach is applicable to simple one-dimensional models. Using the DAE method for realistic two- and three-dimensional models would not be practical as it would require excessive CPU memory and time. The DAE approach would be good for possibly one-dimensional column problems. Another advantage of the DAE method is it doesn't experience convergence problems (Afifi, 1994).

Direct Substitution Approach:

In the direct substitution approach (DSA), the chemical equations are substituted directly into the transport equations resulting in nonlinear PDE's written for each node (Yeh, *et al.*, 1989). The nonlinear PDE's are solved simultaneously for the PDV's. Again, the choice of PDV's governs the methodology of this approach. There are four methods possible with the DSA which are: (1) choosing the PDV's as concentrations of

Reproduced with permission of the copyright owner. Further reproduction prohibited without permission.

aqueous component species, (2) total dissolved concentrations of aqueous components, (3) total analytical concentration of aqueous components, and (4) a hybrid.

Choosing the PDV's as the concentration of aqueous component species or dissolved concentration of aqueous components will not allow the chemical process of precipitation/dissolution. Also the first and third possibility also makes the DSA impractical for two- and three-dimensional problems because PDE's, one for each aqueous component, must be solved simultaneously. Prescribing a hybrid set of PDV's, the fourth possibility, requires one to develop linear and quasi-linear transport equations through algebraic manipulations. This process is only good for extremely simple problems, yet many difficulties can still arise for realistic problems. One such problem is that the type of chemical reactions be known before hand (Yeh *et al.*, 1989).

The DSA for methodology (2) requires less CPU storage and time compared to the DAE approach, but still requires approximately 129.6 MB of storage which can present a problem for some PC users. Only 8 seconds would be needed to compute a single time step, but this is on a CRAY-XMP (Yeh, *et al.*, 1989). Results were not given for the other three methodologies. As with the DAE approach, an advantage of the DSA would be its suitability for one-dimensional problems and lack of convergence problems (Afifi, 1994).

Sequential Iteration Approach:

The sequential iteration approach (SIA) addresses the impractical nature of the DAE and direct substitution approaches to be used for realistic three dimensional simulations. If one recognizes the fact that the PDE's for transport contain the space

Reproduced with permission of the copyright owner. Further reproduction prohibited without permission.

derivatives and the nonlinear algebraic equations represent a batch system, the system can be iterated between sequentially solving the two types of equations (Yeh, *et al.*, 1989).

Yeh, *et al.* (1989) discusses three SIA methods as governed by the choice of PDV's which are: (1) concentrations of aqueous component species as PDV's, (2) total dissolved concentrations of aqueous components as PDV's, and (3) total analytical concentrations of aqueous components as PDV's. Of these three methods, the third is the only method which allows for all the geochemical processes including precipitation/dissolution, but requires many more equations to be solved. Also, the equation developed for the third method must be solved implicitly if one hopes for a steady-state solution.

For the same, small three-dimensional problem, the second SIA choice would require only 1.3 MB of CPU storage and 0.8 seconds of CPU time (using the iteration method). Results for the first and third choices were not given. By far the SIA is better for solving realistic two- and three-dimensional systems when comparing CPU storage and time; however, does have problems with convergence (Yeh *et al.*, 1989; Engesgaard, 1988).

Mixing Cell Approach:

The mixing cell, or reaction splitting approach, is another strategy for solving multi-species contaminant transport in porous media. This approach is similar to the sequential iteration approach in that the transportation and chemical reaction equations are coupled together, but not combined as in the DAE or direct substitution approach. The transport equations are solved first via finite difference, finite element, or another

Reproduced with permission of the copyright owner. Further reproduction prohibited without permission.

such method. After which, the chemical reactions between constituents within an elemental volume are determined, like a batch system.

Narasimhan *et al.* (1986) developed a mixing model, DYNAMIX, which incorporates a modified form of the finite element model, TRUMP (Edwards, 1972), for transport and PHREEQE (Parkhurst *et al.*, 1980) for chemical reactions. Narasimhan *et al.* (1986) discovered that their model, DYNAMIX, was computer intensive in solving the mixing of many chemical species and the migration of the dilution front; hence, limiting there grid size to a few tens of grid cells. DYNAMIX can handle three-dimensional flow with ion exchange and precipitation/dissolution for the chemical reactions.

Afifi (1994), in his study, reviewed other models which utilize the mixing cell approach. Afifi (1994) found that the mixing cell approach, or as he stated the reaction splitting approach, was advantageous for discontinuous models and where different time stepping is required between splitting operators. Two disadvantages of the mixing cell approach were: (1) it yields an approximate solution since transport and chemical reactions are realistically fully coupled and (2) the geochemical reactions are not treated from a physical point of view (Afifi, 1994). On the point of a physical representative model, Narasimhan *et al.* (1986) state, "Considering the present lack of knowledge about the relations that exist between chemical reactions and physical properties, the errors arising due to their omission is not likely to drastically influence the overall results...." However, Bryant, *et al.* (1986) state that a general model of flow through porous media must include the physical and chemical nature of the problem.

Reproduced with permission of the copyright owner. Further reproduction prohibited without permission.

Chemical Equilibrium verses Kinetic Modeling:

One of the contentions in multi-species transport modeling is whether the groundwater is moving slow enough for chemical reactions to take place, reaching equilibrium before the next time step (Jennings, *et al.*, 1984) If one assumes that the groundwater regime is moving slow enough for chemical reactions to occur between time steps, then instantaneous equilibrium can be assumed for the reactions which is mormally the case (Bryant *et al.*, 1986).

This is a major advantage in three respects. The first is that a large database of chemical equilibrium equations exist, and second, they can be incorporated either directly into the transport equations (i.e. DAE or DSA) or coupled to the transport equations (i.e. SIA or mixing cell approach) (Walsh, *et al*, 1984.). The third advantage is a less complex transport model (Jennings, *et al.*, 1984) The kinetic modeling approach requires more equations than the equilibrium approach to be solved and has a less extensive library of thermodynamic equations.

The kinetic modeling approach is more reliable since the instantaneous equilibrium approach produces only approximate results (Jennings, *et al.*, 1984). Because chemical constituents can potentially migrate over distances before equilibrium is reached in quick groundwater regimes, kinetic modeling is a viable option. Some researchers dismiss chemical equilibrium since a critical water flux is difficult to determine (Reardon, 1981).

Reproduced with permission of the copyright owner. Further reproduction prohibited without permission.

Chapter 3

Mathematical Description of Problem

In simulating contaminant transport, the movement of miscible solutes in the groundwater is described by advection, dispersion and diffusion of the solute. It is important to understand each of these processes so as to ascertain a better understanding of actual field measurements and model development. Combining advection, dispersion and diffusion into a mass balance equation describes the movement of solutes in groundwater, though each process is governed by a different physical means.

To ascertain the ground water flow velocities required in determining advection and dispersion, the volumetric flow rates calculated by MODFLOW are used. MODFLOW determines these flow rates by solving the three-dimensional ground water flow equation (see equation 3.1). The volumetric flow rates must first be divided by the saturated grid cell face area to arrive at a Darcy velocity. How this Darcy velocity is used follows in the next section.

$$\frac{\delta}{\delta x}\cdot\left(K_{xx}\cdot\frac{\delta h}{\delta x}\right)+\frac{\delta}{\delta y}\cdot\left(K_{yy}\cdot\frac{\delta h}{\delta y}\right)+\frac{\delta}{\delta z}\cdot\left(K_{zz}\cdot\frac{\delta h}{\delta z}\right)-W=S_s\cdot\frac{\delta h}{\delta t} \qquad 3.1$$

where: K_{xx}, K_{yy}, and K_{zz}: directional hydraulic conductivities (L/T)
h: potentiometric head
W: sink/source (T^{-1})
S_s: specific storage of porous media (L^{-1})

Advection:

Head gradients create a water velocity field throughout the aquifer system. Granted, stresses to the aquifer such as wells, recharge, and discharge, also cause groundwater movement. This velocity is known as the Darcy velocity (see equation 3.2)

Reproduced with permission of the copyright owner. Further reproduction prohibited without permission.

which can be transformed to a seepage velocity by dividing by the aquifer porosity (see equation 3.3).

$$q = -K\left(\frac{dh}{dl}\right) \qquad 3.2$$

where:

q = Darcy velocity (L/T)
K = hydraulic conductivity (L/T)
$\left(\frac{dh}{dl}\right)$ = hydraulic gradient (L/L)

$$v = \frac{q}{\phi} \qquad 3.3$$

where:

ϕ = aquifer porosity

Advection is the movement of solutes with the groundwater at seepage velocities. The mass flux due to advection is the product of the seepage velocity, aquifer porosity, and the concentration of the solute. Equation 3.4 depicts the mass flux in the x-direction.

$$J_A = v_x \cdot \phi C \qquad 3.4$$

where:

J_A = advective mass flux ($M/L^2/T$)
C = solute concentration (M/L^3)

In a similar manner, mass fluxes in the y- and z-directions are determined from those velocities in the respective directions.

Diffusion and Dispersion:

Diffusion and dispersion are related directly to the physical nature of either the solute or the soil. Diffusion (D_d) is a molecular process in which solute is spread due to

Reproduced with permission of the copyright owner. Further reproduction prohibited without permission.

its concentration gradient. A solute moves from higher concentrations to a lower concentrations. The ground water velocity greatly effects the diffusion of a solute as diffusion is only noticeable in extremely slow velocity fields. Typical diffusion values range from 1 x 10^{-3} ft/day to 2 x 10^{-3} ft/day at 76 °F. These values are considered constant throughout the study domain (Bedient, *et al.*, 1994).

Dispersion is dependent on the heterogeneity of the soil. On the microscopic level, three physical properties of the soil causing dispersion of the solute are (1) velocity variation between flow paths, (2) paths of least resistance through the pores, and (3) faster movement through larger pores (see Figure 3.1). Dispersion is described by the product of the seepage velocity, v, and a dispersivity value, α. The dispersivity value is usually divided into a longitudinal and transverse value. The transverse value is typically 1/10 to equaling the longitudinal value.

Hydrodynamic dispersion, which is a combination of dispersion and diffusion, is added to a total mass flux (J_T) to account for the spreading of a solute other than spreading associated with advection. Dispersion dominates hydrodynamic dispersion except in extremely slow flows where the velocity nears zero. Equation 3.5 depicts the hydrodynamic dispersion (D) as the sum of dispersion and diffusion values.

$$D = \alpha v + D_d \qquad 3.5$$

The mass flux describing hydrodynamic dispersion (J_D) is (in the x-direction):

$$J_D = -\phi \left(D_{xi} \frac{\delta C}{\delta i} \right) \quad i = (x,y,z) \qquad 3.6$$

Since first, the change in concentration over space is determined from the concentration at the new location minus the previous location and second, the fact that solute moves

Reproduced with permission of the copyright owner. Further reproduction prohibited without permission.

from a higher to a lower concentration, the mass flux is negated to cancel the negative change; hence, the reason for the negative sign in equation 3.6.

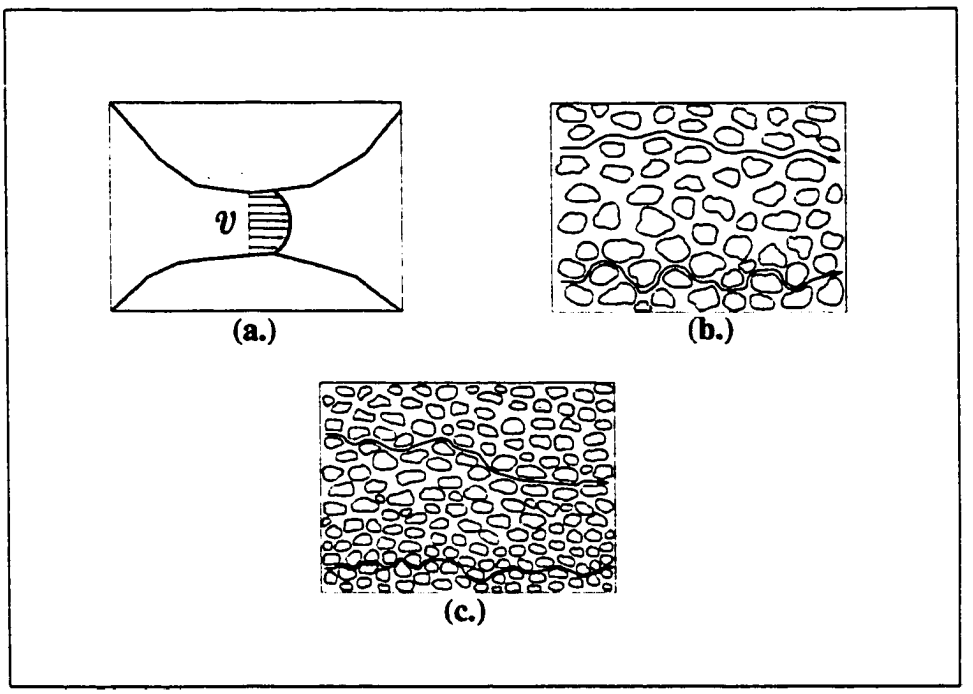

Figure 3.1. The three physical causes of dispersion: (a) velocity variation within a pore, (b) differences in pore sizes, and (c) tortuosity.

The total mass flux is the addition of the advection and hydrodynamic dispersion mass fluxes (see equation 3.7).

$$J_T = J_A + J_D \tag{3.7}$$

or

$$J_T = v_x \cdot \phi C - \phi \left[D_{xi} \cdot \left(\frac{\delta C}{\delta i} \right) \right] \tag{3.8}$$

Reproduced with permission of the copyright owner. Further reproduction prohibited without permission.

Mass Balance Equation:

With the total mass flux now known, the three dimensional, partial differential mass balance equation can be determined using the Taylor series. To describe the PDE, a representative elemental volume (REV) is utilized (see Figure 3.2). Mass balance requires that the difference between the flux in and the flux out equal a rate change of mass. From the Taylor series expansion and representing the x-direction, the following equation is obtained:

$$J_{x_{out}} = J_{x_{in}} + \frac{\delta J_x}{\delta x} \cdot \Delta x + \frac{\delta^2 \cdot J_x}{2! \cdot \delta x^2} \cdot \Delta x^2 + \text{higher order terms} \qquad 3.9$$

The second order term plus all higher order terms are negligible and do not contribute greatly to the overall solution; however, this does induce truncation error. Neglecting these terms and rearranging Equation 3.9, the resulting equation is:

$$J_{(x_{in})} - J_{(x_{out})} = -\frac{\delta J_x}{\delta x} \cdot \Delta x \qquad 3.10$$

Reproduced with permission of the copyright owner. Further reproduction prohibited without permission.

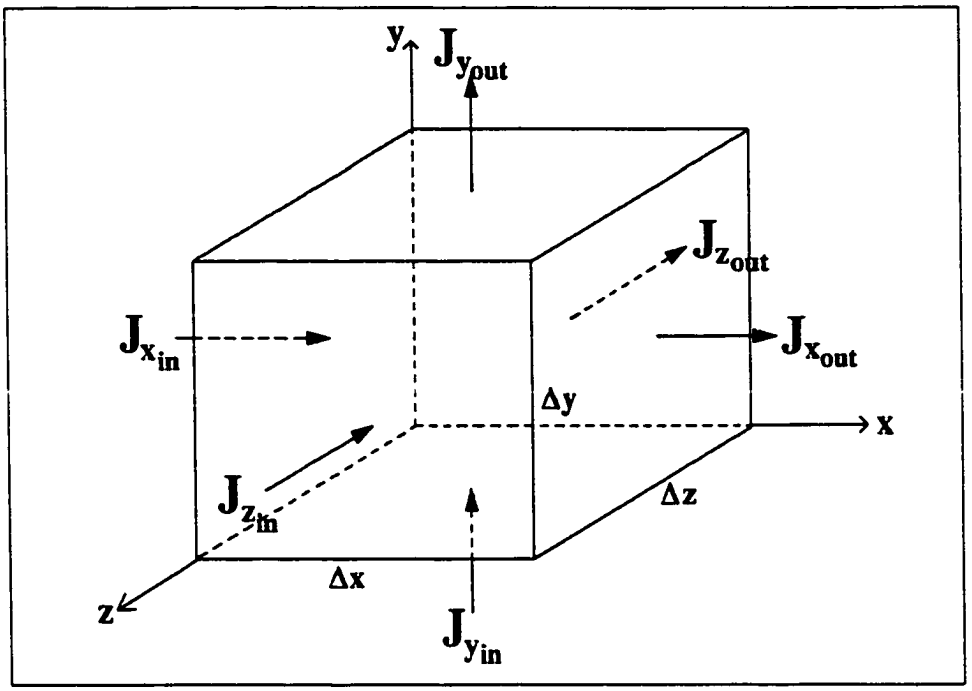

Figure 3.2. An example representative elemental volume (REV) with mass fluxes shown entering and leaving the volume.

Substituting J_T from Equation 3.8 for J_x in Equation 3.10, one obtains the change in flux across the REV surface in the x-direction.

$$-\frac{\delta J_x}{\delta x}\cdot\Delta x = \frac{-\delta\left[\left(\upsilon_x\cdot\phi C - \phi D_{xx}\cdot\frac{\delta C}{\delta x} - \phi D_{xy}\cdot\frac{\delta C}{\delta y} - \phi D_{xz}\cdot\frac{\delta C}{\delta z}\right)\cdot\Delta y\Delta z\right]}{\delta x}\cdot\Delta x \qquad 3.11$$

The cross-sectional area which the mass flux in the x-direction passes through is $\Delta z\Delta y$ as indicated in Figure 3.2. Solute can be present in three phases: (1) solid, (2) liquid, and (3) gaseous. For this study, only solute in the liquid phase is considered. Therefore, the mass rate of change for the solute in the liquid phase is

$$\text{mass rate of change} = \frac{\delta(C\cdot\phi\Delta x\Delta y\Delta z)}{\delta t} \qquad 3.12$$

Reproduced with permission of the copyright owner. Further reproduction prohibited without permission.

Hence setting Equation 3.11 and Equation 3.12 equal for mass balance, the following results:

$$\left[-\frac{\delta}{\delta x}\cdot\left(\upsilon_x\cdot C\right)+\frac{\delta}{\delta x}\cdot\left(D_{xx}\cdot\frac{\delta C}{\delta x}\right)+\frac{\delta}{\delta x}\cdot\left(D_{xy}\cdot\frac{\delta C}{\delta y}\right)+\frac{\delta}{\delta x}\cdot\left(D_{xz}\cdot\frac{\delta C}{\delta z}\right)\right]\cdot\phi\Delta x\Delta y\Delta z=\phi\Delta x\Delta y\Delta z\cdot\frac{\delta C}{\delta t} \qquad 3.13$$

An assumption is made that the volume of the representative element and the porosity do not change; therefore, these terms can be removed from inside the partial derivatives. Dividing both sides of the PDE by the porosity and the volume of the representative element, the PDE becomes (written for all three-dimensions):

$$\begin{aligned}&\frac{\delta}{\delta x}\cdot\left(D_{xx}\cdot\frac{\delta C}{\delta x}\right)+\frac{\delta}{\delta x}\cdot\left(D_{xy}\cdot\frac{\delta C}{\delta y}\right)+\frac{\delta}{\delta x}\cdot\left(D_{xz}\cdot\frac{\delta C}{\delta z}\right)+\frac{\delta}{\delta y}\cdot\left(D_{yy}\cdot\frac{\delta C}{\delta y}\right)+\frac{\delta}{\delta y}\cdot\left(D_{yx}\cdot\frac{\delta C}{\delta x}\right)+\\&\frac{\delta}{\delta y}\cdot\left(D_{yz}\cdot\frac{\delta C}{\delta z}\right)+\frac{\delta}{\delta z}\cdot\left(D_{zz}\cdot\frac{\delta C}{\delta z}\right)+\frac{\delta}{\delta z}\cdot\left(D_{zx}\cdot\frac{\delta C}{\delta x}\right)+\frac{\delta}{\delta z}\cdot\left(D_{zy}\cdot\frac{\delta C}{\delta y}\right)-\\&\frac{\delta\left(\upsilon_x\cdot C\right)}{\delta x}-\frac{\delta\left(\upsilon_y\cdot C\right)}{\delta y}-\frac{\delta\left(\upsilon_z\cdot C\right)}{\delta z}=\frac{\delta C}{\delta t}+\frac{W}{\phi}\cdot\frac{\delta C}{\delta t}+R\end{aligned} \qquad 3.14$$

Equation 3.14 describes three-dimensional contaminant transport through porous media including a sink/source term (W) and a reaction term (R). Possible sink/source terms are discussed and shown in Chapter 5. The reaction term is also discussed further in Chapter 5.

Reproduced with permission of the copyright owner. Further reproduction prohibited without permission.

Chapter 4

Chemical Reactions

Chemical reactions are important factors in the fate of solute transport in groundwater. Retardation of solute movement is caused by sorption and cation exchange reactions. Other chemical reactions, such as acid-base, oxidation-reduction, complexation, precipitation/dissolution, and hydrolysis, affect the dissolved solute concentration. The types of chemical reactions may vary from site to site and may have pronounced to negligible effect on the solute. Understanding the nature of these reactions and their affect on solute transport underlies the development of and the application of appropriate transport models.

Acid-base:

An acid is a substance that donates or loses a proton. A base accepts or adds protons. In a typical acid-base reaction, an acid loses a proton to an accepting base. Consider the following, simple acid-base reaction:

$$HCO^{3-} + H_2O \leftrightarrows H_3O^+ + CO_3^{2-} \qquad 4.1$$

HCO_3^- is the acid that loses a proton to water, the base. On the right hand side of the equation, the base, CO_3^{2-} gains the proton lost from H_3O^+ (Bedient, *et al.*, 1994). H_3O^+ is equated to H^+. If equilibrium of equation 4.1 results in the addition of H^+ ions (reaction moves to the right hand side), then the solution becomes more acidic.

Acidity of a solution is measured by the negative logarithm of hydrogen ions present in the solution; simply termed pH. Hence, the basicity of a solution is the pOH,

Reproduced with permission of the copyright owner. Further reproduction prohibited without permission.

the negative logarithm of hydroxide ions present. However, the pH range is typically used to indicate both the acidity and basicity of a solution. If the pH is less than 7.0, the solution is acidic, becoming more acidic toward zero. A pH of 7.0 is neutral and basic when between 7.0 (lightly basic) and 14.0 (strongly basic).

The equilibrium constant for equation 4.1 using the law of mass action is:

$$K = \frac{[H^+][CO_3^{2-}]}{[HCO^{3-}]} \qquad 4.2$$

The $[H_2O] = 1$ and again note that $[H_3O^+] = [H^+]$ (brackets represent concentrations). Table 4.1 lists some of the important weak acid-base reactions in water (Bedient, *et al.*, 1994). The strength of acids or bases depends on whether protons are lost or gained, respectively. Unlike electrons, protons transport well in water. Consequently, acid-base reactions in water reach equilibrium very rapidly (Devinny, *et al.*, 1990). Acid-base reactions are very important as they affect the pH, a master variable in aqueous systems (Bedient, *et al.*, 1994, and Afifi, 1994).

Cation Exchange:

Cation exchange is not a true chemical reaction though considered one because the exchange process is written in the form of a chemical reaction (McBride, 1994). Cation exchange, also termed absorbent-motivated sorption (Bedient, *et al.*, 1994), is the affinity of the soil for solute due to charge attraction. Typically cation exchange occurs between clayey soils which carry a negative charge and the cations Na^+, K^+, Mg^{2+}, and Ca^{2+}. Ammonia (NH_4^+) and lithium (Li^+) as well as some radioactive species which are also subject to cation exchange (Bedient, *et al.*, 1994). Cations attached to the soil

Reproduced with permission of the copyright owner. Further reproduction prohibited without permission.

surface by this exchange process slow the migration of the solute. This hindrance of solute migration is termed retardation.

Reaction	Mass law equation	- log K (25 C)
$H_2O = H^+ + OH^-$	$K_w = (H^+)(OH^-)$	14.0
$CO_2(g) + H_2O = H_2CO_3$	$K_{CO_2} = \frac{H_2CO_3}{P_{CO_2}(H_2O)}$	1.46
$H_2CO_3 = HCO_3^- + H^+$	$K_1 = \frac{(HCO_3^-)(H^+)}{H_2CO_3}$	6.35
$HCO_3^- = CO_3^{2-} + H^+$	$K_2 = \frac{(CO_3^{2-})(H^+)}{HCO_3^-}$	10.33
$H_2SiO_3 = HSiO_3^- + H^+$	$K = \frac{(HSiO_3^-)(H^+)}{H_2SiO_3}$	9.86
$HSiO_3 = SiO_3^- + H^+$	$K = \frac{(SiO_3^-)(H^+)}{HSiO_3}$	13.1

Source: Bedient et al., 1994.

Table 4.1. Typical acid-base reaction in natural water systems.

Cation exchange is modeled with either the constant charge model or the constant potential model. The constant charge model assumes the charge imbalance on the solute surface to be fixed. The disadvantage of this model is that the sorption of cations and anions must be modeled separately (Engesgaard, *et al.*, 1988). The constant potential model is similar to complexation (discussed later) where the solute surface charge varies according to pH. This model is more realistic of naturally sorbing substrate, but researchers prefer the constant charge model with much success aside from its limitations (Engesgaard, *et al.*, 1988).

An example exchange process is given in equation 4.3:

Reproduced with permission of the copyright owner. Further reproduction prohibited without permission.

$$z_b A_S + z_a B_I^{zb+} \leftrightarrows z_a B_S + z_b A_I^{za+} \qquad 4.3$$

where: A,B: chemical species
z: valence
S,I subscripts: sorbed and dissolved ion, respectively

Using chemical thermodynamics, the equilibrium state of equation 4.3 is:

$$K_{B/A} = \frac{(A_I)^{zb}}{(A_S)^{zb}} \cdot \frac{(B_S)^{za}}{(B_I)^{za}} \qquad 4.4$$

or

$$K_{B/A} = \left(\frac{A_I}{A_S}\right)^{zb} \cdot \left(\frac{B_S}{B_I}\right)^{za} \qquad 4.5$$

where: $K_{B/A}$: selectivity coefficient

The parentheses represent the activities of the ions. The relationship between the ion activity and the concentration (square brackets) is depicted by an activity coefficient (γ).

$$(C) = \gamma \cdot [C] \qquad 4.6$$

where C: chemical species

The activity coefficient approximates unity in dilute solutions in which the solution ionic strength is low. By using or introducing γ, ion activity can be equated to the species concentration (McBride, 1994). Hence, equation 4.5 becomes:

$$K_{B/A} = \left[\frac{A_I}{A_S}\right]^{zb} \cdot \left[\frac{B_S}{B_I}\right]^{za} \qquad 4.7$$

This equation is also known as the Vanselow equation which indicates heterovalent exchange (K_v=$K_{b/a}$, v for Vanselow). In equation 4.7, the exchangeable species, A_S and B_S, are equivalent fractions of sorbed species (mmol/mmol). To model homovalent exchange, the valences (z) in equation 4.7 are equal to one resulting in the form of the Kerr equilibrium equation.

Reproduced with permission of the copyright owner. Further reproduction prohibited without permission.

$$K_{B/A} = \frac{[A_I] \cdot [B_S]}{[A_S] \quad [B_I]} \qquad 4.8$$

Other equations, such as the Gapon and modified Gapon, describe cation exchange. The Gapon equation was introduced first as an empirical representation of Na-Ca exchange, but the equation was later given some thermodynamic justification by other researchers (Engesgaard, *et al.*, 1988). The Gapon equation is as follows:

$$K_{B/A} = \frac{[A_I]^{1/za} \cdot [B_S]}{[A_S] \quad [B_I]^{1/zb}} \qquad 4.9$$

The modified Gapon equation is:

$$K_{B/A} = \frac{[A_I] \cdot [B_S]}{[A_S] \quad [B_I]^{1/zb}} \qquad 4.10$$

Cation exchange is a rapid process compared to average groundwater velocities (Engesgaard, *et al.*, 1988); therefore, giving credence to the equilibrium approach over the kinetic approach as discussed at the end of Chapter 2. Research, as reviewed by Engesgaard *et al.* (1988), indicates that an equilibrium state for cation exchange can be obtained between 2 minutes and 48 hours.

Sorption:

Sorption is a non-chemical process that encompasses two general forms: adsorption and absorption. Adsorption describes the attraction of dissolved solute to particle surfaces, here porous media. Absorption describes solute penetration of the porous media. For this study, only the adsorption process is discussed and simulated. Similar to cation exchange, sorption retards the solute flow in the groundwater.

Reproduced with permission of the copyright owner. Further reproduction prohibited without permission.

Four mechanisms cause adsorption of solute onto the surface of the porous media: (1) chemical bond formation, (2) cation exchange (discussed previously), (3) hydrophobic bonding, and (4) Van der Waals forces.

In chemical bond formation, covalent chemical bonds are formed between the solid and the solute. These covalent bonds are the same as those holding molecules together; therefore, they are very difficult to break. In essence, the solute becomes part of the solid (Devinny, *et al.*, 1990).

Hydrophobic bonding occurs when non-charged particles are attracted to non-charged surfaces. The strength of attraction depends on how much the water rejects the solute molecule. Adsorption due to hydrophobic bonding can be "predicted from the organic content of the soil and the octanol-water partition coefficient for the contaminant" (Devinny, *et al.*, 1990). Typically those molecules which adsorb onto the soil particles have low solubility in water in comparison to more soluble molecules with respect to hydrophobic attraction.

Van der Waals forces may be the dominant factor in adsorption of solute in soils (Devinny, *et al.*, 1990). The electron cloud surrounding a molecule can oscillate back and forth creating alternating dipoles. As this molecule approaches a surface, the electrons on the solid's surface start oscillating inducing oppositely charged dipoles to those of the molecule; thereby, attracting the molecule to the solid's surface. This is termed a Van der Waals force.

A combination of mechanisms can also occur. For instance, complex organic chemicals can undergo ion exchange and hydrophobic bonding at the same time over different regions of its chemical structure (Devinny, *et al.*, 1990). For this study, solute

Reproduced with permission of the copyright owner. Further reproduction prohibited without permission.

adsorption is solved as a combination of these mechanisms. Several methods are available to estimate adsorption such as methods based on octanol-water coefficients, water solubility, molecular structure, surface area, and plume location. Other approaches to determine adsorption are laboratory methods and field column devices. Typically, laboratory methods are performed to determine adsorption concentrations. The laboratory method is expressed by graphing the amount of solutes sorbed to the concentration in solution. These representations are called isotherms (Bedient, *et al.*, 1994). Three types of equilibrium isotherms exist: linear, Freundlich, and Langmuir.

The linear isotherm is described by equation 4.11 (Jury, *et al.*, 1991).

$$S = K_d C \qquad 4.11$$

where: S: sorbed concentration
K_d: distribution coefficient
C: solution concentration

Figure 4.1 depicts the graphical representation of the linear adsorption isotherm.

The Freundlich isotherm is a more general adsorption equation shown graphically in figure 4.2 and expressed as equation 4.12 (Bedient, *et al.*, 1994).

$$S = K_d C^{1/N} \qquad 4.12$$

where: K_d: Freundlich adsorption constant
N: Freundlich exponent

Reproduced with permission of the copyright owner. Further reproduction prohibited without permission.

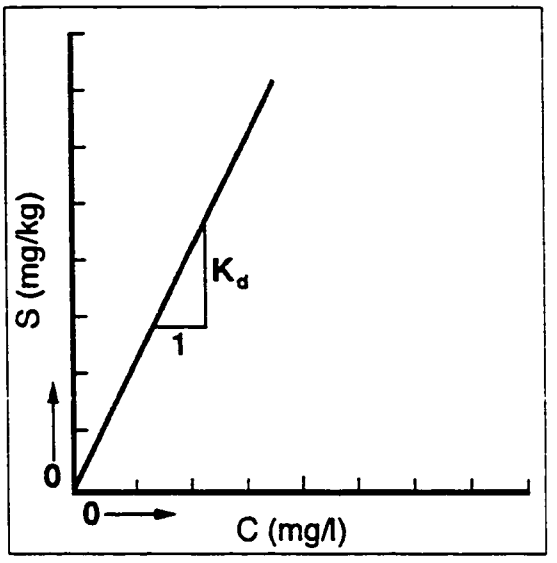

Figure 4.1. Graphical representation of the linear adsorption isotherm. K_d is the slope of the line.

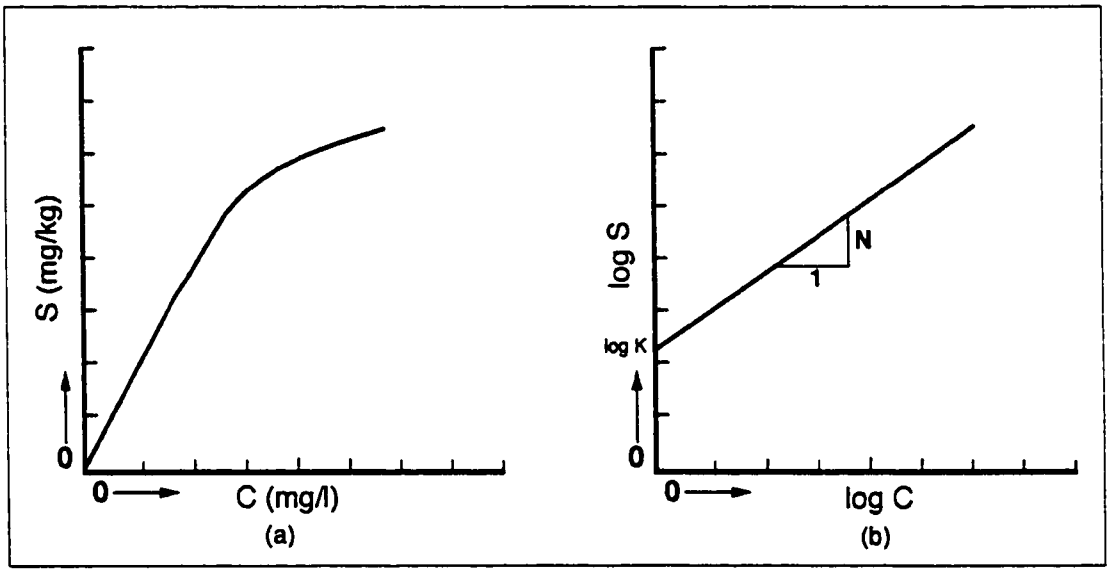

Figure 4.2. Graphical representation of Freundlich adsorption isotherm. (a) isotherm of S verses C. (b) isotherm of log S verses log C.

The linear and Freundlich isotherms assume that there is not a maximum number of sorbing sites. The Langmuir isotherm (see equation 4.13) is based on the fact that a maximum number of sorbing sites does exist. Once all of the sorbing sites are filled,

Reproduced with permission of the copyright owner. Further reproduction prohibited without permission.

solute in solution can no longer sorb, remaining in solution (Bedient, *et al.*, 1994). See figure 4.3 for the Langmuir isotherm graphical representation.

$$S = \frac{kbC}{(1 + kC)} \qquad 4.13$$

Where: k: adsorption constant based on bonding strength;
b: maximum limit of sorbed solute on media.

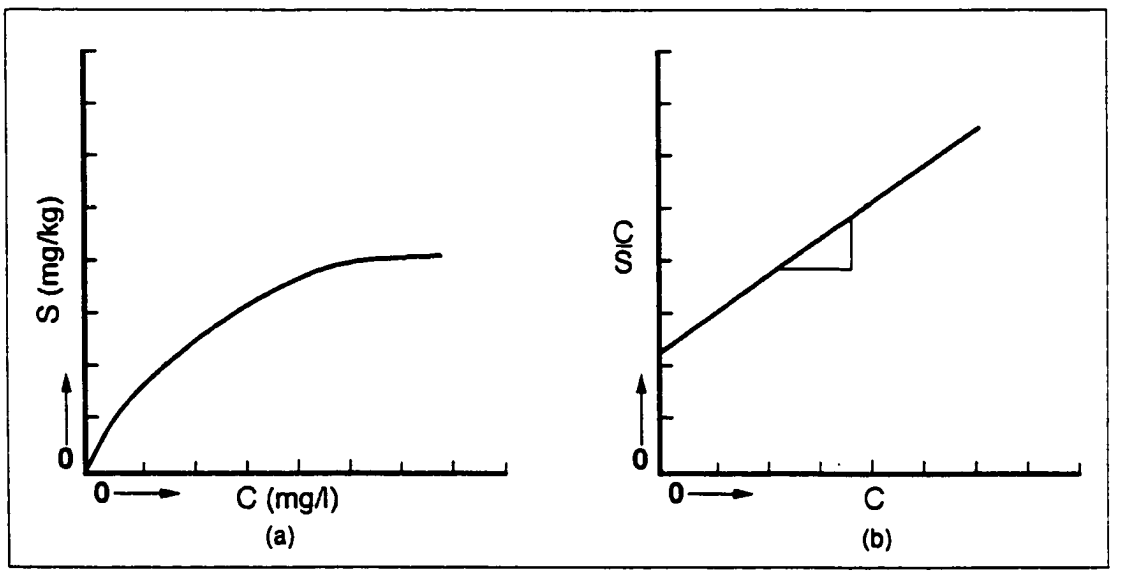

Figure 4.3. Graphical representation of Langmuir adsorption isotherm. (a) nonlinear isotherm of S verses C. (b) linear isotherm of C/S verses C.

Other isotherms are the Langmuir two-surface (see equation 4.14) and the competitive Langmuir (see equation 4.15). The competitive Langmuir isotherm allows for more than one species unlike the aforementioned isotherms. If an ion is absorbed, then another ion must desorb (Engesgaard, *et al.*, 1988).

$$S = \left[\frac{k_1 \cdot b_1 \cdot C}{(1 + k_1 \cdot C)}\right] + \left[\frac{k_2 \cdot b_2 \cdot C}{(1 + k_2 \cdot C)}\right] \qquad 4.14$$

where: 1,2: species one and species

Reproduced with permission of the copyright owner. Further reproduction prohibited without permission.

two, respectively

$$(C_1/C_2)/S = \frac{b_2}{k_1 \cdot b_1} + \frac{C_1}{b_2 \cdot C_2} \qquad 4.15$$

Oxidation-reduction:

Oxidation-reduction reactions are simply termed redox reactions. Redox reactions involve the availability of electrons (e^-). By adding electron(s), negative charge, to a positively charged molecule, the total positive charge is reduced. A reduction of Mn^{3+} by the addition of an electron is expressed by equation 4.16.

$$Mn^{3+} + e^- = Mn^{2+} \qquad 4.16$$

Loss of electrons from a chemical species is an oxidation reaction (see equation 4.17).

$$Mn^{2+} = Mn^{3+} + e^- \qquad 4.17$$

The availability of electrons in groundwater depends mainly on the presence of molecular oxygen, a powerful oxidant. If an abundance of oxygen is present, any available electrons will be readily oxidized. Note that free electrons do not exist in aqueous solutions (McBride, 1994). Conversely, high levels of electrons signify low oxygen levels, which is usually the case in saturated soils. Low oxygen levels are caused by aerobic activity in the aquifer. Biological activity in the aquifer can catalyze the redox reactions (Devinny, *et al.*, 1990). Typically, redox reactions are extremely slow. Therefore redox reactions should be modeled with the kinetic approach.

The general redox half-reaction depicts an ongoing process of electron exchange between oxidants and reductants. In equation 4.18, as negatively charged electrons are gained by an oxidant, there is a reduction in positive valence. If electrons are lost in a

Reproduced with permission of the copyright owner. Further reproduction prohibited without permission.

reducant there is a gain in positive charge in the oxidant. This constant gain and loss of electrons occur freely in the ground water system and this movement constitutes the virtual equilibrium relation.

$$\text{Oxidation (ox)} + ne^- = \text{reduction (red)} \qquad 4.18$$

Redox equations consist of two half-redox reactions since complete reactions can be viewed as two half-reactions. For example, the redox reaction shown in equation 4.19 to the right of the equation is a reduction and to the left an oxidation. A half-reaction stems from the fact that a reaction such as equation 4.19,

$$Zn + 2H^+ \leftrightarrows Zn^{2+} + H_2 \qquad 4.19$$

can be written as two half-reactions (see equations 4.20 and 4.21).

$$Zn \leftrightarrows Zn^{2+} + 2e^- \qquad 4.20$$

$$2H^+ + 2e^- \leftrightarrows H_2\,(gas) \qquad 4.21$$

From the expression in 4.18, virtual equilibrium is written as:

$$K = \frac{[red]}{[ox][e^-]^n} \qquad 4.22$$

"No such reaction can attain equilibrium in isolation, since at least one other redox pair must be present to donate or accept the electrons(s). The 'equilibrium constant' should then be thought of as a virtual or operational constant only." (McBride, 1994)

Redox reactions are important in contaminant transport. Oxidation of already reduced chlorinated hydrocarbons or carbon as solvents catalyzed by biological activity can create carbon dioxide (CO_2). Although CO_2 is a non-toxic product, it is acidic and

Reproduced with permission of the copyright owner. Further reproduction prohibited without permission.

therefore effects the solution pH. Metal ions are also affected by redox reactions (Devinny, *et al.*, 1990, and McBride, 1994).

Complexation:

Complexation is a process whereby free ions combine to form another ion. This complexation product can have different chemical characteristics from the original free ions. The free ions can be simple cations, such as metals, anions (*i.e.* Cl^-, F^-, Br^-, SO_4^{3-}), organic molecules, or even other complexes. The numbers of complexes that can form from these free ions are numerous; however, relatively few complexes are really significant in retrospect to concentrations found in actual cases (Engesgaard, *et al.*, 1988).

Complexation is a very rapid process; usually reaching equilibrium within seconds (Engesgaard, *et al.*, [1988]). Complexation is a very important chemical reaction. Chromium, copper, lead, uranium, and plutonium are heavy metals that may become increasingly mobile (leach) in groundwater through complexation. On the other hand, some complexes can become absorbed onto the soil thereby preventing migration (Bedient, *et al.*, 1994 and Devinny, *et al.*, 1990).

The simplest from of a complexation reaction is shown as the combination of a metal ion (Mn^{2+}) with a chlorine ion (Cl^-) as follows:

$$Mn^{2+} + Cl^- = MnCl^+ \qquad 4.23$$

A complexation reaction will always be between opposite charge attractions. From equation 4.23, the following general equilibrium reaction is expressed as (Engesgaard, *et al.*, 1988):

Reproduced with permission of the copyright owner. Further reproduction prohibited without permission.

$$iA^{za} + jB^{zb} \leftrightarrows A_iB_j^{(iza + jzb)} \qquad 4.24$$

where: i,j: number of moles
A,B: involved ions
z: valence

The equilibrium constant for equation 4.24 using thermodynamics is:

$$K^C_{AB} = \frac{[C_{AB}]}{[C_A][C_B]} \qquad 4.25$$

where: K: equilibrium constant

Equilibrium constants can readily be found in the literature.

Precipitation and Dissolution:

Precipitation and dissolution are other very important chemical processes in solute transport. Large quantities of mass can be transferred between the groundwater and porous media (Bedient, *et al.*, 1994). Free ions can precipitate out of solution as a solid, thereby removing those ions from possible transport. Dissolution is the dissolving of a solid back into free ions.

Reactions involving the solid phase are always slower than reactions between dissolved species (Engesgaard, *et al.*, 1988). Precipitation of a solid is usually a slower process than dissolution, and it occurs when the groundwater is over saturated with chemical species. Nucleation and crystal growth are the two processes of precipitation. Ion and molecules interact to form the nuclei of the solid. After nucleation, crystal growth starts by material buildup on the nuclei (Engesgaard, *et al.*, 1988).

Dissolution depends on the solubility of the solid in groundwater. Solubility of the solid decreases if similar ions to those that result from the dissolution process exists within the solution (Bedient, *et al.*, 1994). The equilibrium coefficient discussed for

Reproduced with permission of the copyright owner. Further reproduction prohibited without permission.

previous chemical reactions is termed the solubility coefficient here. For the dissolution of a solid containing three ions, the equilibrium equation is written:

$$A_iB_jC_k = iA^{za} + jB^{zb} + kC^{zc} \qquad 4.26$$

where: i,j,k: number of moles

Hence, the solubility coefficient is expressed as (Engesgaard, *et al.*, 1988):

$$K^S_{ABC} = [C_A]^i[C_B]^j[C_C]^k \qquad 4.27$$

where: $iz_a + jz_b + kz_c = 0$

Note that the activity of a solid is unity.

Precipitation and dissolution are slow processes as mentioned previously. Reactions involved with dissolved species including complexation will often reach equilibrium long before equilibrium occurs in precipitation/dissolution reactions (Sposito, 1994). Therefore, the kinetic approach should be used to model precipitation and dissolution reactions (Sparks, 1986).

Hydrolysis:

Hydrolysis is a common chemical process involving organic molecules interacting with water (Bedient, *et al.*, 1994 and Devinny, *et al.*, 1990). An organic species, RX, combines with water forming a hydroxyl group (-OH) (see equation 4.28). Typically organic species are degraded by hydrolysis reactions (see Table 4.2) although there are some organic compounds inert to hydrolysis (see Table 4.3).

$$RX + H_2O \leftrightarrows ROH + H^+ + X^- \qquad 4.28$$

where: RX: organic molecule

Although risking oversimplification of most hydrolysis reactions, the first-order rate constant for a hydrolysis reaction is expressed as follows: (Bedient, *et al.*, 1994).

Reproduced with permission of the copyright owner. Further reproduction prohibited without permission.

$$-\frac{d[RX]}{dt} = k_T[RX] \qquad 4.28$$

where: k_T: hydrolysis rate constant

Alkanes	Aromatic amines
Alkenes	Alchohols
Alkynes	Phenols
Benzenes/biphenyls	Glycols
Polcyclic aromatic hydrocarbons	Ethers
Heterocyclic polycyclic aromatic hydrocarbons	Aldehydes
	Ketones
Halogenated aromatics/PCBs	Carboxylic acids
Dieldrin/aldrin and related halogenated hydrocarbon pesticides	Sulfonic acids
Aromatic nitro compounds	

Source: Bedient et al., 1994.

Table 4.2. Organic compounds degraded by hydrolysis.

Alkyl halides	Nitriles
Amides	Phosphonic acid esters
Amines	Phosphoric acid esters
Carbamates	Sulfinic acid esters
Carboxylic acid esters	Sulfuric acid esters
Epoxides	

Source: Bedient et al., 1994.

Table 4.3. Organic compounds inert to hydrolysis.

Reproduced with permission of the copyright owner. Further reproduction prohibited without permission.

Chapter 5

Model Development

Modeling multi-species contaminant transport requires that the number of equations equal the number of unknowns. Discussed in this chapter are the necessary equations for modeling the chemical reactions and subsequent transport of the chemical species. The PDV's are equivalent to the concentrations of the aqueous components. Therefore from equations 5.1 and 5.2, the aqueous calcium component concentration, C_1, is equivalent to the cumulative concentrations of all species containing calcium (see Equation 5.3). The component concentrations are also shown for the remaining PDV's: Na, SO_4, and Cl (see Equations 5.4-5.6, respectively).

$$C_{(CaSO_4)} + 2 \cdot C_{(NaCl)} = C_{(Na_2 \cdot SO_4)} + C_{(CaCl_2)} \qquad 5.1$$

$$C_{Ca} + 2 \cdot X_{Na} = X_{Ca} + 2 \cdot C_{Na} \qquad 5.2$$

where: C: species concentration
X: ion exchanged species

$$C_1 = C_{Ca} + C_{(CaSO_4)} + C_{(CaCl_2)} \qquad 5.3$$

$$C_2 = C_{Na} + C_{(NaSO_4)} + 2 \cdot C_{(Na_2 \cdot Cl)} \qquad 5.4$$

$$C_3 = C_{(CaSO_4)} + C_{(Na_2 \cdot SO_4)} \qquad 5.5$$

$$C_4 = 2 \cdot C_{(CaCl_2)} + C_{NaCl} \qquad 5.6$$

Note that the sorbed calcium component (X_{Ca}) in equation 5.2 does not enter into equation 5.3. The sorbed concentration of each species is substituted directly into the

Reproduced with permission of the copyright owner. Further reproduction prohibited without permission.

respective transport equation (see Equation 5.7) (Yeh, *et al.*, 1989). The component concentrations are typically calculated in terms of molar concentration (M).

The respective transport equations for each of the aforementioned aqueous components are as follows:

$$D_{xx}\cdot\frac{\delta^2\cdot C_1}{\delta x^2} - v_x\cdot\frac{\delta\cdot C_1}{\delta x} = \frac{\delta C_1}{\delta t} + \frac{\delta X_{Ca}}{\delta t} \qquad 5.7$$

$$D_{xx}\cdot\frac{\delta^2\cdot C_2}{\delta x^2} - v_x\cdot\frac{\delta\cdot C_2}{\delta x} = \frac{\delta C_2}{\delta t} + \frac{\delta X_{Na}}{\delta t} \qquad 5.8$$

$$D_{xx}\cdot\frac{\delta^2\cdot C_3}{\delta x^2} - v_x\cdot\frac{\delta\cdot C_3}{\delta x} = \frac{\delta C_3}{\delta t} \qquad 5.9$$

$$D_{xx}\cdot\frac{\delta^2\cdot C_4}{\delta x^2} - v_x\cdot\frac{\delta\cdot C_4}{\delta x} = \frac{\delta C_4}{\delta t} \qquad 5.10$$

The partial differential equation for this study is discussed more fully later in this chapter.

Another set of equations necessary for model development constitutes the algebraic equations that are derived from the chemical reactions. Descriptions of these derived algebraic equations as well as descriptions of chemical reaction modeling techniques, such as operational electrons and the proton condition, are discussed here more fully.

Reproduced with permission of the copyright owner. Further reproduction prohibited without permission.

Algebraic Equations for Chemical Reactions:

Aqueous Complexation:

Aqueous complexation is solved via a mass action equation where an equation is written for each complex species. From the transformation of equation 4.25, the complexed species, C_{AB}, is equal to the equilibrium constant times the chemical products.

$$C_{AB} = K_{AB} [C_A][C_B] \qquad 5.11$$

Redefining C_{AB} as X_i, the concentration of the i^{th} component species, Yeh *et al.* (1991) expresses the aqueous complexation mass action equation as

$$X_i = \alpha_i \cdot \prod_{k=1}^{N_a} (C_k)^{a_{ik}} \qquad i = 1, 2, \ldots, M_x \qquad 5.12$$

where

$$\alpha_i = K_i \cdot \prod_{k=1}^{N_a} \frac{(\gamma_k)^{a_{ik}}}{\gamma_i} \qquad i = 1, 2, \ldots, M_x \qquad 5.13$$

where: X_i: concentration of the i^{th} complexed species (M/L^3)
α_i: stability constant of the i^{th} complexed species
N_a: number of aqueous components
C_k: concentration of the k^{th} aqueous component species (M/L^3)
a_{ik}: stoichiometric coefficient of the k^{th} aqueous component in the i^{th} complexed species
M_x: number of complexed species
K_i: thermodynamic equilibrium constant of the i^{th} complexed species
γ_k: activity coefficient of the k^{th} aqueous component species (L^3/M)
γ_i: activity coefficient of the i^{th} complexed species (L^3/M).

Since γ is approximately unity or one for dilute species, α_i is simply equal to the thermodynamic equilibrium constant. Therefore, substitution of 5.13 into 5.12 becomes

Reproduced with permission of the copyright owner. Further reproduction prohibited without permission.

$$X_i = K_i \cdot \prod_{k=1}^{N_a} (C_k)^{a_{ik}} \qquad i = 1, 2, \ldots, M_x \qquad 5.14$$

Hence, the complex species concentration is the thermodynamic equilibrium constant times the product of each aqueous component species raised to the power of its stoichiometric coefficient. If an aqueous component is not involved in the formation of the complex species, X_i, then its result in the product of C_k is one because its stoichiometric coefficient would be zero. Equation 5.13 is written for M_x unknowns.

Sorption:

Sorption, as discussed in Chapter 4, can be modeled by a cation exchange or by adsorption isotherms. Sorption has been successfully modeled exclusively as cation exchange (Afifi, 1994, Cernik, *et al.*, 1994, Lewis, *et al.*, 1987). The value of using cation exchange to model sorption is when simulating multispecies transport. For single species, sorption can be estimated with either the linear, Freundlich, or Langmuir isotherms. The use of isotherms to calculate a retardation factor is mentioned later in the transport modeling section of this chapter.

Both the equilibrium equation and the cation exchange capacity (CEC) equation are needed to model the cation exchange process. Several expressions exist for representing the equilibrium equation such as the Kerr, Vanselow, Gaines-Thomas, and Gapon equations. The Gaines-Thomas equation is used widely in representing ion-exchange mass action processes (Walter, *et al.*, 1994, Afifi, 1994, Bjerg, *et al.*, 1993, Yeh, *et al.*, 1991, Yeh, *et al.*, 1989). The Gaines-Thomas equation assumes that the sorption sites are initially occupied with exchangeable ions and that the site's surface

Reproduced with permission of the copyright owner. Further reproduction prohibited without permission.

charge and cation exchange capacity (CEC) are fixed (Walter, *et al.*, 1994). Similar to the Vanselow equation in Chapter 4 (equation 4.7), the exchanged species (z_i, z_J) are the equivalent fractions of the sorbed species (z_i or z_J) concentration (M/L^3) to the total concentration of all sorbed species, s_T, (M/L^3).

Rewriting equation 4.4 becomes

$$K_{iJ} = \frac{(a_J)^{v_i}}{(z_J)^{v_i}} \cdot \frac{(z_i)^{v_J}}{(a_i)^{v_J}} \qquad i = 1, 2, \ldots, M_s \qquad 5.15$$

where: a: dissolved concentration (M/L^3)
z: equivalent sorbed concentration
v: valence
K_{iJ}: selectivity coefficient

Assuming the activity of any sorbed species to be proportional to its molar concentration (Yeh, *et al.*, 1991), the terms in equation 5.15 become

$$a_i = \gamma_i \cdot a_i \qquad 5.16a$$

$$a_J = \gamma_J \cdot a_J \qquad 5.16b$$

$$z_i = \frac{z_i}{s_T} \qquad 5.16c$$

$$z_J = \frac{z_J}{s_T} \qquad 5.16d$$

where

$$s_T = \sum_{i=1}^{M_s} z_i \qquad 5.17$$

Reproduced with permission of the copyright owner. Further reproduction prohibited without permission.

The term, s_T, in equation 5.17 is the total concentration of all sorbed species (M/L^3). Again under the assumption that γ is equal to unity, equation 5.15 with substitution of equations 5.16a to 5.16d and 5.17 becomes

$$K_{iJ} = \frac{\left(a_J\right)^{v_i}}{\left(\frac{z_J}{s_T}\right)^{v_i}} \cdot \frac{\left(\frac{z_i}{s_T}\right)^{v_J}}{\left(a_i\right)^{v_J}} \qquad 5.18$$

Solving for the concentration of the i^{th} ion exchanged species, Z_i becomes

$$\left(\frac{z_i}{s_T}\right)^{v_J} = K_{iJ} \cdot \left[\frac{\left(a_i\right)^{v_J}}{\left(a_J\right)^{v_i}}\right] \cdot \left(z_J\right)^{v_i} \cdot \left(s_T\right)^{-v_i} \qquad 5.19$$

or more simply the equilibrium equation for z_i is

$$z_i = \left[K_{iJ} \cdot \left[\frac{\left(a_i\right)^{v_J}}{\left(a_J\right)^{v_i}}\right] \cdot \left(z_J\right)^{v_i} \cdot \left(s_T\right)^{v_J - v_i} \right]^{\frac{1}{v_J}} \qquad 5.20$$

The cation exchange equation is simply the sum of the concentrations of all the exchanged cations (see Equation 5.21).

$$CEC = \sum_{i=1}^{M_s} v_i \cdot z_i \qquad 5.21$$

Precipitation and Dissolution:

Reproduced with permission of the copyright owner. Further reproduction prohibited without permission.

The precipitation and dissolution chemical reactions are not simulated in this model. These reactions are extremely slow, thereby requiring the kinetic approach for modeling. Aside from not being able to utilize the local equilibrium approach, high concentrations of contaminants are required to reach an over saturation limit where precipitation can occur. Precipitation under these conditions is unusual and occurs under extreme conditions atypical of most situtations.

Hydrolysis:

Hydrolysis was reviewed as a specific chemical reaction in Chapter 4 based on references by Bedient (1994) and Devinny *et al.* (1990). However, in multi-species transport, hydrolysis can be simulated as an acid-base reaction (Yeh, *et al.*, 1991, Afifi, 1994) since the hydrolysis equation is similar to the acid-base reaction equation.. Therefore, hydrolysis reactions are modeled as acid-base reactions.

Acid-base:

For acid-base reactions, the chemical species involved are modeled in the transport equations as chemical components. However, an additional parameter is needed to describe the acidity of the system for hydrogen components (Yeh, *et al.*, 1991). This parameter is the proton activity or better termed the pH. The pH can be determined by using either the electroneutrality approach or the proton condition. These two approaches are mathematically equivalent but not computationally equivalent (Morel, *et al.*, 1972). It is best to use the proton condition for computing the pH of the system (Yeh, *et al.*, 1989). The proton condition states that the concentration of the excess proton (H) is the difference between the total hydrogen component and the hydroxide component (see

Reproduced with permission of the copyright owner. Further reproduction prohibited without permission.

Equation 5.22). Hence, the excess proton is then substituted into the transport equation (PDE).

$$\text{excess protons} = T_H - T_{OH} \qquad 5.22$$

The total hydrogen and hydroxide components are determined from the mole balance equation. The law of mole balance states that the total number of moles of a chemical component equals the molar sum of all species containing that chemical component within a unit solution volume. Though the mole balance equation is used to determine T_H and T_{OH} for acid-base reactions, the total component molar concentration of all species in solution is determined with the mole balance equation. Each chemical component is represented by its own mole balance equation. The mole balance equation is expressed as

$$T_j = C_j + \sum_{i=1}^{M_x} a_{ij} \cdot X_i + \sum_{i=1}^{M_s} a_{ij} \cdot Z_i \qquad 5.23$$

Hence, the mole balance equation includes the chemical components contained in the aqueous state, the complexation reactions, and ion exchange. Because the mass action equation for acid-base, hydrolysis, and redox reactions are similar to the complexation mass action equation, these four chemical processes are represented in equation 5.23 with the complexation reaction term. Since precipitation/dissolution is not included in this model, any possible contribution it may make to the mole balance equation is eliminated.

Redox:

Reproduced with permission of the copyright owner. Further reproduction prohibited without permission.

As stated in Chapter 4, redox reactions are slow, and these reactions are often treated in a kinetic modeling approach. However, Yeh *et al.* (1991) and Afifi (1994) assume redox reactions to occur under the local equilibrium approach since they may have sufficient time to occur within a finite difference cell due to the length of time it takes for the chemical components to traverse the cell. Therefore, redox reactions are modeled using the local equilibrium approach. Should redox reactions initially occur too slowly for an equilibrium modeling approach, the grid cell size may be increased to accommodate the completion of the redox reaction.

Redox reactions, like acid-base reactions, do not need special mathematical treatment (Yeh, *et al.*, 1991). However, the conservation of electrons must be satisfied. Therefore, the principle of an operational electron is used to treat an electron like an aqueous component subject to transport. For instance (referring to equation 4.16), Mn^{3+}, Mn^{2+} and e^- as well will be subject to transport with e^- being treated as an operational electron.

To find the resulting aqueous chemical concentrations, equations 5.14, 5.20 and 5.23 are solved simultaneously using the Newton-Raphson method. There are a number of root-locating methods, but the Newton-Raphson method is the most widely used (Pfingsten, 1996, Bajracharya, *et al.*, 1995, Afifi, 1994, Walter, *et al.*, 1994, Liu, *et al.*, 1989, Chapra, *et al.*, 1988). The equation for this method can be determined by using a geometrical interpretation or by applying a Taylor series.

Using the geometrical derivation and an initial estimate of x_i, a tangent is drawn (see Figure 5.1) from the point $[x_i, f(x_i)]$ to the x-axis. The point where the tangent

Reproduced with permission of the copyright owner. Further reproduction prohibited without permission.

intercepts the x-axis usually represents a new estimate, x_{i+1}. The first derivative at the first estimate is synonymous to the slope:

$$\frac{df}{dx} \approx \frac{f(x_i) - 0}{x_i - x_{i+1}} \qquad 5.24$$

Rearranging, equation 5.24 becomes

$$f(x_i) = f'(x_i)(x_i - x_{i+1}) \qquad 5.25$$

which is called the Newton-Raphson formula (Chapra, *et al.*, 1988).

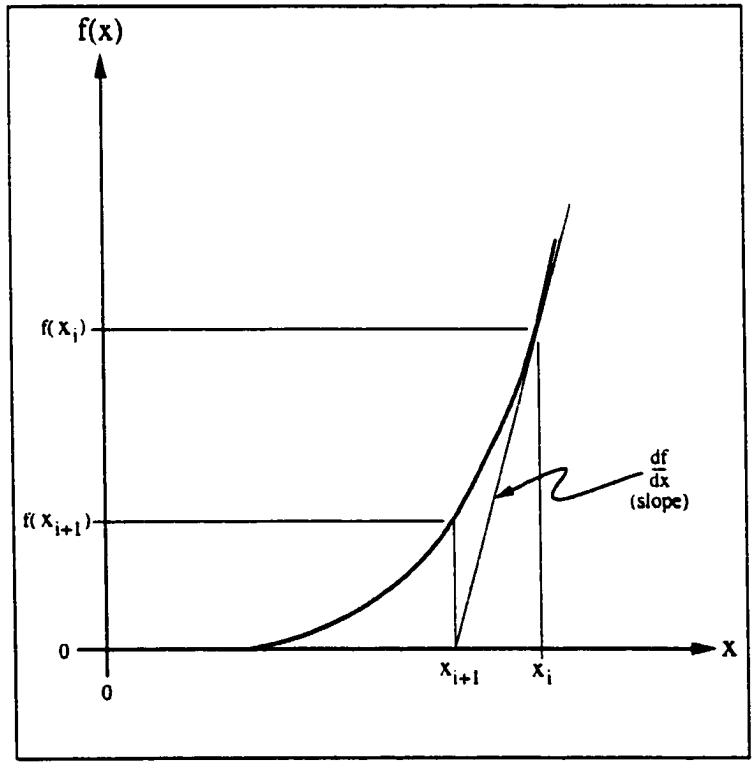

Figure5.1. Graphical representation of Newton-Raphson technique.

Reproduced with permission of the copyright owner. Further reproduction prohibited without permission.

Writing equation 5.25 in matrix form becomes,

$$[Z^n]\{\Delta x\} = \{Y^n\} \qquad 5.26$$

The vector, $\{Y^n\}$, is the residual which approaches zero as convergence is reached. The matrix, $[Z^n]$, is better known as the Jacobian matrix, which is the partial derivative of Y with respect to x. The vector, $\{\Delta x\}$, is the change in the parameter values where $\Delta x = x^n + x^{n+1}$ where n represents the initial estimate and n+1 is the prediction.

With the Newton-Raphson briefly explained, one must now derive both a function, $f(x^n)$, for the residual vector, $\{Y^n\}$, and a function derivative, $f'(x^n)$, for the Jacobian matrix, $[Z^n]$, and estimate the parameter, x^n. For this study, the function is defined by equations 5.14, 5.20 and 5.24, and it is expressed as

$$Y^n = C_j + \sum_{i=1}^{M_x} a_{ij} \cdot X_i + \sum_{i=1}^{M_s} a_{ij} \cdot Z_i - T_j \qquad j = 1, 2, \ldots, Na \qquad 5.27$$

C_j is chosen as the parameter, x^n. Hence, the partial derivative of equation 5.27 with respect to the parameter, C_j, and with the substitution of X_i and Z_i, is as follows:

$$\frac{\delta Y^n}{\delta C_j} = \frac{\delta}{\delta C_j} \cdot \left[C_j + \sum_{i=1}^{M_x} a_{ij} \cdot \left[K_i \cdot \prod_{j=1}^{N_a} (C_j)^{a_{ij}} \right] + \sum_{i=1}^{M_s} a_{ij} \cdot \left[K_{ij} \cdot \left[\frac{(a_i)^{v_j}}{(a_j)^{v_i}} \right] \cdot (z_j)^{v_i} \cdot (s_T)^{v_j - v_i} \right]^{\frac{1}{v_j}} - T_j \right] \qquad 5.28$$

$$j = 1, 2, \ldots, Na$$

Following through the derivation, equation 5.28 becomes

Reproduced with permission of the copyright owner. Further reproduction prohibited without permission.

$$\frac{\delta Y^n}{\delta C_j} = 1 + \sum_{i=1}^{Mx} a_{ij} \cdot \left[a_{ik} \cdot (C_k)^{a_{ik}-1} \cdot K_i \cdot \prod_{j=1}^{Na} (C_j)^{a_{ij}}, j \neq k \right] + \sum_{i=1}^{M_s} a_{ij} \cdot \left[(K_{ij})^{\frac{1}{v_j}} \cdot C_i \cdot (C_j)^{-\frac{v_i}{v_j}} \cdot (Z_j)^{\frac{v_i}{v_j}} \cdot (S_T)^{\frac{v_j - v_i}{v_j}} \right] \quad 5.29$$

$$j = 1, 2, \ldots, Na \qquad k = 1, 2, \ldots, Na$$

The resulting partial derivative of the function, Y^n, is

$$\frac{\delta Y^n}{\delta C_j} = 1 + \sum_{i=1}^{M_x} a_{ij} \cdot a_{ik} \cdot \frac{X_i}{C_k} + \sum_{i=1}^{M_s} a_{ij} \cdot \left(-\frac{v_i}{v_j} \cdot \frac{Z_i}{C_j} \right) \qquad j = k = 1, 2, \ldots, Na \quad 5.30$$

To determine the solution of equation 5.26, Afifi (1994) describes a four step process: (1) knowing the initial parameter, x^n (or C_j), compute the residual using equation 5.27, (2) compute the Jacobian, Z^n, (3) solve equation 5.26 for the vector, $\{\Delta x\}$, and (4) obtain the new iterate by equation 5.31. These four steps are repeated until the solution converges (Afifi, 1994).

$$x^{n+1} = x^n - \Delta x \quad 5.31$$

Transport Modeling:

Once the component concentrations are determined from the chemical reaction model for each finite difference cell, each component's migration is simulated using the following finite difference equation for multispecies modeling:

$$\frac{\delta}{\delta x} \cdot \left(D_{xx} \cdot \frac{\delta C}{\delta x} \right) + \frac{\delta}{\delta x} \cdot \left(D_{xy} \cdot \frac{\delta C}{\delta y} \right) + \frac{\delta}{\delta x} \cdot \left(D_{xz} \cdot \frac{\delta C}{\delta z} \right) + \frac{\delta}{\delta y} \cdot \left(D_{yy} \cdot \frac{\delta C}{\delta y} \right) + \frac{\delta}{\delta y} \cdot \left(D_{yx} \cdot \frac{\delta C}{\delta x} \right) +$$

$$\frac{\delta}{\delta y} \cdot \left(D_{yz} \cdot \frac{\delta C}{\delta z} \right) + \frac{\delta}{\delta z} \cdot \left(D_{zz} \cdot \frac{\delta C}{\delta z} \right) + \frac{\delta}{\delta z} \cdot \left(D_{zx} \cdot \frac{\delta C}{\delta x} \right) + \frac{\delta}{\delta z} \cdot \left(D_{zy} \cdot \frac{\delta C}{\delta y} \right) -$$

5.32

Reproduced with permission of the copyright owner. Further reproduction prohibited without permission.

$$\frac{\delta(v_x \cdot C)}{\delta x} - \frac{\delta(v_y \cdot C)}{\delta y} - \frac{\delta(v_z \cdot C)}{\delta z} = \frac{\delta C}{\delta t} + \frac{W}{\phi} \cdot C + \frac{\delta C_s}{\delta t} + \lambda\left(C + C_s\right)$$

where: W is the volumetric flux of sources (+) and sinks (-) per unit volume of aquifer (T^{-1});
ϕ is the aquifer porosity;
C_s is the cation exchange concentration(MM^{-1});
λ is the first-order irreversible reaction rate constant.

If only one species is being modeled within the system (not multispecies), then the following variant of equation 5.32 is used:

$$\frac{\delta}{\delta x} \cdot \left(D_{xx} \cdot \frac{\delta C}{\delta x}\right) + \frac{\delta}{\delta x} \cdot \left(D_{xy} \cdot \frac{\delta C}{\delta y}\right) + \frac{\delta}{\delta x} \cdot \left(D_{xz} \cdot \frac{\delta C}{\delta z}\right) + \frac{\delta}{\delta y} \cdot \left(D_{yy} \cdot \frac{\delta C}{\delta y}\right) + \frac{\delta}{\delta y} \cdot \left(D_{yx} \cdot \frac{\delta C}{\delta x}\right) +$$

$$\frac{\delta}{\delta y} \cdot \left(D_{yz} \cdot \frac{\delta C}{\delta z}\right) + \frac{\delta}{\delta z} \cdot \left(D_{zz} \cdot \frac{\delta C}{\delta z}\right) + \frac{\delta}{\delta z} \cdot \left(D_{zx} \cdot \frac{\delta C}{\delta x}\right) + \frac{\delta}{\delta z} \cdot \left(D_{zy} \cdot \frac{\delta C}{\delta y}\right) -$$

$$\frac{\delta(v_x \cdot C)}{\delta x} - \frac{\delta(v_y \cdot C)}{\delta y} - \frac{\delta(v_z \cdot C)}{\delta z} = R \cdot \frac{\delta C}{\delta t} + \frac{W}{\phi} \cdot C + \lambda\left(C + \frac{\rho_b}{\phi} \cdot C_s\right) \qquad 5.33$$

In equation 5.33, the cation exchange term is removed and replaced with a retardation factor, R, that describes species sorption where

$$R = 1 + \frac{\rho_b}{\phi} \cdot \frac{\delta C_s}{\delta C} \qquad 5.34$$

where: ρ_b is the media bulk density.

The $\delta C_s/\delta C$ can be modeled using either the linear, Freundlich, or Langmuir isotherm as indicated respectively in equations 5.35 to 5.37.

$$C_s = K_d \cdot C \qquad 5.35$$

$$C_s = K_f \cdot C^a \qquad 5.36$$

Reproduced with permission of the copyright owner. Further reproduction prohibited without permission.

$$C_s = \frac{K_l \cdot C_s \cdot C}{1 + K_l \cdot C} \qquad 5.37$$

Accordingly, the expression of the retardation factor changes upon the choice of either the linear, Freundlich, or Langmuir isotherm as indicated by equations 5.38 to 5.40, respectively.

$$R = 1 + \frac{\rho_b}{\phi} \cdot K_d \qquad 5.35$$

Where: K_d is the distribution coefficient.

$$R = 1 + \frac{\rho_b}{\phi} \cdot a \cdot K_f \cdot C^{a-1} \qquad 5.36$$

Where: K_f is the Freundlich constant
a is the Freundlich exponent.

$$R = 1 + \frac{\rho_b}{\phi} \cdot \left[\frac{K_l \cdot b}{(1 + K_l \cdot C)^2} \right] \qquad 5.37$$

Where: K_l is the Langmuir constant
b is the maximum limit of sorbed solute on media.

The retardation factor is only used in single species transport. Since multispecies transport is the main thrust of this study, the topic of retardation factors is disregarded until Chapter 6.

The volumetric flux term, W, represents sink/sources such as constant heads, wells, rivers, and streams, exclusive sources like recharge and general head boundary conditions, and exclusive sinks such as evapotranspiration and drains. Sinks to the system are added to the left-hand side of equation 5.32 as their value depends on the changing concentration within those cells the sinks reside. Sources are considered to remain constant during a stress period; therefore, source terms are added as constants to

Reproduced with permission of the copyright owner. Further reproduction prohibited without permission.

the right-hand side. Of a special note, typically contaminants remain in the ground water system during evapotranspiration. However, an amount of contaminant can be released from ground water if a plant root system invades a shallow flow system (such as cattails drawing up heavy metals). Therefore, if a known amount of contaminant is removed via evapotranspiration, then this amount is subtracted from the right-hand side.

The radioactive decay or possible biodegradation term in equation 5.32 is expressed by the dissolved and sorbed concentrations multiplied by the rate constant, λ. The rate constant is customarily stated in terms of the half-life of radioactive or biodegradable materials (see equation 5.41).

$$\lambda = \frac{\ln(2)}{\sqrt{t}} \qquad 5.41$$

where: λ: rate constant (T^{-1})
t: half-life of radioactive contaminant (T)

If a contaminant has a half-life of 40 days, then the concentration of that contaminant will be reduced by half in 40 days of simulation. Similar to MT3D (Zheng, 1996), two rate constants can be specified in cases where sorbed concentrations reduce at a different rate other than dissolved phase contaminants such as the case with some biodegradation problems.

The decay or biodegradation term depends on the concentration of the cells that are unknown at the beginning of the time step. Therefore, this term is added to the unknowns on the left-hand side. The exception to this method is for cation exchange reactions involving multiple species. The exchange species is held constant during a time

Reproduced with permission of the copyright owner. Further reproduction prohibited without permission.

step that results in the decay or degradation of the exchange species to be added to the RHS.

There is further discussion on the specification of sink/source and rate constant terms in Chapter 6. Next, it is necessary to expand the partial differential equation into an ordinary differential equation.

Equation 5.32 is expanded using centered in space (central difference) for the second order derivatives, backward in space (upwinding) for the advection terms, and implicit in time. For the space derivatives represented as centered in space, there is no numerical dispersion. Numerical dispersion does occur with upwinding of the quantity ($0.5v\Delta x$). The numerical dispersion is positive for implicit in time, and is of the quantity ($0.5v^2\Delta t$).

Numerical dispersion for implicit in time and upwinding enters the equation through the exclusion of the second order terms within the Taylor series expansion (see equation 3.8). This numerical dispersion ultimately resembles an added dispersion value; hence, the name numerical dispersion. One accounts for numerical dispersion by simply subtracting the calculated numerical dispersion from the actual dispersion value (see Equation 5.38); hence, maintaining second order accuracy. The derivation of numerical dispersion for both the time and advection terms is shown in Appendix A. The actual dispersion terms for each direction are calculated from equations 5.39 to 5.44.

$$D = D_{actual} - \frac{v^2 \cdot \Delta t}{2} \qquad 5.38$$

Reproduced with permission of the copyright owner. Further reproduction prohibited without permission.

$$D_{xx} = \alpha_L \cdot \frac{(v_x)^2}{|v|} + \alpha_{TH} \cdot \frac{(v_y)^2}{|v|} + \alpha_{TV} \cdot \frac{(v_z)^2}{|v|} + D_{diff} \quad 5.39$$

$$D_{yy} = \alpha_L \cdot \frac{(v_y)^2}{|v|} + \alpha_{TH} \cdot \frac{(v_x)^2}{|v|} + \alpha_{TV} \cdot \frac{(v_z)^2}{|v|} + D_{diff} \quad 5.40$$

$$D_{zz} = \alpha_L \cdot \frac{(v_z)^2}{|v|} + \alpha_{TV} \cdot \frac{(v_x)^2}{|v|} + \alpha_{TV} \cdot \frac{(v_y)^2}{|v|} + D_{diff} \quad 5.41$$

$$D_{xy} = D_{yx} = (\alpha_L - \alpha_{TH}) \cdot \frac{v_x \cdot v_y}{|v|} \quad 5.42$$

$$D_{xz} = D_{zx} = (\alpha_L - \alpha_{TV}) \cdot \frac{v_x \cdot v_z}{|v|} \quad 5.43$$

$$D_{yz} = D_{zy} = (\alpha_L - \alpha_{TV}) \cdot \frac{v_y \cdot v_z}{|v|} \quad 5.44$$

To expand the first derivative terms associated with the advection terms, upwinding is used. Upwinding is derived from the backward Taylor series, resulting in equation 5.45 for variable sized cells.

$$\frac{\delta C}{\delta x} = \frac{C_{i+1} - C_{i-1}}{.5 \cdot \Delta x_{i+1} + \Delta x_i + .5 \cdot \Delta x_{i-1}} \quad 5.45$$

The second order derivatives can be represented by the second central difference equation (see Equation 5.46). Equation 5.46 is derived by adding the forward and backward Taylor series. The squared distance term represents a change in distance across variable sized cells.

$$\frac{\delta C}{\delta x} = \frac{C_{i+1} - 2 \cdot C_i + C_{i-1}}{\left(\frac{\Delta x}{2}\right)^2} \quad 5.46$$

Reproduced with permission of the copyright owner. Further reproduction prohibited without permission.

Another method of solving the second order derivatives is to take the first central difference twice, but over half a step (.5Δx) rather than a full Δx. This alternative method for representing the second order derivatives is used in this study.

With the knowledge of how the derivative terms are represented, the choice of a grid stencil is made. A grid stencil defines how many cells contribute to the calculation of the space derivatives. Referring to Figure 5.2a, a five point stencil includes the center cell (the cell in question) and the top, bottom and side cells. The diagonal cells, shaded gray, are do not contribute to the calculation. A nine point stencil (see Figure 5.2b) includes the cells represented by the five point stencil as well as the diagonal grid cells. Although the nine point stencil requires more calculations than the five point stencil, it is more accurate. For this study, the nine point stencil is utilized.

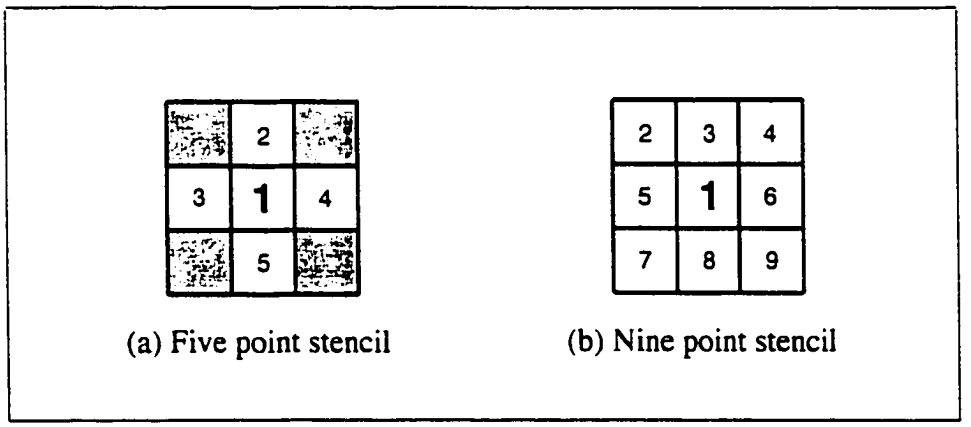

Figure 5.2. Depiction of a five and nine point stencil.

Equation 5.32 is expanded using the implicit method for the time derivatives, upwinding for the first order derivative terms, and the first central difference performed twice over half a step for the second order derivative. Dispersion is calculated at the cell

Reproduced with permission of the copyright owner. Further reproduction prohibited without permission.

face for each direction. Therefore, by reference to equations 5.38 to 5.44, the component velocities must be known at each of the cell faces.

MODFLOW outputs the x-, y-, and z-directional volumetric flux exiting the right, front, and bottom face, respectively, for each cell. Therefore, there are potentially three volumetric flux values for each cell in the finite difference grid. These volumetric fluxes are calculated using Darcy's equation. Hence, the volumetric flux equals the change in head between adjacent cell centers multiplied by the harmonic average of the hydraulic conductivity times the saturated area of the cell face.

Referring to Figure 5.3, the seepage velocity is determined by dividing the volumetric flux by the saturated area of the cell face and the porosity of the system. The notation for dispersion in the x-direction at the right hand face of cell (j,i,k) is $D_{xx\,j,i+\frac{1}{2},k}$. Using equation 5.39,

$$D_{xx_{j,i+\frac{1}{2},k}} = \alpha_L \cdot \frac{\left(\upsilon_{x_{j,i+\frac{1}{2},k}}\right)^2}{\left|\upsilon_{j,i+\frac{1}{2},k}\right|} + \alpha_{TH} \cdot \frac{\left(\upsilon_{y_{j,i+\frac{1}{2},k}}\right)^2}{\left|\upsilon_{j,i+\frac{1}{2},k}\right|} + \alpha_{TV} \cdot \frac{\left(\upsilon_{z_{j,i+\frac{1}{2},k}}\right)^2}{\left|\upsilon_{j,i+\frac{1}{2},k}\right|} \qquad 5.47$$

Again referring to Figure 5.3, $\upsilon_{x\,j,i+\frac{1}{2},k}$ is easily calculated. However, $\upsilon_{y\,j,i+\frac{1}{2},k}$ and $\upsilon_{z\,j,i+\frac{1}{2},k}$ must be determined. Piecewise linear interpolation is used between the velocity points 1, 2, 3, and 4 in Figures 5.4 and 5.5 to determine υ_y and υ_z at the cell interface (j, i+½,k), respectively. This method assumes that the velocity component in a specific direction is linear across a finite difference cell. This procedure is repeated for each cell face.

Reproduced with permission of the copyright owner. Further reproduction prohibited without permission.

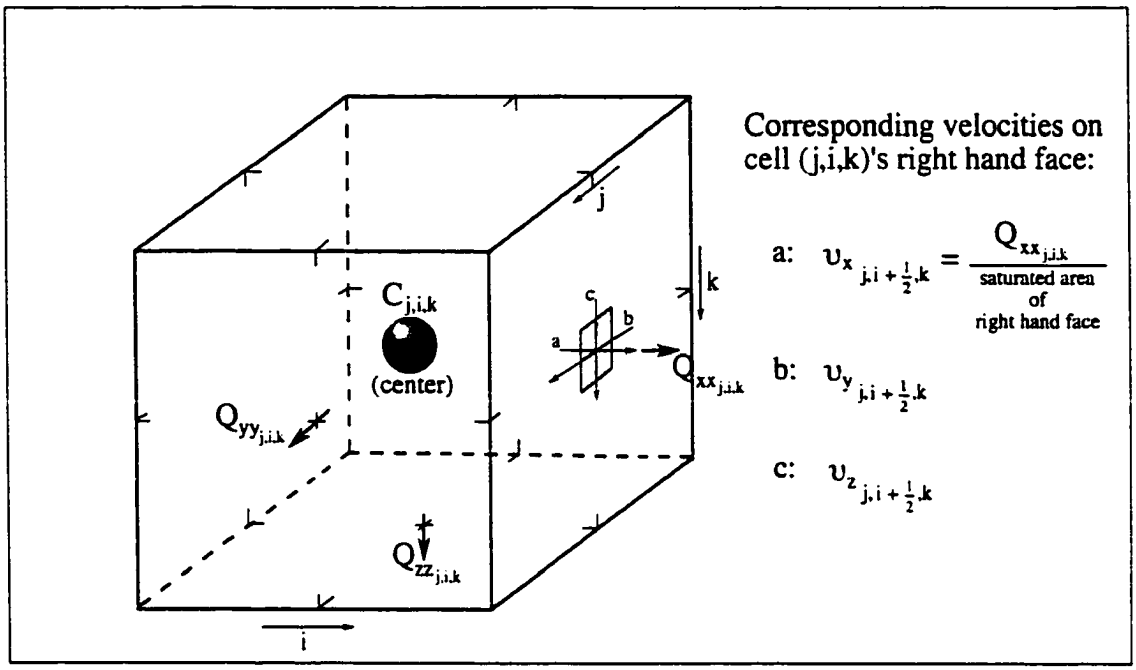

Figure 5.3. Depiction of component velocities in x-, y-, and z-directions at the right hand face of cell (j,i,k).

Reproduced with permission of the copyright owner. Further reproduction prohibited without permission.

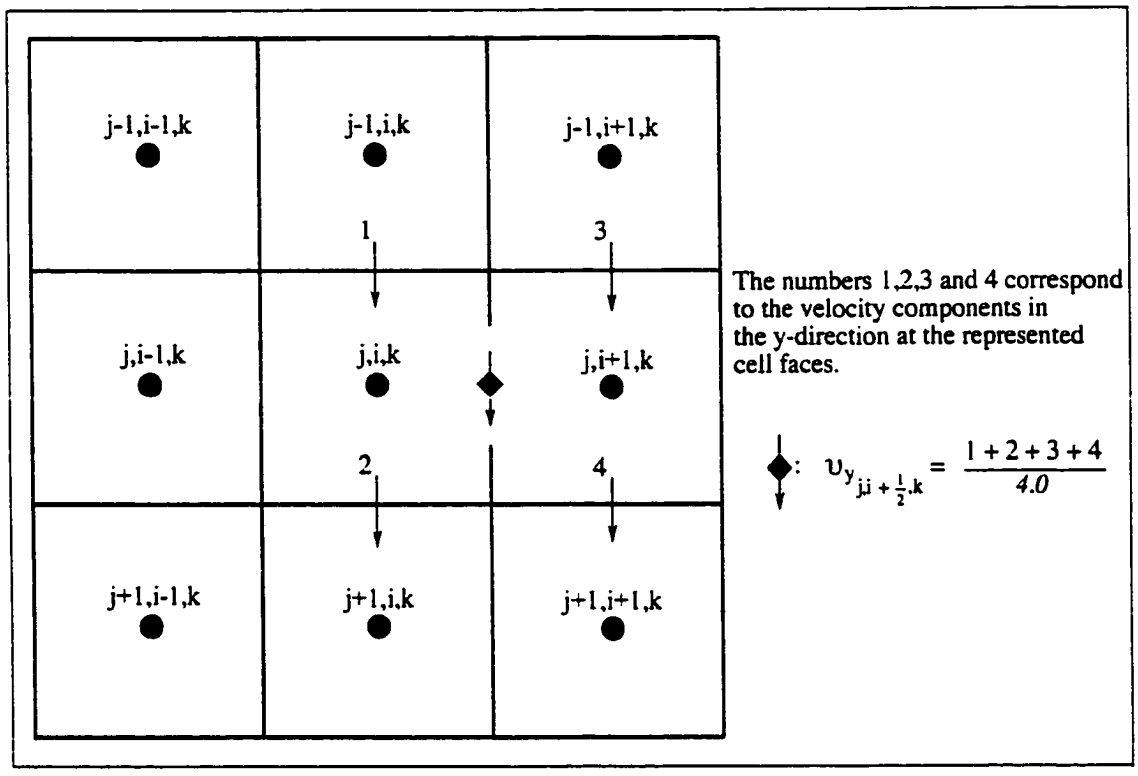

Figure 5.4. Representation of calculation of the v_y component velocity at the right hand face of cell (j,i,k).

Reproduced with permission of the copyright owner. Further reproduction prohibited without permission.

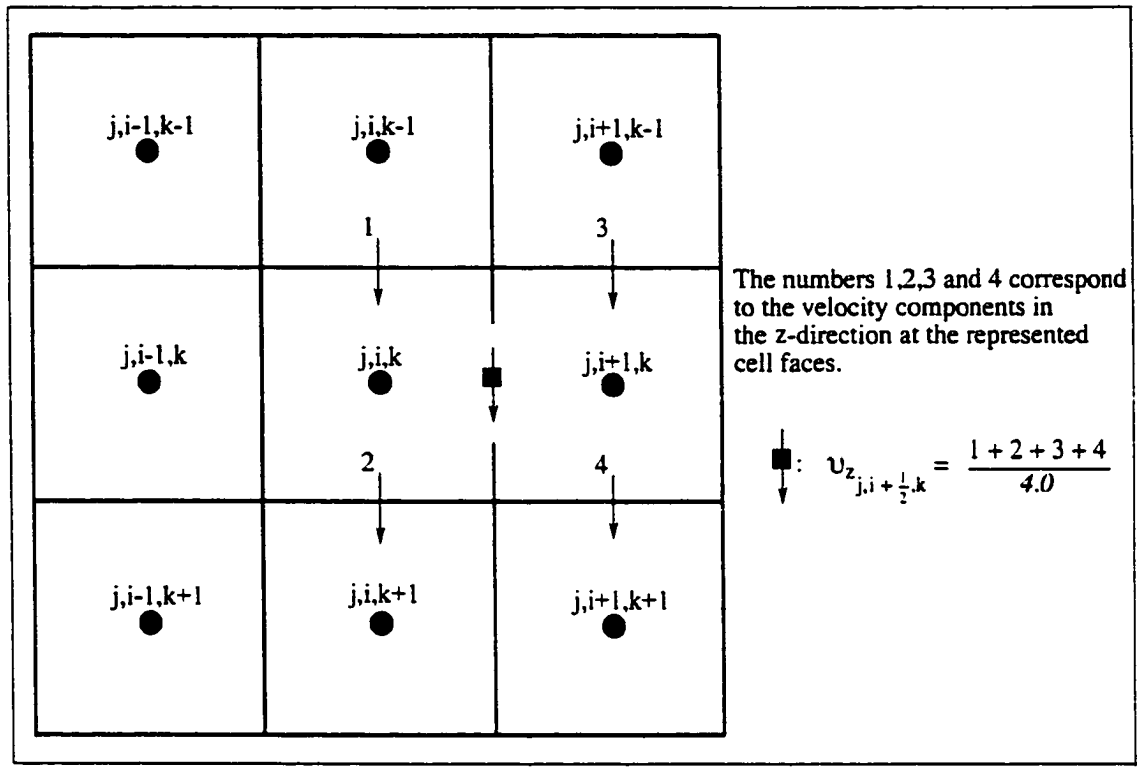

Figure 5.5. Representation of calculation of the υ_z component velocity at the right hand face of cell (j,i,k).

Calculation of the dispersion values for the cell faces of each finite difference grid cell is only a small part of solving equation 5.32. Equation 5.32 must be expanded using finite difference notation. Equation 5.48 is the finite difference interpolation of equation 5.32. The expansion of the second order derivative terms indicates the dispersion and concentration values at the cell faces. The expansion of the advection terms indicates the velocities and concentrations at the cell centers. The "t" superscript denotes previous time step information while the "t+Δt" superscript refers to new time step information. The concentration within source terms is held constant during a stress period in which time steps occur. Cation exchange concentrations are assumed constant during a time step with sequential iteration between the algebraic chemical reaction

Reproduced with permission of the copyright owner. Further reproduction prohibited without permission.

equations for chemical equilibrium. Lastly, the radioactive decay term, λ, is separated into decay of the aqueous concentration and cation exchange concentration.

$$\left[D_{xx}{}_{j,i+\frac{1}{2},k} \cdot \left[\frac{C_{j,i+\frac{1}{2},k}}{\overline{\Delta x}} \right] - D_{xx}{}_{j,i-\frac{1}{2},k} \cdot \left[\frac{C_{j,i-\frac{1}{2},k}}{\overline{\Delta x}} \right] \right]^{t} \cdot \frac{1}{\Delta x_{j,i,k}}$$

$$+ \left[D_{xy}{}_{j,i+\frac{1}{2},k} \cdot \left[\frac{C_{j,i+\frac{1}{2},k}}{\overline{\Delta y}} \right] - D_{xy}{}_{j,i-\frac{1}{2},k} \cdot \left[\frac{C_{j,i-\frac{1}{2},k}}{\overline{\Delta y}} \right] \right]^{t} \cdot \frac{1}{\Delta x_{j,i,k}}$$

$$+ \left[D_{xz}{}_{j,i+\frac{1}{2},k} \cdot \left[\frac{C_{j,i+\frac{1}{2},k}}{\overline{\Delta z}} \right] - D_{xz}{}_{j,i-\frac{1}{2},k} \cdot \left[\frac{C_{j,i-\frac{1}{2},k}}{\overline{\Delta z}} \right] \right]^{t} \cdot \frac{1}{\Delta x_{j,i,k}}$$

$$+ \left[D_{yy}{}_{j+\frac{1}{2},i,k} \cdot \left[\frac{C_{j+\frac{1}{2},i,k}}{\overline{\Delta y}} \right] - D_{yy}{}_{j-\frac{1}{2},i,k} \cdot \left[\frac{C_{j-\frac{1}{2},i,k}}{\overline{\Delta y}} \right] \right]^{t} \cdot \frac{1}{\Delta y_{j,i,k}}$$

$$+ \left[D_{yx}{}_{j+\frac{1}{2},i,k} \cdot \left[\frac{C_{j+\frac{1}{2},i,k}}{\overline{\Delta x}} \right] - D_{yx}{}_{j-\frac{1}{2},i,k} \cdot \left[\frac{C_{j-\frac{1}{2},i,k}}{\overline{\Delta x}} \right] \right]^{t} \cdot \frac{1}{\Delta y_{j,i,k}}$$

$$+ \left[D_{yz}{}_{j+\frac{1}{2},i,k} \cdot \left[\frac{C_{j+\frac{1}{2},i,k}}{\overline{\Delta z}} \right] - D_{yz}{}_{j-\frac{1}{2},i,k} \cdot \left[\frac{C_{j-\frac{1}{2},i,k}}{\overline{\Delta z}} \right] \right]^{t} \cdot \frac{1}{\Delta y_{j,i,k}}$$

$$+ \left[D_{zz}{}_{j,i,k+\frac{1}{2}} \cdot \left[\frac{C_{j,i,k+\frac{1}{2}}}{\overline{\Delta z}} \right] - D_{zz}{}_{j,i,k-\frac{1}{2}} \cdot \left[\frac{C_{j,i,k-\frac{1}{2}}}{\overline{\Delta z}} \right] \right]^{t} \cdot \frac{1}{\Delta z_{j,i,k}}$$

$$+ \left[D_{zx}{}_{j,i,k+\frac{1}{2}} \cdot \left[\frac{C_{j,i,k+\frac{1}{2}}}{\overline{\Delta x}} \right] - D_{zx}{}_{j,i,k-\frac{1}{2}} \cdot \left[\frac{C_{j,i,k-\frac{1}{2}}}{\overline{\Delta x}} \right] \right]^{t} \cdot \frac{1}{\Delta z_{j,i,k}}$$

$$+ \left[D_{zy}{}_{j,i,k+\frac{1}{2}} \cdot \left[\frac{C_{j,i,k+\frac{1}{2}}}{\overline{\Delta y}} \right] - D_{zy}{}_{j,i,k-\frac{1}{2}} \cdot \left[\frac{C_{j,i,k-\frac{1}{2}}}{\overline{\Delta y}} \right] \right]^{t} \cdot \frac{1}{\Delta z_{j,i,k}}$$

$$- \left[\frac{C_{j,i,k} \cdot (v_x)_{j,i,k} - C_{j,i-1,k} \cdot (v_x)_{j,i-1,k}}{.5 \cdot \Delta x_{j,i,k} + .5 \cdot \Delta x_{j,i-1,k}} \right]^{t}$$

Reproduced with permission of the copyright owner. Further reproduction prohibited without permission.

$$
\begin{aligned}
&- \left[\frac{C_{j,i,k}\cdot\left(v_y\right)_{j,i,k} - C_{j-1,i,k}\cdot\left(v_y\right)_{j-1,i,k}}{.5\cdot\Delta y_{j,i,k} + .5\cdot\Delta y_{j-1,i,k}}\right]^t \\
&- \left[\frac{C_{j,i,k}\cdot\left(v_z\right)_{j,i,k} - C_{j,i,k-1}\cdot\left(v_z\right)_{j,i,k-1}}{.5\cdot\Delta z_{j,i,k} + .5\cdot\Delta z_{j,i,k-1}}\right]^t \\
= \frac{\left(C_{j,i,k}\right)^{t+\Delta t} - \left(C_{j,i,k}\right)^t}{\Delta t} &+ \frac{W}{\phi}\cdot\left(C_{j,i,k}\right)^t + \left[\left(C_s\right)_{j,i,k}\right]^t + \lambda\cdot\left[C_{j,i,k} + \frac{\rho_b}{\phi}\cdot\left(C_s\right)_{j,i,k}\right]^t \qquad 5.48
\end{aligned}
$$

Equation 5.48 is expanded further to reveal the cells contributing to the calculation of $C_{j,i,k}$ (C) in equation 5.32. The resulting equation is as follows:

$$
\begin{aligned}
&\left[D_{xx}{}_{j,i+\frac{1}{2},k}\cdot\left(\frac{C_{j,i+1,k} - C_{j,i,k}}{.5\cdot\Delta x_{j,i+1,k} + .5\cdot\Delta x_{j,i,k}}\right) - D_{xx}{}_{j,i-\frac{1}{2},k}\cdot\left(\frac{C_{j,i,k} - C_{j,i-1,k}}{.5\cdot\Delta x_{j,i,k} + .5\cdot\Delta x_{j,i-1,k}}\right)\right]^t\cdot\frac{1}{\Delta x_{j,i,k}} \\
&+ \left(D_{xy}{}_{j,i+\frac{1}{2},k}\right)\cdot\left[\frac{\left(\frac{C_{j+1,i+1,k} - C_{j-1,i+1,k}}{.5\cdot\Delta y_{j+1,j+1,k} + \Delta y_{j,i+1,k} + .5\cdot\Delta y_{j-1,i+1,k}}\right) + \left(\frac{C_{j+1,i,k} - C_{j-1,i,k}}{.5\cdot\Delta y_{j+1,i,k} + \Delta y_{j,i,k} + .5\cdot\Delta y_{j-1,i,k}}\right)}{2}\right]^t\cdot\frac{1}{\Delta x_{j,i,k}} \\
&- \left(D_{xy}{}_{j,i-\frac{1}{2},k}\right)\cdot\left[\frac{\left(\frac{C_{j+1,i,k} - C_{j-1,i,k}}{.5\cdot\Delta y_{j+1,i,k} + \Delta y_{j,i,k} + .5\cdot\Delta y_{j-1,i,k}}\right) + \left(\frac{C_{j+1,i-1,k} - C_{j-1,i-1,k}}{.5\cdot\Delta y_{j+1,i-1,k} + \Delta y_{j,i-1,k} + .5\cdot\Delta y_{j-1,i-1,k}}\right)}{2}\right]^t\cdot\frac{1}{\Delta x_{j,i,k}} \\
&+ \left(D_{xz}{}_{j,i+\frac{1}{2},k}\right)\cdot\left[\frac{\left(\frac{C_{j,i+1,k+1} - C_{j,i+1,k-1}}{.5\cdot\Delta z_{j,i+1,k+1} + \Delta z_{j,i+1,k} + .5\cdot\Delta z_{j,i+1,k-1}}\right) + \left(\frac{C_{j,i,k+1} - C_{j,i,k-1}}{.5\cdot\Delta z_{j,i,k+1} + \Delta z_{j,i,k} + .5\cdot\Delta z_{j,i,k-1}}\right)}{2}\right]^t\cdot\frac{1}{\Delta x_{j,i,k}} \\
&- \left(D_{xz}{}_{j,i-\frac{1}{2},k}\right)\cdot\left[\frac{\left(\frac{C_{j,i,k+1} - C_{j,i,k-1}}{.5\cdot\Delta z_{j,i,k+1} + \Delta z_{j,i,k} + .5\cdot\Delta z_{j,i,k-1}}\right) + \left(\frac{C_{j,i-1,k+1} - C_{j,i-1,k-1}}{.5\cdot\Delta z_{j,i-1,k+1} + \Delta z_{j,i-1,k} + .5\cdot\Delta z_{j,i-1,k-1}}\right)}{2}\right]^t\cdot\frac{1}{\Delta x_{j,i,k}} \\
&+ \left[D_{yy}{}_{j+\frac{1}{2},i,k}\cdot\left(\frac{C_{j+1,i,k} - C_{j,i,k}}{.5\cdot\Delta y_{j+1,i,k} + .5\cdot\Delta y_{j,i,k}}\right) - D_{yy}{}_{j-\frac{1}{2},i,k}\cdot\left(\frac{C_{j,i,k} - C_{j-1,i,k}}{.5\cdot\Delta y_{j,i,k} + .5\cdot\Delta y_{j-1,i,k}}\right)\right]^t\cdot\frac{1}{\Delta y_{j,i,k}}
\end{aligned}
$$

Reproduced with permission of the copyright owner. Further reproduction prohibited without permission.

$$+\left(D_{yx}{}_{j+\frac{1}{2},i,k}\right)\cdot\left[\frac{\left(\frac{C_{j+1,i+1,k}-C_{j+1,i-1,k}}{.5\cdot\Delta x_{j+1,i+1,k}+\Delta x_{j+1,i,k}+.5\cdot\Delta x_{j+1,i-1,k}}\right)+\left(\frac{C_{j,i+1,k}-C_{j,i-1,k}}{.5\cdot\Delta x_{j,i+1,k}+\Delta x_{j,i,k}+.5\cdot\Delta x_{j,i-1,k}}\right)}{2}\right]^{t}\cdot\frac{1}{\Delta y_{j,i,k}}$$

$$-\left(D_{yx}{}_{j-\frac{1}{2},i,k}\right)\cdot\left[\frac{\left(\frac{C_{j,i+1,k}-C_{j,i-1,k}}{.5\cdot\Delta x_{j,i+1,k}+\Delta x_{j,i,k}+.5\cdot\Delta x_{j,i-1,k}}\right)+\left(\frac{C_{j-1,i+1,k}-C_{j-1,i-1,k}}{.5\cdot\Delta x_{j-1,i+1,k}+\Delta x_{j-1,i,k}+.5\cdot\Delta x_{j-1,i-1,k}}\right)}{2}\right]^{t}\cdot\frac{1}{\Delta y_{j,i,k}}$$

$$+\left(D_{yz}{}_{j+\frac{1}{2},i,k}\right)\cdot\left[\frac{\left(\frac{C_{j+1,i,k+1}-C_{j+1,i,k-1}}{.5\cdot\Delta z_{j+1,i,k+1}+\Delta z_{j+1,i,k}+.5\cdot\Delta z_{j+1,i,k-1}}\right)+\left(\frac{C_{j,i,k+1}-C_{j,i,k-1}}{.5\cdot\Delta z_{j,i,k+1}+\Delta z_{j,i,k}+.5\cdot\Delta z_{j,i,k-1}}\right)}{2}\right]^{t}\cdot\frac{1}{\Delta y_{j,i,k}}$$

$$-\left(D_{yz}{}_{j-\frac{1}{2},i,k}\right)\cdot\left[\frac{\left(\frac{C_{j,i,k+1}-C_{j,i,k-1}}{.5\cdot\Delta z_{j,i,k+1}+\Delta z_{j,i,k}+.5\cdot\Delta z_{j,i,k-1}}\right)+\left(\frac{C_{j-1,i,k+1}-C_{j-1,i,k-1}}{.5\cdot\Delta z_{j-1,i,k+1}+\Delta z_{j-1,i,k}+.5\cdot\Delta z_{j-1,i,k-1}}\right)}{2}\right]^{t}\cdot\frac{1}{\Delta y_{j,i,k}}$$

$$\left[D_{zz}{}_{j,i,k+\frac{1}{2}}\cdot\left(\frac{C_{j,i,k+1}-C_{j,i,k}}{.5\cdot\Delta z_{j,i,k+1}+.5\cdot\Delta z_{j,i,k}}\right)-D_{zz}{}_{j,i,k-\frac{1}{2}}\cdot\left(\frac{C_{j,i,k}-C_{j,i,k-1}}{.5\cdot\Delta z_{j,i,k}+.5\cdot\Delta z_{j,i,k-1}}\right)\right]^{t}\cdot\frac{1}{\Delta z_{j,i,k}}$$

$$+\left(D_{zx}{}_{j,i,k+\frac{1}{2}}\right)\cdot\left[\frac{\left(\frac{C_{j,i+1,k+1}-C_{j,i-1,k+1}}{.5\cdot\Delta x_{j,i+1,k+1}+\Delta x_{j,i,k+1}+.5\cdot\Delta x_{j,i-1,k+1}}\right)+\left(\frac{C_{j,i+1,k}-C_{j,i-1,k}}{.5\cdot\Delta x_{j,i+1,k}+\Delta x_{j,i,k}+.5\cdot\Delta x_{j,i-1,k}}\right)}{2}\right]^{t}\cdot\frac{1}{\Delta z_{j,i,k}}$$

$$-\left(D_{zx}{}_{j,i,k-\frac{1}{2}}\right)\cdot\left[\frac{\left(\frac{C_{j,i+1,k}-C_{j,i-1,k}}{.5\cdot\Delta x_{j,i+1,k}+\Delta x_{j,i,k}+.5\cdot\Delta x_{j,i-1,k}}\right)+\left(\frac{C_{j,i+1,k-1}-C_{j,i-1,k-1}}{.5\cdot\Delta x_{j,i+1,k-1}+\Delta x_{j,i,k-1}+.5\cdot\Delta x_{j,i-1,k-1}}\right)}{2}\right]^{t}\cdot\frac{1}{\Delta z_{j,i,k}}$$

$$+\left(D_{zy}{}_{j,i,k+\frac{1}{2}}\right)\cdot\left[\frac{\left(\frac{C_{j+1,i,k+1}-C_{j-1,i,k+1}}{.5\cdot\Delta y_{j+1,i,k+1}+\Delta y_{j,i,k+1}+.5\cdot\Delta y_{j-1,i,k+1}}\right)+\left(\frac{C_{j+1,i,k}-C_{j-1,i,k}}{.5\cdot\Delta y_{j+1,i,k}+\Delta y_{j,i,k}+.5\cdot\Delta y_{j-1,i,k}}\right)}{2}\right]^{t}\cdot\frac{1}{\Delta z_{j,i,k}}$$

$$-\left(D_{zy}{}_{j,i,k-\frac{1}{2}}\right)\cdot\left[\frac{\left(\frac{C_{j+1,i,k}-C_{j-1,i,k}}{.5\cdot\Delta y_{j+1,i,k}+\Delta y_{j,i,k}+.5\cdot\Delta y_{j-1,i,k}}\right)+\left(\frac{C_{j+1,i,k-1}-C_{j-1,i,k-1}}{.5\cdot\Delta y_{j+1,i,k-1}+\Delta y_{j,i,k-1}+.5\cdot\Delta y_{j-1,i,k-1}}\right)}{2}\right]^{t}\cdot\frac{1}{\Delta z_{j,i,k}}$$

$$-\left[\frac{C_{j,i+1,k}\cdot\left(\frac{q_{x}{}_{j,i+\frac{1}{2},k}+q_{x}{}_{j,i,k}}{2\cdot\theta}\right)-C_{j,i-1,k}\cdot\left(\frac{q_{x}{}_{j,i-\frac{3}{2},k}+q_{x}{}_{j,i-\frac{1}{2},k}}{2\cdot\theta}\right)}{.5\cdot\Delta x_{j,i,k}+.5\cdot\Delta x_{j,i-1,k}}\right]^{t}$$

Reproduced with permission of the copyright owner. Further reproduction prohibited without permission.

$$
- \left[\frac{C_{j+1,i,k} \cdot \left(\frac{q_{y\,j+\frac{1}{2},i,k} + q_{y\,j,i,k}}{2 \cdot \theta} \right) - C_{j-1,i,k} \cdot \left(\frac{q_{y\,j-\frac{3}{2},i,k} + q_{y\,j-\frac{1}{2},i,k}}{2 \cdot \theta} \right)}{.5 \cdot \Delta y_{j,i,k} + .5 \cdot \Delta y_{j-1,i,k}} \right]^t
$$

$$
- \left[\frac{C_{j,i,k+1} \cdot \left(\frac{q_{z\,j,i,k+\frac{1}{2}} + q_{z\,j,i,k}}{2 \cdot \theta} \right) - C_{j,i,k-1} \cdot \left(\frac{q_{z\,j,i,k-\frac{3}{2}} + q_{z\,j,i,k-\frac{1}{2}}}{2 \cdot \theta} \right)}{.5 \cdot \Delta z_{j,i,k} + .5 \cdot \Delta z_{j,i,k-1}} \right]^t
$$

$$
= \frac{(C_{j,i,k})^{t+\Delta t} - (C_{j,i,k})^t}{\Delta t} + \frac{W}{\phi} \cdot (C_{j,i,k})^t + \left[(C_s)_{j,i,k} \right]^t + \lambda \cdot \left[C_{j,i,k} + \frac{\rho_b}{\phi} \cdot (C_s)_{j,i,k} \right]^t \qquad 5.49
$$

As mentioned previously, the second order derivatives are expanded by using the first central difference twice, but at half a step (.5Δx). Half a step distance would require the concentration to be known at the face of cell, $C_{j,i,k}$. Therefore, using the D_{xy} term as an example, the first central difference is first applied to the cells in the i+1 column between j+1 and j-1 (■) (see Figure 5.6). This resulting value is the concentration for cell (j,i+1,k). The same procedure is performed for the cells in column i between j+1 and j-1 (●) resulting in a value for cell (j,i,k). With the concentration value determined for cells (j,i,k) and (j,i+1,k) for contributions due to changes in the y-direction, the arithmetic average of the values results in the dispersion value at the right hand face of cell $C_{j,i,k}$ (▲). The same procedure is performed for the cells $C_{j,i-1,k}$ and $C_{j,i,k}$ to obtain the concentration at the left hand face of cell $C_{j,i,k}$ (◆).

With the concentrations known at the right and left hand faces of cell, $C_{j,i,k}$, the first central difference is performed a second time, but in the x-direction over the distance $\Delta x_{j,i,k}$. The resulting value is the representative concentration of $C_{j,i,k}$ for dispersion in the xy-direction (D_{xy}). This procedure is performed for each second order derivative term in equation 5.32 using the templates in Figure 5.7.

Reproduced with permission of the copyright owner. Further reproduction prohibited without permission.

One should also note the terminology for the velocity expressions. MODFLOW outputs the volumetric fluxes at the cell faces, not at their center. Therefore, using v_x as an example, the seepage velocity at i+1/2 and i-1/2 represents the velocities at the right and left hand cell faces, respectively, of cell (j,i,k) (■) (see Figure 5.8). The average velocity at cell (j,i,k) is the arithmetic average of the two face velocities. The same method is applied to the cell (j,i-1,k) (▲). Hence, upwinding is applied between the average velocity values of cells (j,i,k) (■) and (j,i-1,k) (▲) to obtain the x-directional velocity for cell (j,i,k) (■).

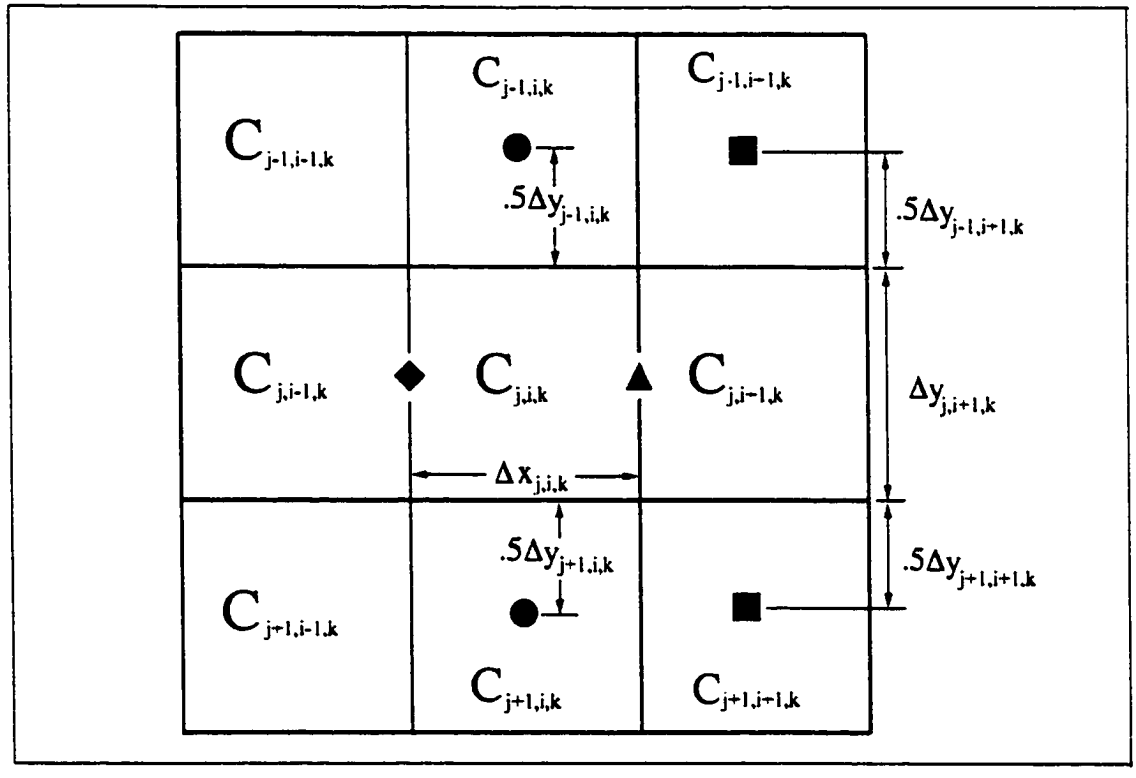

Figure 5.6. Illustration of determining the second order derivative for the D_{xy} term in equation 5.32.

Reproduced with permission of the copyright owner. Further reproduction prohibited without permission.

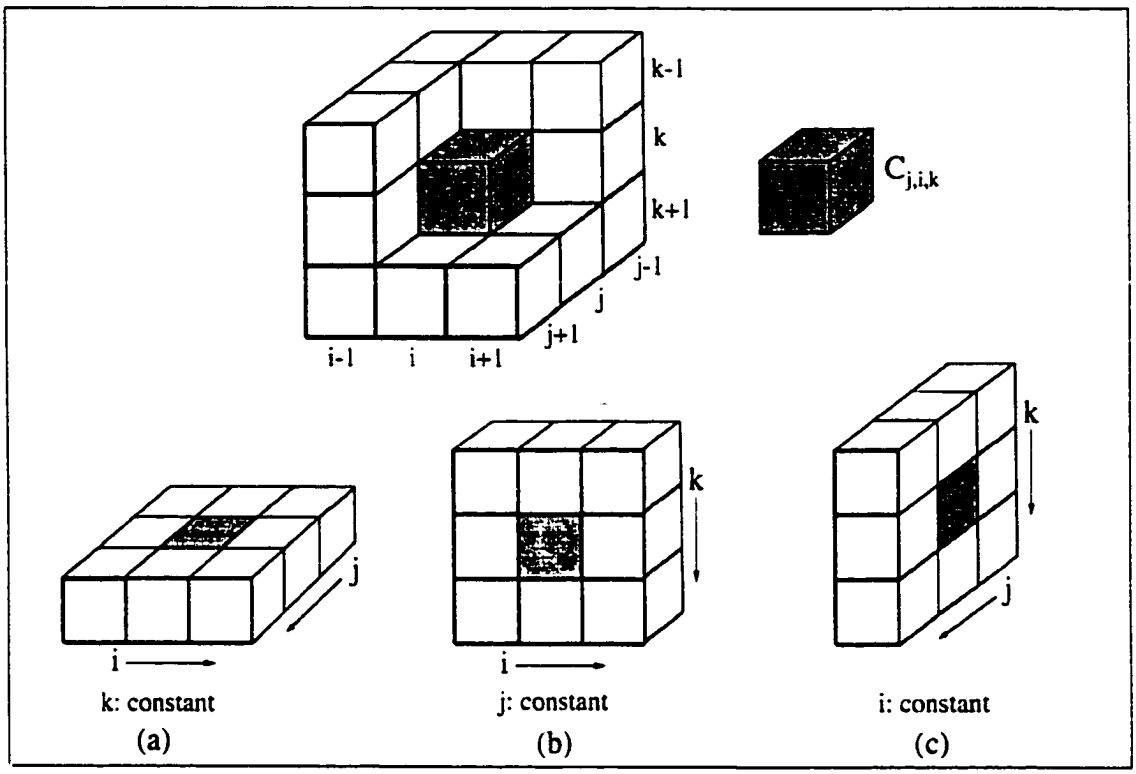

Figure 5.7. Templates utilized for determining the partial derivative terms: (a) D_{xx}, D_{xy}, D_{yy}, D_{yx}, v_x, and v_y; (b) D_{xz}, D_{zx}, D_{zz}, and v_z; (c) D_{yz} and D_{zy}.

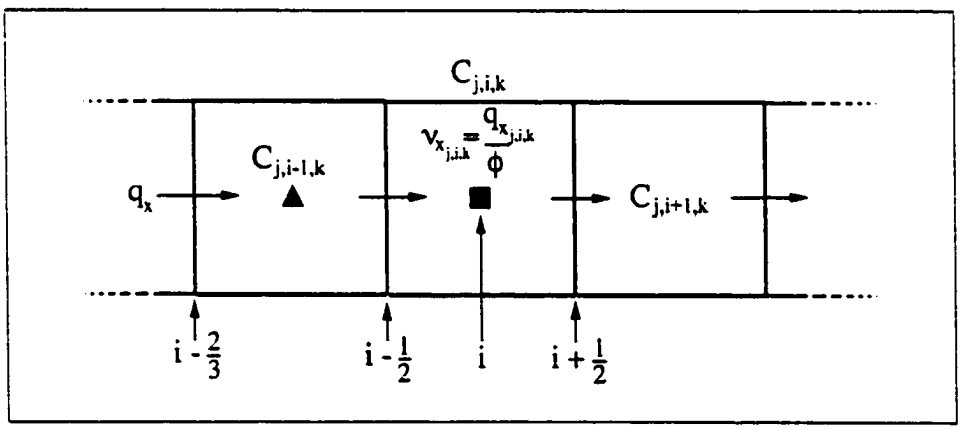

Figure 5.8. Illustration of determining $\delta(Cv_x)/\delta x$.

Reproduced with permission of the copyright owner. Further reproduction prohibited without permission.

The actual number of cells used in the calculations of the first and second order derivatives is 19, not 27. Figure 5.9 depicts the cells used as well as representation of those cells which coincide between templates (▲,●,■,). The eight cells, $C_{j+1,i+1,k+1}$, $C_{j+1,i+1,k-1}$, $C_{j-1,i+1,k+1}$, $C_{j-1,i+1,k-1}$, $C_{j+1,i-1,k+1}$, $C_{j+1,i-1,k-1}$, $C_{j-1,i-1,k+1}$, and $C_{j-1,i-1,k-1}$, are not used in the calculations. Cells solely used within a template are indicated in Figure 5.9 with a "x". This information will be used later to simplify the calculation of the matrix coefficient weights.

Equation 5.49 is written for each cell in the finite domain; these equations defining a system of equations into the A-matrix ([A]). This system of linear equations is solved simultaneously via equation 5.50.

$$[A]\{x\} = \{b\} \qquad 5.50$$

The vector, {b}, contains the known values such as well discharge and cation exchange. The vector, {x}, represents the unknown concentrations for each cell at the new iteration. Therefore, the inverse of [A] must be multiplied with {b} to obtain {x}.

The inverse of [A] is very tedious for large systems of equations. A method for solving equation 5.50 is the preconditioned biconjugate gradient squared method. This method is reviewed later in this chapter, but the development of [A] is discussed here.

Each row of [A] contains the coefficient weights of each cell used in equation 5.49; hence, 19 coefficient weights. Therefore if a row in [A] represents a single cell, then the number of rows in [A] equals the number of columns by the number of rows by the number of layers in the system. The number of columns in [A] equals the number of rows in [A].

Reproduced with permission of the copyright owner. Further reproduction prohibited without permission.

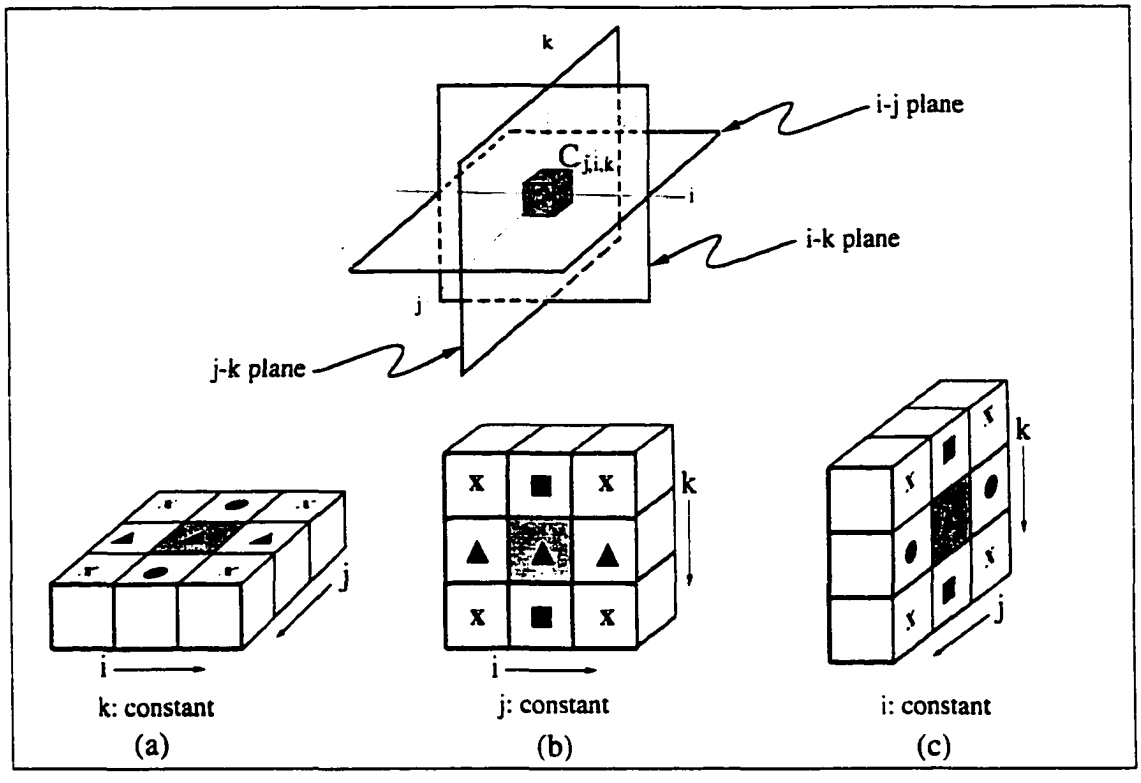

Figure 5.9. Plane view of cells used as well as representation of coinciding cells on templates (a), (b), and (c) as indicated by the symbols ▲,●, and ■.

Recall that the concentrations of the 18 cells surrounding the one cell in question results in the number of coefficient weights. To obtain the coefficient weights, equation 5.49 is expanded further to collect terms for each of the 19 cells. For example, collecting terms for $C_{i+1,j,k}$ is as follows:

$$C_{i+1,j,k}: \left(\frac{D_{xx_{i+1,j,k}} + D_{xx_{i,j,k}}}{2}\right) \cdot \frac{1}{.5\cdot\Delta x_{i+1,j,k} + .5\cdot\Delta x_{i,j,k}} \cdot \frac{1}{\Delta x_{i,j,k}} +$$

$$\left(\frac{D_{yx_{i,j+1,k}} + D_{yx_{i,j,k}}}{2}\right) \cdot \frac{1}{2} \cdot \frac{1}{.5\cdot\Delta x_{i+1,j,k} + \Delta x_{i,j,k} + .5\cdot\Delta x_{i-1,j,k}} \cdot \frac{1}{\Delta y_{i,j,k}} -$$

$$\left(\frac{D_{yx_{i,j,k}} + D_{yx_{i,j-1,k}}}{2}\right) \cdot \frac{1}{2} \cdot \frac{1}{.5\cdot\Delta x_{i+1,j,k} + \Delta x_{i,j,k} + .5\cdot\Delta x_{i-1,j,k}} \cdot \frac{1}{\Delta y_{i,j,k}} +$$

$$\left(\frac{D_{zx_{i,j,k+1}} + D_{zx_{i,j,k}}}{2}\right) \cdot \frac{1}{2} \cdot \frac{1}{.5\cdot\Delta x_{i+1,j,k} + \Delta x_{i,j,k} + .5\cdot\Delta x_{i-1,j,k}} \cdot \frac{1}{\Delta z_{i,j,k}} -$$

Reproduced with permission of the copyright owner. Further reproduction prohibited without permission.

$$\left(\frac{D_{zz_{i,j,k}} + D_{zz_{i,j,k-1}}}{2}\right)\cdot\frac{1}{2}\cdot\frac{1}{.5\cdot\Delta x_{i+1,j,k} + \Delta x_{i,j,k} + .5\cdot\Delta x_{i-1,j,k}}\cdot\frac{1}{\Delta z_{i,j,k}} -$$
$$\left[\frac{q_{x_{i+\frac{3}{2},j,k}} + q_{x_{i+\frac{1}{2},j,k}}}{2\cdot\theta}\right]\cdot\frac{1}{.5\cdot\Delta x_{i+1,j,k} + \Delta x_{i,j,k} + .5\cdot\Delta x_{i-1,j,k}} \qquad 5.51$$

The coefficient weights for each of the 19 cells in equation 5.49 are shown in Appendix B. Similarities among the weights can be seen both in the weights shown in Appendix B and by the templates in Figure 5.9. The number of initial calculations required per finite difference grid cell for the 19 coefficient weights as input into a row in [A] is approximately 800. Taking advantage of the similarities among the weights, the number of calculations can be reduced by 75%. The reduced form of the coefficient weights can also be found in Appendix B.

With the coefficients determined, [A] can be built with each matrix row representing a cell in the finite difference grid. An algorithm (see Equation 5.52) is utilized to number the grid cells that correspond to the row number in [A].

$$L = [(j-1)n + i\,] + (k-1)nm \qquad 5.52$$

where: L: number of grid cell and matrix row
j: row counter of finite difference grid
i: column counter of finite difference grid
k: layer counter of finite difference grid
n: number of columns in the finite difference grid
m: number of rows in the finite difference grid

An example of applying equation 5.52 is found in Figure 5.10.

Reproduced with permission of the copyright owner. Further reproduction prohibited without permission.

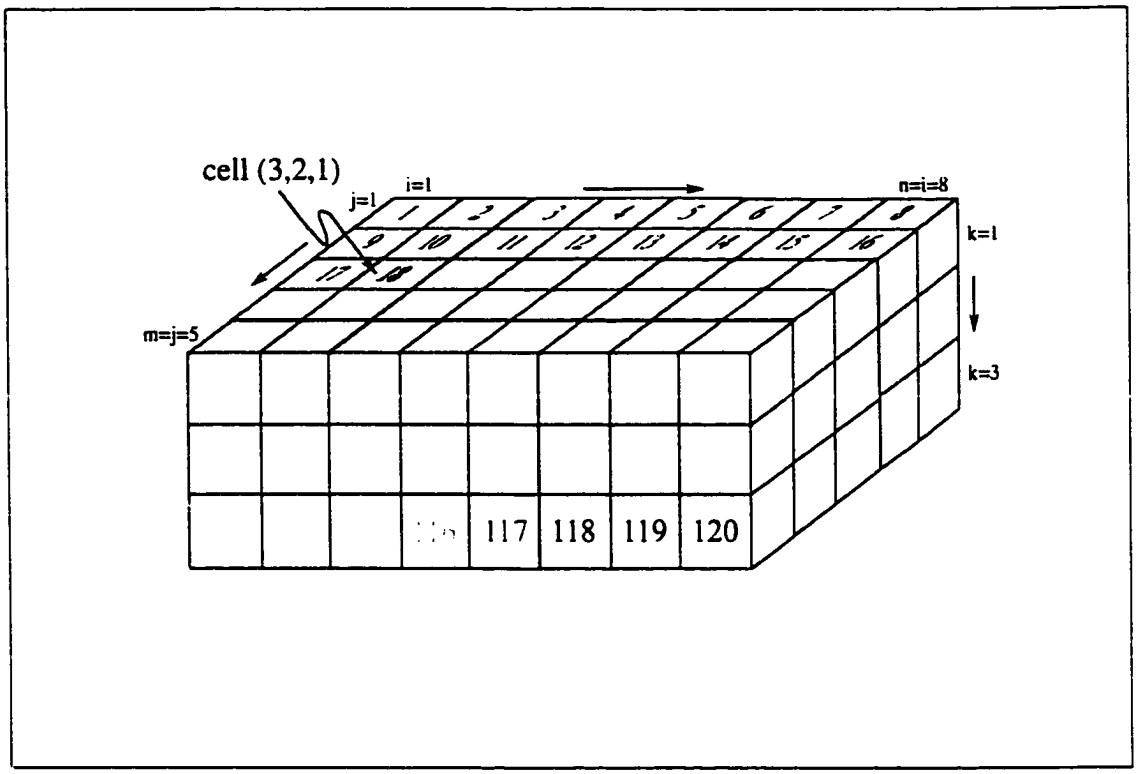

Figure 5.10. Depiction of grid cell numbering using the algorithm L=[(j-1)n + i] + (k-1)nm.

In Figure 5.10, the grid has 8 columns, 5 rows and 3 layers. Therefore, n equals 8 with i ranging from 1 to n, m equals 5 with j ranging from 1 to m, and k ranges from 1 to the total number of layers, or 3. Using the same coordinate orientation shown in Figure 5.7, the numbering of the cells start at cell (1,1,1) moving across the rows for each row of the first layer, then back to the first row/column cell of the second layer. Hence by utilizing equation 5.52, the corresponding number for the cell (3,2,1) is 18. Equation 5.52 determines the row of the coefficient weights in [A] for a finite difference cell as well as the column location of $C_{j,i,k}$ in [A]. Therefore, cell (3,2,1) is placed in the 18^{th} row of [A] and equation 5.49 is written for cell (3,2,1) respective to its placement in row 18.

Reproduced with permission of the copyright owner. Further reproduction prohibited without permission.

The concentration for cell (3,2,1), $C_{j,i,k}$, is located in the 18^{th} row and 18^{th} column of [A]. To find the coefficient weight of one of the 18 subset cells for cell (3,2,1), substitute the j,i,k subscripts into equation 5.52. For the subset cell, $C_{j-i,i+1,k}$, equation 5.52 becomes

$$L = [((j-1)-1)n + (i+1)\ ] + (k-1)nm. \qquad 5.53$$

The corresponding number for the $C_{j-1,i+1,k}$ coefficient weight is 11. Therefore, the coefficient weight of $C_{j-1,i+1,k}$ for cell (3,2,1) is placed in row 18, column 11 of [A]. Equation 5.53 is used to determine the column locations of the deviations of $C_{j,i,k}$ for a finite difference grid cell. This operation is repeated to determine the column location for each of cell (3,2,1)'s eighteen subset cells.

To solve the system of linear equations as shown by equation 5.50, the matrix A must be inverted. The inversion of [A] can be very memory intensive and computationally inefficient for large systems. To solve this dilemma, iterative techniques have been developed which are typically more memory efficient and require fewer cycles to solve (Kaushik, *et al.*, 1992). Iterative routines require less memory because only the nonzero values in [A] are needed along with their position. Fewer cycles, or iterations, are required for iterative routines in which the [A] is preconditioned. Preconditioning [A] also eliminates the possible singularity of [A]. Another advantage of iterative methods over direct methods is that they preserve the sparsity of the [A] (Brussino, *et al.*, 1989).

A popular preconditioner is the incomplete L-U decomposition where L and U are the lower and upper triangular matrices. The theory behind incomplete L-U decomposition is to redefine [A] so that it is closer to the identity matrix and that this

Reproduced with permission of the copyright owner. Further reproduction prohibited without permission.

refinement of [A] is easier to solve (Chen, *et al.*,1989). Therefore, the system, $[A]\{x\}=\{b\}$, can be preconditioned as follows:

$$[L^{-1} A U^{-1}] [U x] = [L^{-1}]\{b\}. \qquad 5.54$$

The lower and upper triangular matrices can be determined simply by incomplete Crout decomposition (Kaushik, *et al.*, 1992).

The preconditioned conjugate gradient iterative method has been very successful in the solution of symmetric problems (Zoran, *et al.*, 1985). However, there are difficulties with the conjugate gradient method solving asymmetric problems (Kaushik, *et al.*, 1992); therefore, alternative conjugate gradient methods are used such as the preconditioned biconjugate gradient (PBCG) algorithm, the preconditioned conjugate gradient squared (PCGS) algorithm, and the diagonally scaled conjugate gradient method (DSCG).

The PBCG and PCGS algorithms are quite similar except for the treatment of the residual error. The residual error for the PBCG algorithm at each iteration, k, is

$$r_k = \phi_k \cdot A \cdot r_o \qquad 5.59$$

where $\phi_k A$ is a k order polynomial generated by the PBCG algorithm. The PCGS algorithm determines the square of $\phi_k A$, $\phi_k^2 A$, which, in theory, converges twice as fast as the PBCG algorithm (Kaushik, *et al.*, 1992).

In Kaushik's *et al.* (1992) study comparing the PBCG and PCGS algorithms, the PCGS algorithm converges 20% faster than the PBCG algorithm. Chen *et al.* (1989) found the PBCG algorithm to converge in 20-50% fewer iterations than the standard preconditioned conjugate gradient algorithm for an 11-banded, asymmetric system of

Reproduced with permission of the copyright owner. Further reproduction prohibited without permission.

linear equations. Chen, *et al.* (1989) also states that the DSCG algorithm should converge just as fast as the PBCG and PCGS algorithms. In brief, the DSCG method normalizes the matrix system by dividing each linear equation by the diagonal element value such that the resulting matrix diagonal has all ones (Chen, *et al.*, 1989).

Very robust iterative solvers are available for public use. For this study, three modified conjugate gradient algorithms written in FORTRAN 77 where obtained from the Netlib repository at the Oak Ridge National Laboratory. The three routines are somewhat similar to the aforementioned algorithms which are as follows: preconditioned biconjugate gradient (DBCG) method; preconditioned biconjugate gradient squared (DCGS) method; and the diagonally scaled biconjugate gradient (DSDBCG) method. The "D" in the acronyms indicates FORTRAN double precision which is important in bridling truncation error.

To compare the different iterative solvers, a test system is created using the two-dimensional Laplacian difference equation shown below.

$$U_{i+1,j} + U_{i-1,j} + U_{i,j+1} + U_{i,j-1} - 4U_{i,j} = 0. \qquad 5.60$$

A Dirichlet boundary condition is enforced on the condition $x^2 - y^2$. Hence, the exact solution of the system for each difference cell is $x^2 - y^2$. Since only the nonzero elements of [A] are passed to the iterative routines, the maximum dimension of the [A] array is the number of rows (m) by the number of columns (n) times the number of cells represented in the difference equation. For example, in equation 5.60 five cells are represented. However for memory allocation information, the [A] array in each of the iterative methods is allocated using the number of cells represented in equation 5.49, or 19 cells.

Reproduced with permission of the copyright owner. Further reproduction prohibited without permission.

The size of the system ranges from 10 rows and columns to 410 rows and columns with matrix orders (N) of N=100 and N=168100, respectively. For each algorithm the number of iterations required for convergence, the time in seconds for convergence, and the root mean square (RMS) error are determined. The RMS error is calculated from the algorithm output and the exact solution using equation 5.61.

$$RMS = \sqrt{\frac{\left[\sum_{i=1}^{N} \left(x_i - exact_i\right)\right]}{N}} \qquad 5.61$$

Also calculated are the percent maximum difference and the maximum percent error. The cell that results in the maximum discrepancy between the exact solution and the model result constitutes the calculation of the percent maximum difference. The most informative type of error is the maximum percent error. For this error type, the cell that has the largest ratio between the exact solution minus the model result and the exact solution constitutes the determination of the maximum percent error.

A Silicon Graphics, 180MHz dual processor, Octane workstation is used for running these test cases. The workstation has 256 megabytes of RAM. Because of computer memory allocation sizes, the maximum allowable dimensions for the acquired DBCG algorithm is 245 by 245, or a matrix order of approximately N=60,000. The maximum matrix order limits for the DCGS and DSDBCG algorithms are approximately N=119,000 and N=168,000, respectively. Of the three iterative solvers presented, the DCGS algorithm performs best. Respectively, for any given matrix order, the DCGS

Reproduced with permission of the copyright owner. Further reproduction prohibited without permission.

algorithm converges in fewer iterations, in generally equal or less time, and with significantly greater accuracy than the other iterative solvers.

In Table 5.1, the computed maximum difference between the DCGS and the exact solution for N=90,000 is approximately 8.18 at cell (156,246) compared to 122.74 for the DSDBCG iterative solution at cell (174,245). The computed maximum different results in a percent error of approximately 0.027% and 0.41%, respectively. The RMS error for the DCGS solver is significantly lower than the DSDBCG solver: approximately 3.73 compared to 44.71, respectively. The time to solution and the number of iterations to convergence are both lower for the DCGS solver. In Table 5.2, the maximum percent error for the DCGS solver is approximately 0.07 which is roughly two orders of magnitude less than the DSDBCG result of 6.82. From the results shown in Tables 5.1 and 5.2, the DCGS solver out performs the DSDBCG solver each time.

The only advantage to the DSDBCG solver is the number of cells that can be modeled. However upon closer inspection of the DCGS FORTRAN coding, placement of the five prominent arrays into common statements allows a greater number of cells to be simulated. In brief, the three arrays associated with the [A] (IA, JA, A), an integer working array (IWORK), and a real working array (RWORK) are placed into common statements. By improving the solver's capability, the DCGS solver can simulate 1,690,000 cells. For this study, the goal of one million cells is met.

From Tables 5.3 and 5.4, the DCGS solver has consistently low maximum percent differences and remarkably low maximum percent errors. Typically, a percent error of less than 5% is acceptable. For the Laplacian difference test equation, the DCGS solver

Reproduced with permission of the copyright owner. Further reproduction prohibited without permission.

runs at reasonable times and in few iterations. Therefore, the DCGS algorithm is used as this study's iterative solver.

Reproduced with permission of the copyright owner. Further reproduction prohibited without permission.

Grid Information			Maximum Difference Error						Grid	Number of	Iterative Time
rows (i)	columns (j)	N	max. difference	row (i)	column (j)	exact solution	model value	% diff.	RMS	Iterations	(minutes)
300	300	90000									
		DCGS	8.18	156	246	36180	36171.82	0.027	3.73	94	1.05
		DSDBCG	122.74	174	245	29749	29871.74	0.41	44.71	373	2.27
345	345	119025									
		DCGS	11.14	180	283	47689	47677.86	0.029	5.06	108	1.63
		DSDBCG	175.29	200	280	38400	38575.29	0.46	65.4	423	3.47
400	400	160000									
		DCGS	*	*	*	*	*	*	*	*	*
		DSDBCG	255.65	232	321	49217	49472.65	0.52	99.14	483	5.12
410	410	168100									
		DCGS	*	*	*	*	*	*	*	*	*
		DSDBCG	268.7	240	329	50641	50909.7	0.53	104.26	495	5.53

Table 5.1 Maximum Difference Error Comparison Between the DCGS and DSDBCG Methods.

Reproduced with permission of the copyright owner. Further reproduction prohibited without permission.

Grid Information			Maximum Percent Error				
rows (i)	columns (j)	N	exact solution	model value	row (i)	column (j)	max. %
300	300	90000					
		DCGS	163	163.11	81	82	0.07
		DSDBCG	83	88.66	41	42	6.82
345	345	119025					
		DCGS	195	195.14	97	98	0.071
		DSDBCG	83	111.04	41	42	6.82
400	400	160000					
		DCGS	*	*	*	*	*
		DSDBCG	129	140.34	64	65	8.8
410	410	168100					
		DCGS	*	*	*	*	*
		DSDBCG	133	144.85	66	67	8.91

Table 5.2. Maximum Percent Error Comparison Between the DCGS and DSDBCG Methods.

Reproduced with permission of the copyright owner. Further reproduction prohibited without permission.

Reproduced with permission of the copyright owner. Further reproduction prohibited without permission.

Grid Information			Maximum Difference Error						Grid	Number of	Iterative Time
rows (i)	columns (j)	N	max. difference	row (i)	column (j)	exact solution	model value	% diff.	RMS	Iterations	(minutes)
400	400	160000	15.38	208	328	64320	64304.62	0.024	6.97	125	2.48
410	410	168100	16.51	212	336	67952	67935.49	0.024	7.46	128	2.7
500	500	250000	24.9	259	409	100200	100175.1	0.025	11.23	156	4.85
600	600	360000	40.2	308	490	145236	145195.8	0.028	18	186	8.3
700	700	490000	54.8	360	571	196441	196386.2	0.028	24.54	217	13.17
800	800	640000	81.8	411	653	257488	257406.2	0.032	36.35	246	20.02
900	900	810000	102.2	461	734	326235	326132.8	0.031	45.42	277	27.73
1000	1000	1000000	138.2	512	816	403712	403573.8	0.034	61.23	306	37.6
1300	1300	1690000	241.3	664	1058	678468	678226.7	0.036	106.83	397	82.68

Table 5.3. Maximum Difference Error Comparison Between the DCGS and DSDBCG Methods for Large Grid Cell Sizes.

Grid Information			Maximum Percent Error				
rows (i)	columns (j)	N	exact solution	model value	row (i)	column (j)	max. %
400	400	160000	211	211.15	105	106	0.073
410	410	168100	215	215.16	107	108	0.075
500	500	250000	257	257.19	128	129	0.076
600	600	360000	325	325.28	162	163	0.085
700	700	490000	373	373.32	186	187	0.085
800	800	640000	433	433.42	216	217	0.097
900	900	810000	481	481.46	240	241	0.096
1000	1000	1000000	545	545.57	272	273	0.105
1300	1300	1690000	697	697.76	348	349	0.109

Table 5.4. Maximum Percent Error Comparison Between the DCGS and DSDBCG Methods for Large Grid Cell Sizes.

Reproduced with permission of the copyright owner. Further reproduction prohibited without permission.

Before moving into the actual coding of MULTRAN, three more areas of modeling must be covered. The first two areas are the computation of the transport time step and the determination of mass balance. The transport time step is essential in maintaining numerical stability. If the time step is too large, oscillation can occur and result in divergence of the solution. Mass balance allows a check to be conducted on the system to determine if the difference between mass into and out of the system matches the mass change in storage within the system. Low mass balance errors, measured in this study as a percent error, typically implies a balanced system.

The stability criteria for the transport time step is identical to the Courant number (see Equation 5.62).

Rearranging equation 5.62 results in a minimum time step criteria of

However, in conducting a minor test of this time step criteria with the following criteria:

Semi-infinite column	
Number of cells:	1000
Δx:	1 ft.
Δt (time step):	1 and .5 days
Total time:	5 days
seepage velocity:	1 ft/day
Source concentration:	1 mg/L

there exist inherent errors during the first few iterations (see Figures 5.11 and 5.12). Using a 1 day time step, there exists an oscillation that becomes smoother after the third iteration (3rd day). Decreasing the time step to 0.5 days presents the same oscillation anomaly again becoming smoother after the third iteration (1 ½ days). From this analysis, an additional time step stipulation is implemented which requires at least 10 transport

Reproduced with permission of the copyright owner. Further reproduction prohibited without permission.

time steps. With at least 10 transport time steps, the possible effects of oscillations occurring early on in the iterative process will be far removed from the resulting solution.

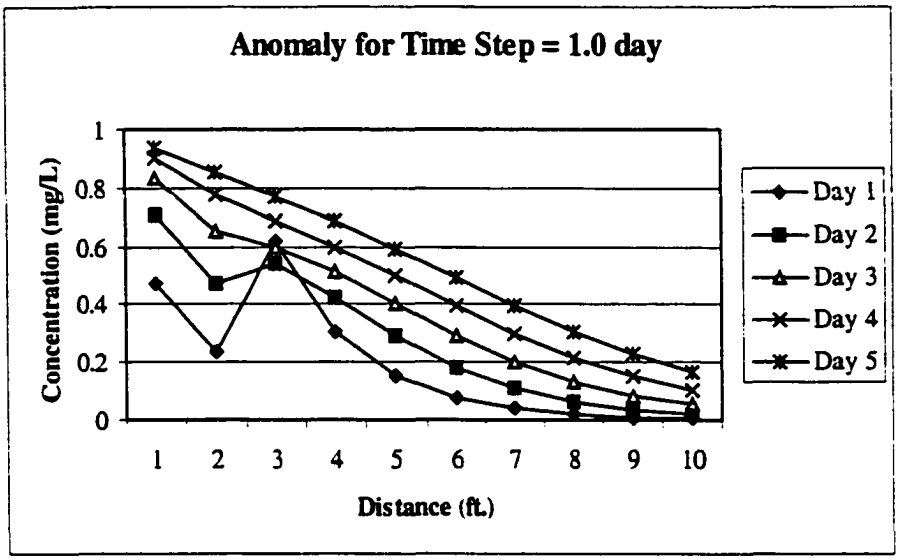

Figure 5.11. Depiction of oscillation anomaly for a time step of 1 day.

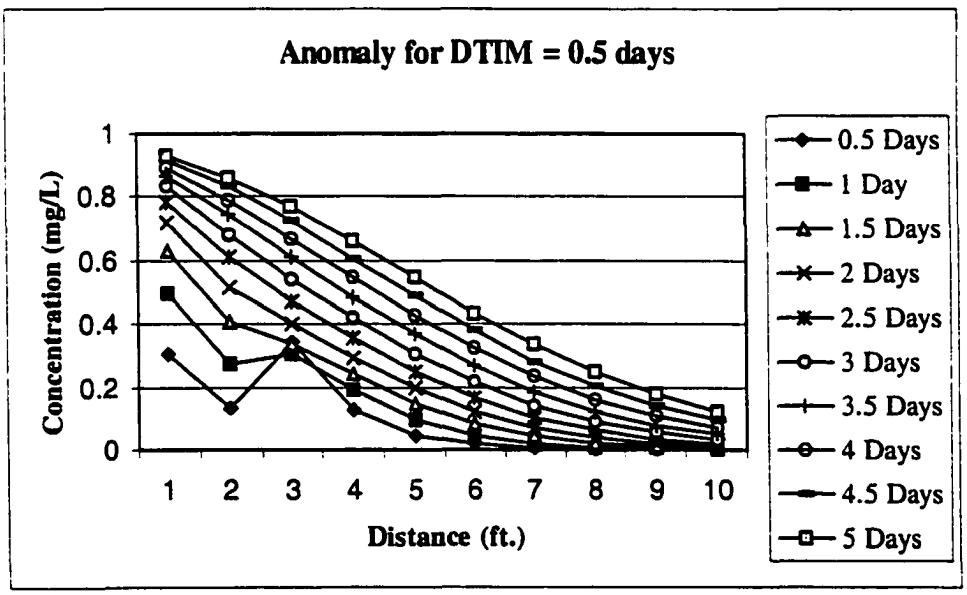

Figure 5.12. Depiction of oscillation anomaly for a time step of 0.5 days.

In determining the accuracy of the solution using mass balance, the cumulative mass into the system minus the removed mass (by sinks, sorption, or

Reproduced with permission of the copyright owner. Further reproduction prohibited without permission.

decay/biodegradation) must equal the mass in storage. To determine the mass balance percent error, the following equation which is similar to MODFLOW and MT3D, is used:

******equation******

The third remaining area of interest is the specification and implementation of boundary conditions. The first boundary condition is a Dirichlet boundary condition in which the concentration is either a specified concentration amount at the boundary or a specified concentration through a sink or source. Having a specified concentration (C_j) amount at a boundary, the RHS is set equal to the concentration amount, C_j, and the diagonal value within the [A], A_{jj}, is set to one with all other entries, $A_{ji;\ (j \text{ not equal to } i)}$, set to zero. In specifying a concentration through a source term, the source flux limited concentration ($WC_j/\Phi\Delta x\Delta y\Delta z$) is added to the RHS with the j^{th} row of terms in the [A] left unchanged. Typically, concentrations are not specified for sink terms except in the case of known evapotranspiration processes. The sink flux is determined as the sink rate divided by the porosity and cell volume. In the case of evapotranspiration, the sink flux rate is multiplied by the specified concentration and is subtracted from the RHS. The j^{th} row of terms in the [A] still remains unchanged. For all other sink cases, the sink rate is added to the corresponding [A] diagonal value, A_{jj}. The RHS entry is not changed for j^{th} row.

The second type of boundary condition is the Neumann condition. For this condition, the concentration gradient is known across a boundary. This is commonly found along impermeable boundaries where the ground water flux is zero. For cells residing along model boundaries, the calculation of those cells' terms within the [A] do

Reproduced with permission of the copyright owner. Further reproduction prohibited without permission.

not include contributions of the hidden, surrounding noflow cells that border model boundaries.

In the case of noflow cells residing within the model boundaries, a combination of the Dirichlet and Neumann is implemented. A cell that borders such a noflow cell excludes within the calculation of the cell's coefficients the term from the noflow cell (se equations 5.49 and 5.51). For representing noflow cells, the [A] diagonal, A_{jj}, is set to one and the RHS entry is set to zero for the j^{th} row.

Reproduced with permission of the copyright owner. Further reproduction prohibited without permission.

Chapter 6

MULTRAN Computer Coding

In order to simulate multispecies contaminant transport for this study, three general models are required. They are a groundwater flow model, a transport model, and a chemical reaction model. The USGS program, MODFLOW, is used as the necessary groundwater model which supplies the cell size information, head distribution, cell-by-cell velocity terms, and timing information. A transport model using an implicit finite difference scheme is developed within this study to determine the aqueous chemical component concentration distributions. Lastly, Afifi's (1994) chemical reaction scheme is taken from REACTRAN3D and is utilized to solve the nonlinear algebraic equations representing chemical reactions and to determine the aqueous component input concentrations for transport. The contributions from these general models are integrated into a single model called MULTRAN. The purpose of this chapter is to elaborate on MULTRAN's computer coding structure.

An overview of MULTRAN's methodology is shown in Figure 6.1. Each item in the flowchart is a synopsis for more detailed programming. With the exception of the "START" and "END" items, each item will be further expanded with a more detailed flowchart followed by a brief description.

Reproduced with permission of the copyright owner. Further reproduction prohibited without permission.

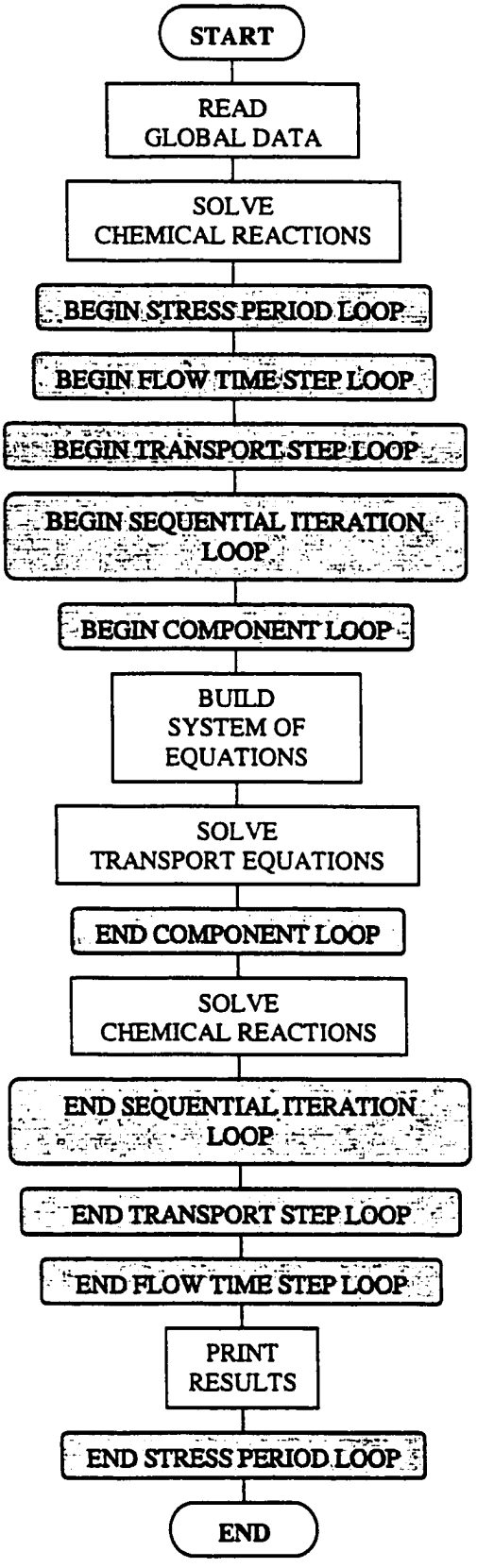

Figure 6.1. Flowchart depicting MULTRAN's program methodology.

Reproduced with permission of the copyright owner. Further reproduction prohibited without permission.

Read Global Data:

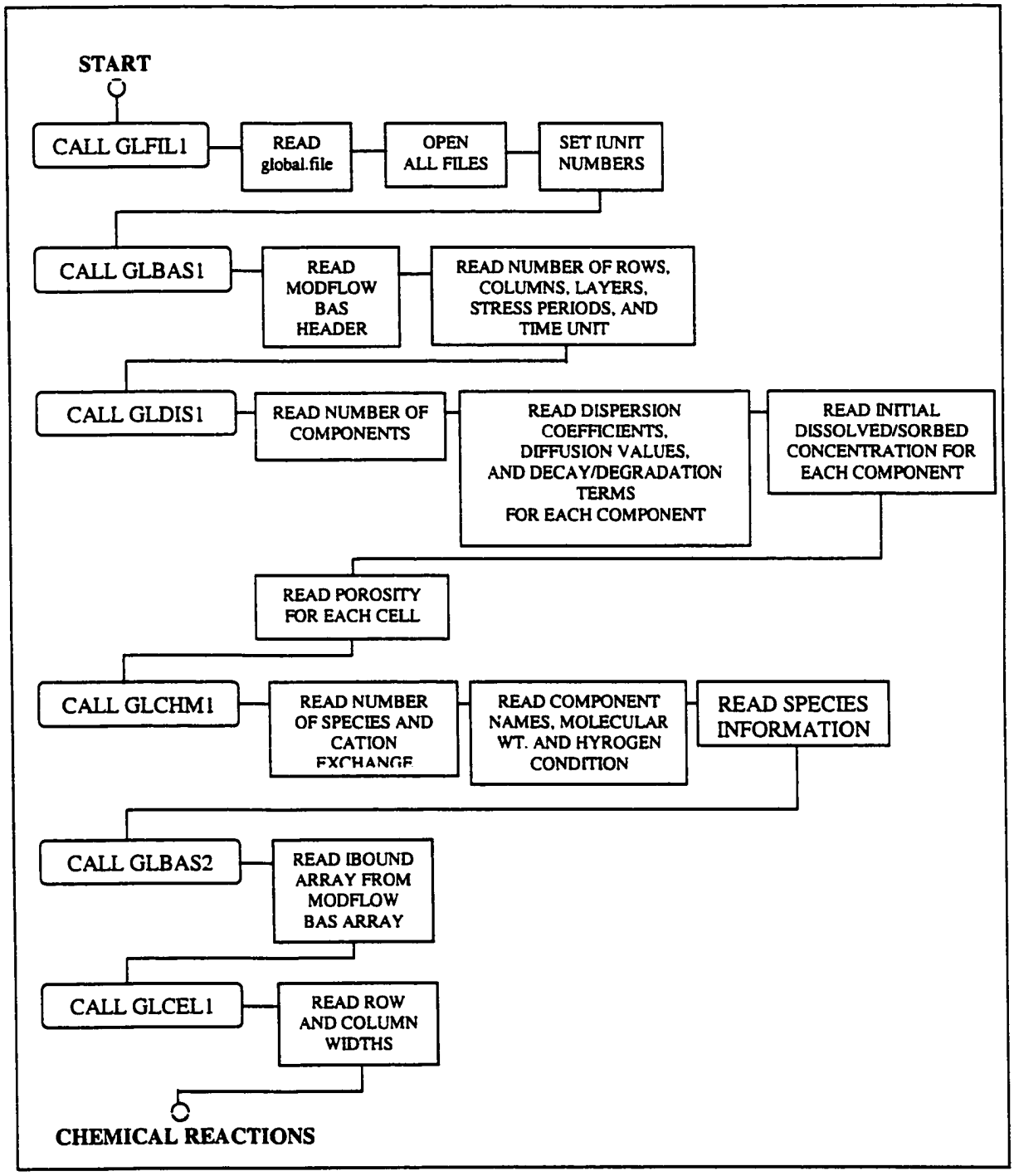

Figure 6.2. Flowchart of Read Global Data routine.

Reproduced with permission of the copyright owner. Further reproduction prohibited without permission.

GLFIL1: All of the external data files read by MULTRAN are input into a file called global.file. This file has the format (A3,A3,I7,1x,A20) with an example appearance as follows:

```
BAS    50 expl.bas
BCF    60 expl.bcf
...
       76 expl.ibound
       78 expl.head
       80 expl.conc
...
EOF
```

The user supplies the file names and unit numbers with the only restriction that the names or numbers not be used twice. All of the files are opened here. MULTRAN requires eight specific files to exist. The first two files are the MODFLOW input files BAS and BCF. The flag for these files in the global.file are BAS and BCF, respectively. The third file is the MODFLOW cell-by-cell budget file that is designated by the LKM flag. The fourth file contains the chemical species characteristics and is specified by the CHM flag. The DIS flag specifies a file containing the dispersivity coefficients, the decay/biodegradation parameters, and the initial dissolved and sorbed component concentrations for each chemical component as well porosity values and possible sorption terms for single species sorption.. The constant concentration cells for each component (specified for each stress period) are located in another file flagged with the CON code. The seventh file contains the sink/source locations and concentrations, and is designated with the SSM flag in the global.file. Lastly, the eighth file has data on the maximum allowed number of iterations, desired model accuracy, and timing information required

Reproduced with permission of the copyright owner. Further reproduction prohibited without permission.

for steady state flow problems. The eighth file is designated by the OUT flag in the global.file. Exact specifications for each of the required eight files are given in Appendix C. Any of the files listed in the global.file can be either formatted or unformatted. Unformatted files must have negative unit numbers.

GLBAS1: The purpose of the GLBAS1 subroutine is simple: to read from the MODFLOW BAS input file the header information, the number of rows, columns, layers, and stress periods and the time unit flag which specifies days, seconds, years, or other measures of time. Excluding the header information, the variables NROW, NCOL, NLAY, NPER, and ITMUNI are set, respectively.

GLDIS1: As mentioned previously, a file is supplied by the user containing the dispersivity coefficients, decay/biodegradation parameters, and initial dissolved and initial sorbed concentrations for each modeled component as well as other parameters. This file is flagged with the DIS code in the global.file. For each component, a longitudinal, horizontal, and transverse dispersivity coefficient as well as a diffusivity value is set respectively to the variables AL(L), ATH(L), ATV(L), and DIFSION(L) with L ranging over the number of components, or NCOMP. On the same read line, the following decay/biodegradation terms are read: LAMCODE(L), LAMDA1(L), and LAMDA2(L). Description of these terms can be found in Appendix C. The initial dissolved and sorbed concentrations for each component are recorded into the two dimensional arrays, CONC(NUM,L) and CSCONC(NUM,L), respectively. The variable NUM ranges from one to the number of finite

Reproduced with permission of the copyright owner. Further reproduction prohibited without permission.

difference grid cells, and is calculated using equation 5.52. CSCONC(NUM,L) is not read if only one component is being modeled. Instead the IISO flag is read with the possibility of assigning single component sorption parameters such as the soil bulk density (RHOB), equilibrium coefficient (KISO), Freundlich exponent (AEXPO), and the maximum number of sorption sites (BMAX). Chapter 5 comments more on the use of these parameters. The porosity of the system is recorded into the three dimensional array, PHI(J,I,K) , with J, I, and K representing the number of rows, columns, and layers, respectively.

GLCHM1: When more than one component is specified, the ICHM file is read. The file contains the number of dissolved species (NSPECIES), the number of cation exchange species (NCATEXH) and component and species information. There are four pieces of component information which are the component name, its molecular weight, a binary-type condition where a value of one specifies a hydrogen component and a zero all other components, and the stoichiometric coefficient for each component. The cation exchange capacity of the soil is set to the variable, CEC. Lastly, the follow six parameters are read for each species: (1) name of the cation exchange species, (2) stoichiometric coefficient, (3) selectivity coefficient (equilibrium constant), (4) the aqueous cation number, (5) the replaced cation number, and (6) the valance of the cation.

GLBAS2: MODFLOW requires each cell to be specified as a constant head cell, noflow cell, or a variable head cell. IBOUND, a three dimensional integer array,

Reproduced with permission of the copyright owner. Further reproduction prohibited without permission.

contains this information. A negative value specifies a constant head cell, a value of zero signifies a noflow cell, and a positive value represents a variable head cell. The IBOUND array is read from the MODFLOW BAS input file. The array values are rewritten with variable head cells represented as zero values and all other cells given a value of one. This is done so constant cells (constant head and noflow) can be recognized and blasted with the value, 1.0E30. Blasting is a very common method for retaining constant cell values. The values are recorded in the three dimensional array, IBNDCON(J,I,K).

GLCEL1: The finite difference grid does not change throughout the simulation; therefore, row and column widths remain constant. This width information is located in the MODFLOW BCF file. The widths along a row, as requested by MODFLOW, are actually the column dimensions. Hence, the widths specified along a column are the row dimensions. The row and column widths are recorded respectively into the one dimensional arrays, DCCELL(I) and DRCELL(J). The row and columns widths are the same for all layers.

Chemical Reactions:

To solve the chemical reactions, Afifi's (1994) chemical reaction routine is called. Passed to the routine is the necessary data read from the CHM flagged file (as mentioned in the GLFIL1 routine discussed under "Read Global Data"). The estimated sorbed concentrations for each component is returned to the main program through the common array, DEL_S(NUM,L).

Reproduced with permission of the copyright owner. Further reproduction prohibited without permission.

Begin Stress Period and Flow Time Step Loop:

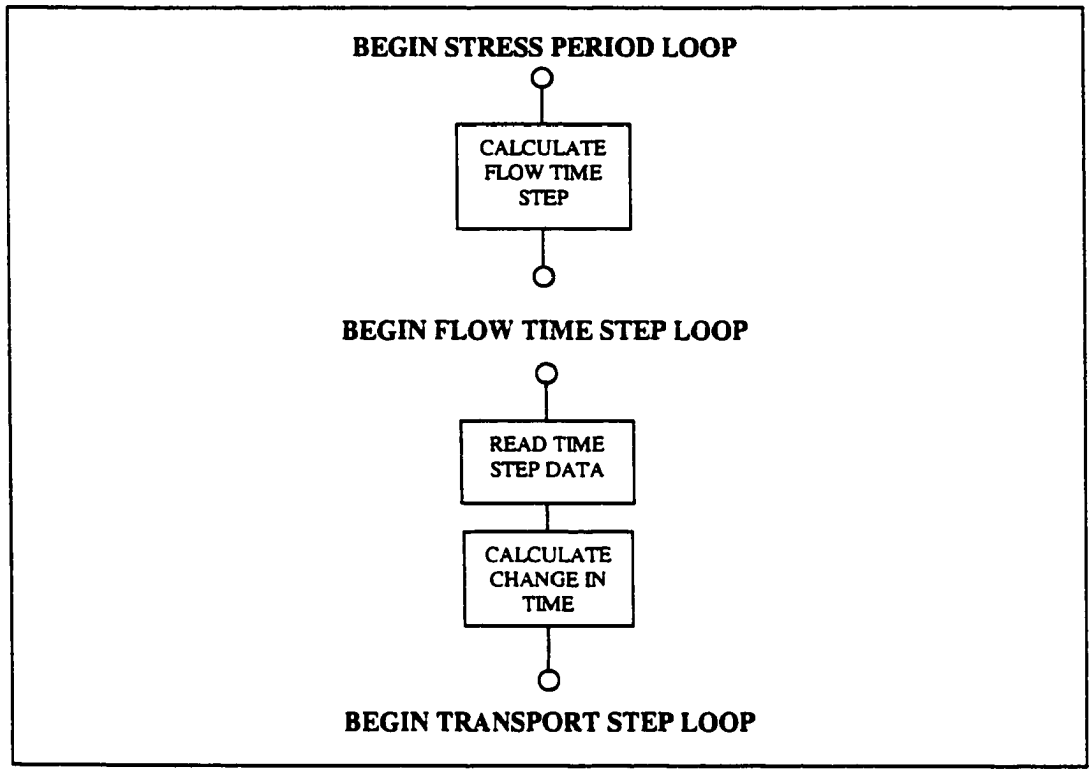

Figure 6.3. Flowchart of beginning stress period loop.

Stress periods represent time periods in which external stresses applied to the system remain constant. For example, two stress periods may exist within a simulated year where one period represents well pumping for summer irrigation and for the second period, well pumping remains off during the winter season. Stress periods are for transient studies. Steady state studies have only one stress period. Therefore, the computational steps for contaminant transport within this loop are recursive for transient cases. Before the flow time step loop begins, the time step information is obtained from the MODFLOW BAS input file. This data includes the length of the stress period, the number of time steps within the stress period, and the time step multiplier that allows for variable time step increments. The flow time step is calculated using the same equation

Reproduced with permission of the copyright owner. Further reproduction prohibited without permission.

as specified in the MODFLOW manual. The necessary transport time step value, DELT, is then calculated based upon the Pelcet number.

Begin Transport Step Loop:

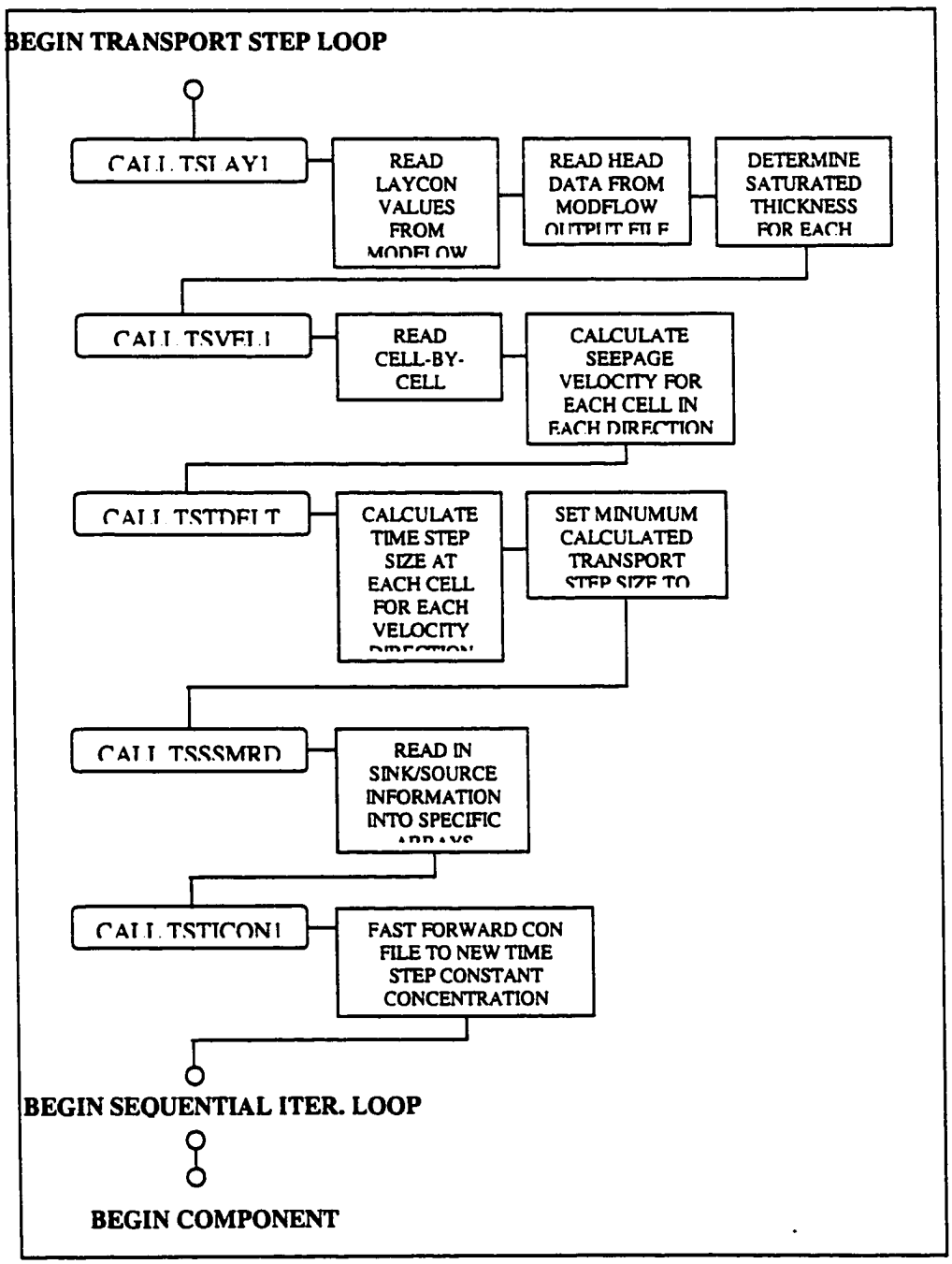

Figure 6.4. Flowchart of beginning time step loop.

Reproduced with permission of the copyright owner. Further reproduction prohibited without permission.

TSLAY1: For each time step, MODFLOW outputs the resulting heads, the cell-by-cell flux terms, and the sink/source information because these values probably vary from time step to time step. Consequently, the saturated thickness varies. Four layer designations are allowed by MODFLOW. They are confined (flagged zero), unconfined (1), confined/unconfined with constant transmissivity (2), and confined/unconfined with variable transmissivity (3). The saturated thickness is simple to solve for the first and second layer type; however, the third and fourth layer types are more difficult. A check on whether the resulting head is above or below the top of the layer for the latter two types results in a more intensive process for solving the saturated thickness of the cells. The saturated thickness is recorded into the three dimensional array, DLLAY(J,I,K).

TSVEL1: As mentioned previously, MODFLOW saves the cell-by-cell fluxes. MULTRAN requires these fluxes as seepage velocities. Therefore, the x-, y-, and z-directional fluxes for each cell are divided by the respective saturated areas and the layer porosity. The x-, y-, and z-directional seepage velocities are respectively placed into the following three dimensional arrays: QXX(J,I,K), QYY(J,I,K), and QZZ(J,I,K).

TSTDELT: Though MODFLOW determines the time step size for the flow equation, sometimes further time discretion is required to meet the stability criteria discussed at the end of Chapter 5. This addition time disjunction results in transport time steps within the MODFLOW flow time steps. Therefore, the minimum transport time step based upon the stability criteria is determined

Reproduced with permission of the copyright owner. Further reproduction prohibited without permission.

by calculating the corresponding cell dimensions divided by the component seepage velocities. The minimum transport time step size is returned as the variable, DTIM.

TSSSMRD: For ease of calculating the concentration amounts into sinks and out of sources, each of the sink/source types are recorded into individual, three dimensional arrays. These arrays are as follow: SSMCST(J,I,K) for constant heads, SSMWEL(J,I,K) for wells, SSMDRN(J,I,K) for drains, SSMRCH(J,I,K) for recharge, SSMEVT(J,I,K) for evapotranspiration, SSMRIV(J,I,K) for rivers, SSMSTR(J,I,K) for streams, and SSMGHB(J,I,K) for general head boundaries. The values for each of the sink/source terms are read from the MODFLOW unformatted, cell-by-cell budget file. If a value is negative; hence, a sink, then the value is recorded in the SSMOUT(J,I,K) array for addition to the left-hand side of equation 5.49. This holds true except in the case of evapotranspiration as discussed in Chapter 5.

TSICON1: This subroutine is a minor routine that fast forwards to the next time step set of constant concentration cell values. At the new time step, new constant concentration values are read, if any.

Reproduced with permission of the copyright owner. Further reproduction prohibited without permission.

Component Loop:

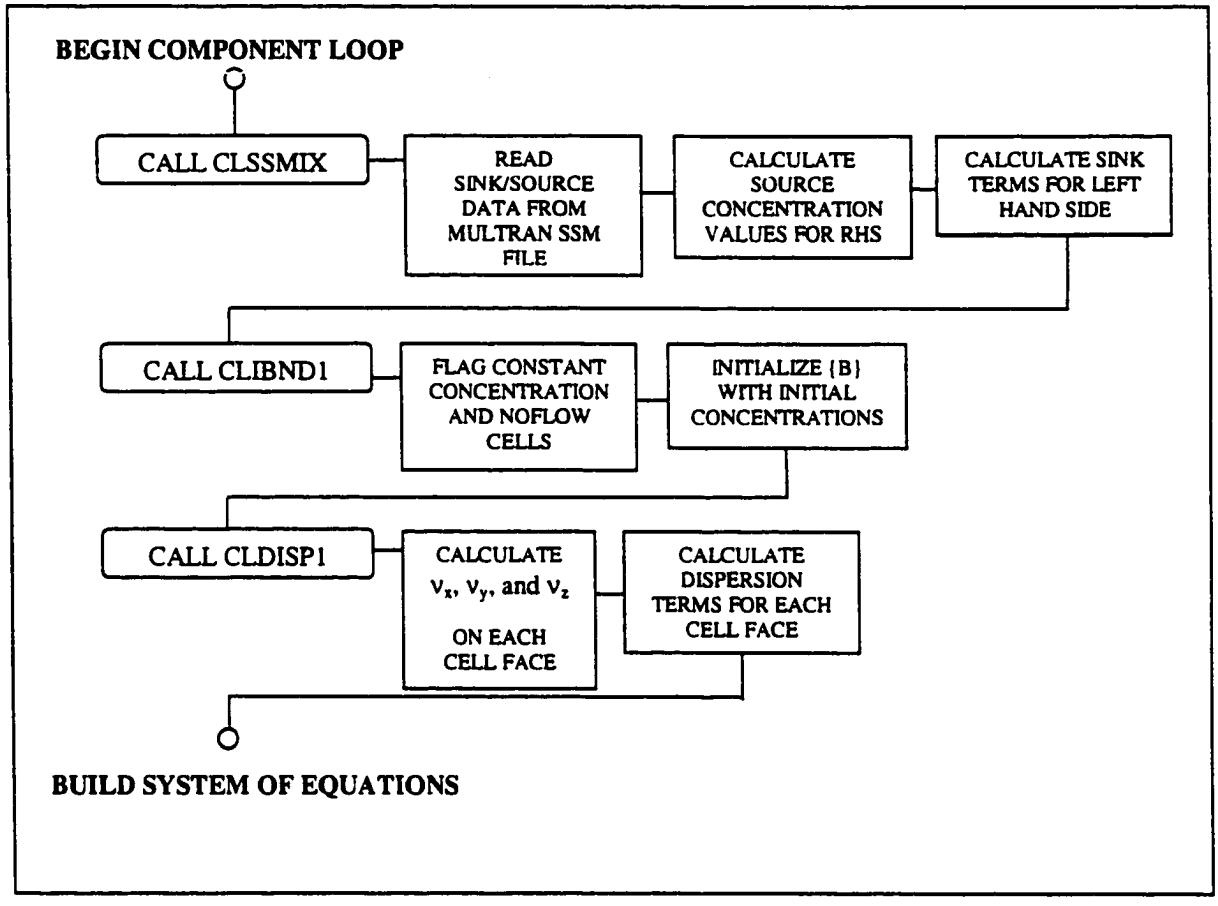

Figure 6.5. Flowchart of beginning component loop.

CLSSMIX: Sink/source values are held constant during stress period time steps within MODFLOW. The same is true here in MULTRAN, and additionally the sink/source values remain constant during the transport time steps. Hence, an additional MULTRAN input file, coded SSM in the "global.file," is required for all possible sink/source terms. The types of sink/source terms are wells, drains, rivers, streams, recharge, evapotranspiration, and general

Reproduced with permission of the copyright owner. Further reproduction prohibited without permission.

head boundaries. Also included are constant head cells. For each possible sink/source type, the input or output concentration is read from the coded SSM input file (see Appendix C). Next, the prerecorded sink/source flow rates are analyzed. If the flow term is positive, representing a source, then this flow term is multiplied by the input concentration, added to the SSMIN(J,I,K) array, and reserved for addition to the RHS. If no concentration is specified by the user, then the SSMIN(J,I,K) value is zero. If the flow term is negative, the sink is skipped. Concentrations are not specified for sinks except in special cases of evapotranspiration as discussed in Chapter 5. If a concentration is specified for an evapotranspiration process within a cell, then it is multiplied by the respective SSMEVT(J,I,K) term and subtracted from the RHS.

CLDISP1: The mathematics of equation 5.49 requires dispersion values to be known at the cell faces; therefore, the directional seepage velocities must be calculated for each cell's six faces as well as the magnitude of those velocities. Hence, there is a possibility of 24 calculated velocity values for each cell. The determination of the z-directional velocity values is skipped if there is only one layer. Since the dispersion factors are calculated cell by cell, the velocity values are not placed in computer memory. If the velocity magnitude for a cell face equals zero, the value is set to 1.0E-30 to avoid division by zero. Once the velocity components are known, the dispersion values are calculated using equations 5.38 and 5.39 to 5.44. If more than one layer is modeled, then 18 dispersion values must be determined; else, only 8 values are

Reproduced with permission of the copyright owner. Further reproduction prohibited without permission.

calculated. The dispersion values are saved into the two dimensional array, DISP(NUM,18).

CLIBND1: Constant concentration cells are listed in a user-defined file that is flagged with the CON code in the global.file. The number of constant concentration cells for a single component is supplied followed by the row, column, layer, and concentration value for the specified number of cells (see Appendix C). A zero must be designated as the number of constant concentration cells for components without specific constant concentration cells. A list of constant concentration cells for each component is supplied for each stress period. Therefore, concentrations are allowed to vary over time; such is the case with landfill leachate. The IBNDCON array value for each constant concentration cell is set to one. Noflow cells are designated within MULTRAN with an IBNDCON of 2. Any initial concentration amounts residing in the modeled system before simulation is recorded into a temporary array, BTMP(NUM), for equation to the RHS.

Reproduced with permission of the copyright owner. Further reproduction prohibited without permission.

Build System of Equations:

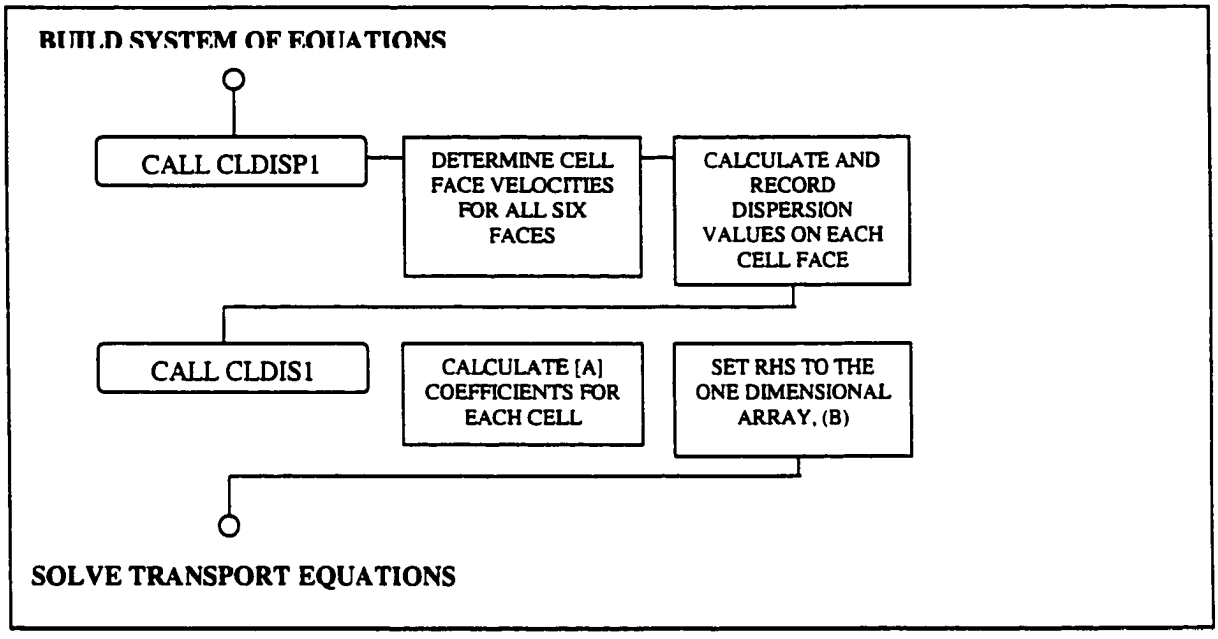

Figure 6.6. Flowchart of building system of equations.

CLDISP1: Before the dispersion values can be calculated for each of the cell faces of which there are at most six, the components of velocity (v_x, v_y, v_z) need to be determined. These cell face velocities are not saved. For this subroutine, all of its calculations for each cell are performed in a large FORTRAN "DO" loop. Also, to conserve computation time, different sets of calculations exist for either multi-layered systems or single layer systems. For single layered systems, calculations for the top and bottom faces of each cell are not necessary. Dispersion values are calculated and saved in the two-dimensional array, DISP(NUM,X), with X equaling 18 for multi-layered systems and 8 for single layered systems. It is also within this routine that numerical dispersion is taken into account.

Reproduced with permission of the copyright owner. Further reproduction prohibited without permission.

CLDIS1: Again, there exist two sets of calculations for either single or multi-layered systems. Based upon equation 5.49, the [A] coefficients are calculated for each cell. The contributions of sinks, decay/degradation and noflow cells are accounted for within this subroutine. All of these values are saved within a one-dimensional, double-precision array called A of the dimension (19*J*I*K). The multiplication of 19, as discussed in Chapter 5, stems from the cell in question plus the 18 possible contributing cells. After the [A] coefficients are determined, the RHS is calculated based on initial concentrations, constant concentrations, and contributing sources. The RHS is saved in the one-dimensional array, B(NUM).

Reproduced with permission of the copyright owner. Further reproduction prohibited without permission.

Begin Transport Loop:

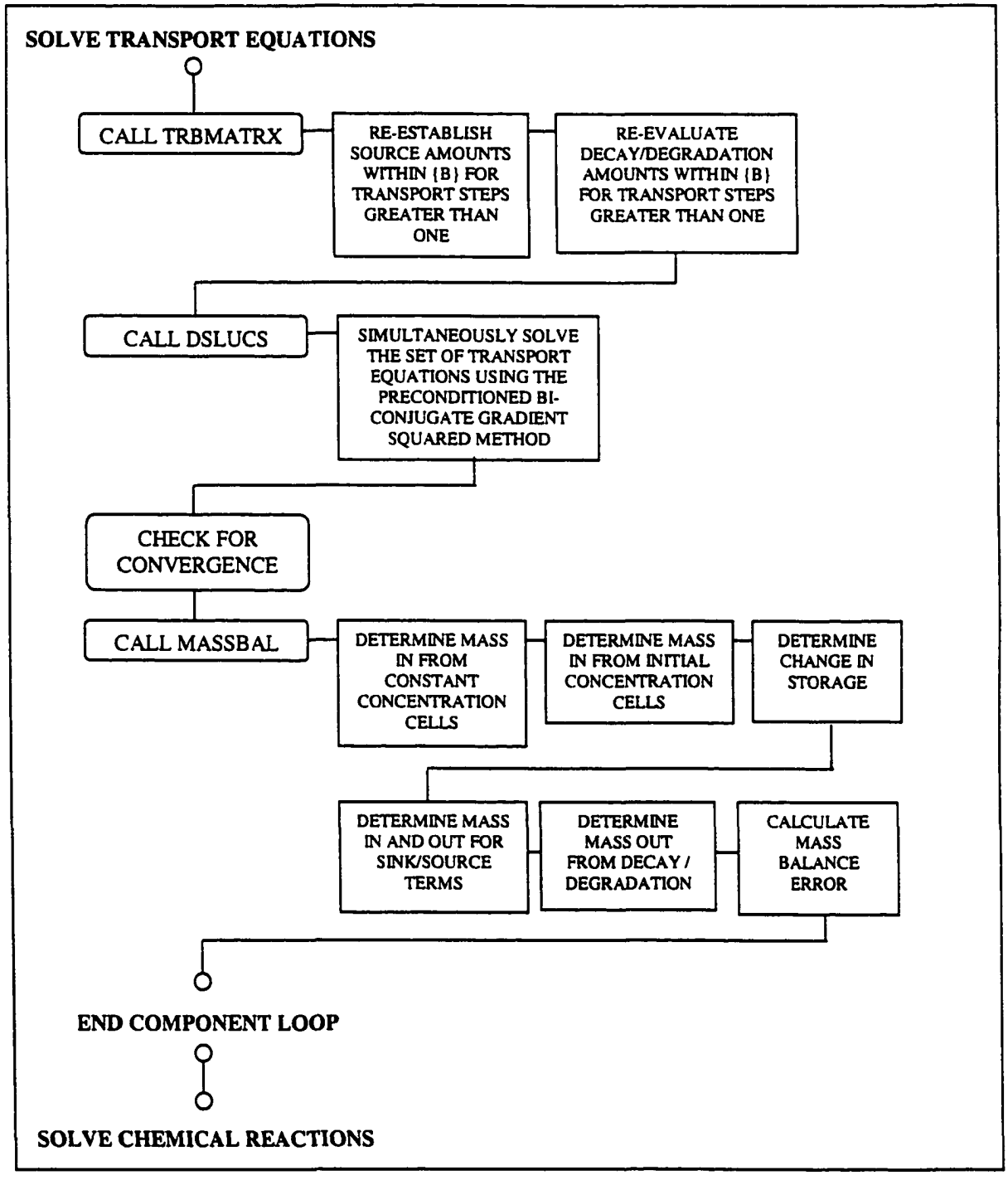

Figure 6.7. Flowchart of beginning transport loop.

Reproduced with permission of the copyright owner. Further reproduction prohibited without permission.

TRBMATRX: For transport time steps greater than one, the TRBMATRX subroutine is accessed. Within this subroutine, any source term amounts are re-established within the {B} as well as the contribution of decay/degradation on cation exchange species.

DSLUCS: To solve the set of transport equations simultaneously, the preconditioned, bi-conjugate gradient squared method is used. The subroutine reads in the [A] and {b} arrays and outputs the {x} array which are the results.

MASSBAL: The accuracy of the model as to mass in, mass out, and change in storage is determined within the MASSBAL subroutine. The mass in is accumulated in the MASSIN variable, the mass out in the MASSOUT variable, and the change in storage in the CHGSTRG variable. The error is calculated using equation 5.*XX*. Also calculated are the concentration amounts into and out of the system as accumulated over time for individual processes such as sink/sources, sorption, and decay/degradation.

Solve Chemical Reactions...End:

After each component is transported, the chemical reaction subroutine, PREGEOCHEM, is called to determine the final adsorbed concentrations for each component. If convergence is not met, sequential iteration between transport and chemical reactions begins though calculations have already been performed for the first sequential iteration loop.

Reproduced with permission of the copyright owner. Further reproduction prohibited without permission.

Once convergence is met, calculations begin for the next transport step and ultimately for the next flow time step. The results are printed at the end of each time step loop before the new stress period begins. After the last stress period is simulated, the program ends.

Reproduced with permission of the copyright owner. Further reproduction prohibited without permission.

Chapter 7

Model Verification

Development of a numerical model requires model verification. Verification typically entails matching model output for ideal cases to analytical solutions. Analytical solutions exist for one-, two-, and three-dimensional contaminant transport. Beyond typical model verification with analytical solutions, verification can also be conducted by comparing results with other models. For the verification of MULTRAN, six verifications are performed as well as two example case studies. Each simulation hereafter is labeled as a "Case." The structure for this chapter is as follows:

One-dimensional:
- Case 1: Conservative, single species, semi-infinite column compared with analytical solution and MT3D.
- Case 2: Reactive via sorption, single species, semi-infinite column compared with analytical solution
- Case 3: Reactive via radioactive decay, single species, semi-infinite column compared with analytical solution
- Case 4: Reactive via cation exchange, multi-species, semi-infinite column compared with analytical solution

Two-dimensional:
- Case 5: Conservative transport compared to the analytical solution and MT3D
- Case 6: Conservative transport in a heterogeneous aquifer example case

Three-dimensional:
- Case 7: Conservative transport compared to the analytical solution and MT3D

Example site analysis:
- Case 8: Two-dimensional, multi-species, reactive transport site remediation including MT3D.

Case 1. Semi-infinite column with conservative contaminant transport.

For a semi-infinite column, the boundary conditions are as follows:

$$t <= 0 \qquad x >= 0 \qquad C = 0$$

Reproduced with permission of the copyright owner. Further reproduction prohibited without permission.

$t > 0$	$x = 0$	$C = C_o$
$t > 0$	$x =$ infinity	$C = 0.$

The partial differential equation to solve is the transport equation in the x-direction.

Hence,

$$D \cdot \frac{\delta^2 \cdot C}{\delta x^2} - V \cdot \frac{\delta C}{\delta x} = \frac{\delta C}{\delta t} \qquad 7.1$$

The analytical solution to equation 7.1 is

$$C(x,t) = \frac{1}{2} \cdot C_o \cdot \left(\operatorname{erfc}\left(\frac{x - vt}{2 \cdot \sqrt{Dt}} \right) + \exp\left(\frac{xv}{D} \right) \cdot \operatorname{erfc}\left(\frac{x + vt}{2 \cdot \sqrt{Dt}} \right) \right) \qquad 7.2$$

For this case, the model parameters are as follows:

Cell length (Δx):	10 ft.
Cell width (Δy):	1 ft.
Cell depth (Δz):	1 ft.
Seepage velocity (ft/day):	0.24 ft/day
Dispersivity (ft.):	10 ft.
Length of simulation time (days):	2000 days

The location where 50% of the contaminant has passed is equal to the seepage velocity multiplied by the simulation time. Here, the distance to the 50% mark is 500 ft. With the 50% mark known (x=500 ft.), the numerical results from MULTRAN and those from the analytical solution can be aligned at x=0. The results from this case are depicted in Figure 7.1. There is a very good correlation between MULTRAN, the analytical solution, and MT3D.

Reproduced with permission of the copyright owner. Further reproduction prohibited without permission.

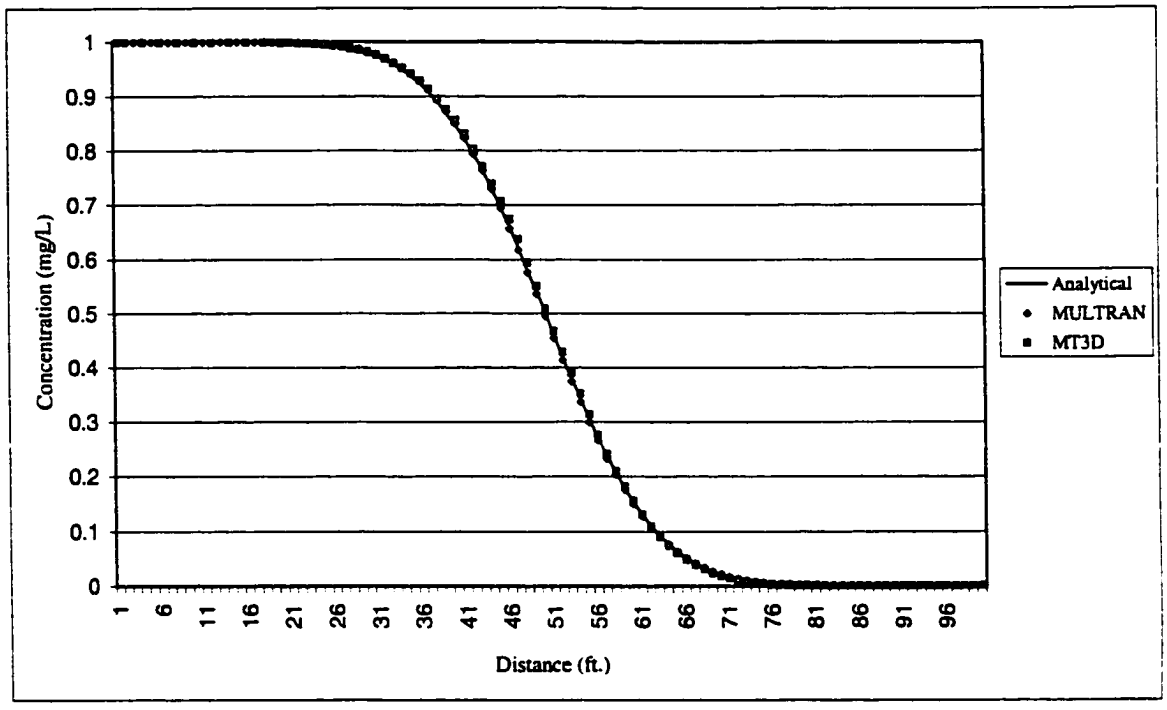

Figure 7.1. Comparison of MULTRAN, MT3D, and the analytical solution for conservative transport in a semi-infinite column.

Of special interest is the correlation between this case and MULTRAN's result when not accounting for numerical dispersion. From Figure 7.2, one realizes the importance of accounting for the effects of numerical dispersion. Though mass balance may be maintained, the concentration front profile is inaccurate.

Reproduced with permission of the copyright owner. Further reproduction prohibited without permission.

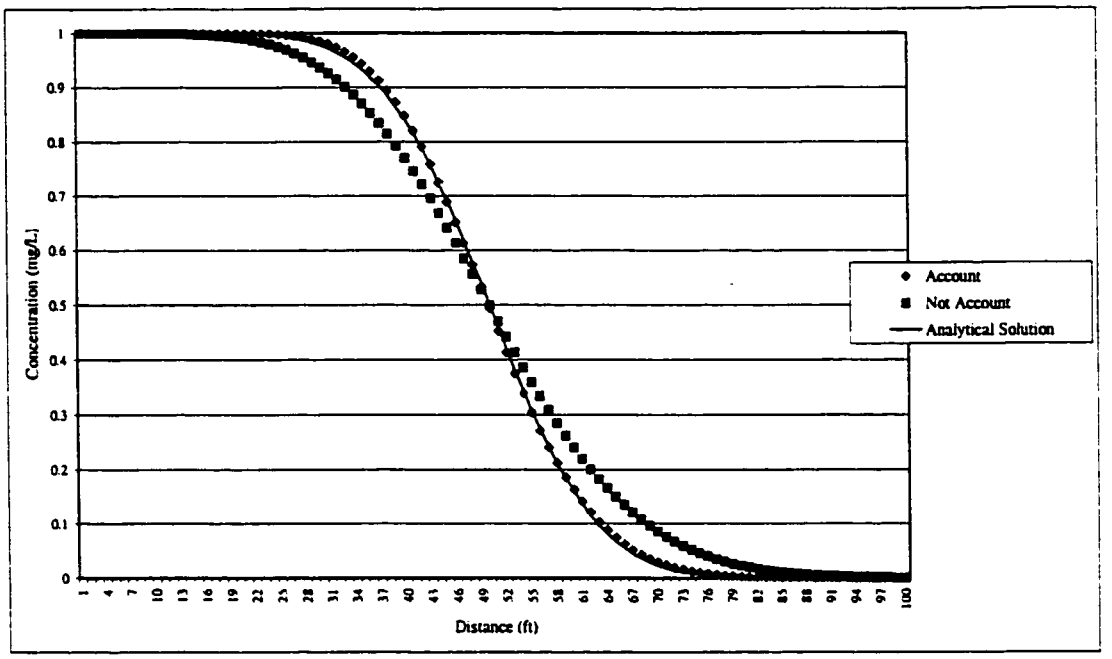

Figure 7.2. Comparison of MULTRAN and analytical solution for conservative contaminant transport in a semi-infinite column accounting for and disregarding numerical dispersion.

Reproduced with permission of the copyright owner. Further reproduction prohibited without permission.

Case 2. Semi-infinite column with reactive contaminant transport via sorption.

The boundary conditions for this case are the same as in Case 1. The partial differential equation is the transport equation in the x-direction including sorption. Hence,

$$D\cdot\frac{\delta^2\cdot C}{\delta x^2} - V\cdot\frac{\delta C}{\delta x} = R\cdot\frac{\delta C}{\delta t} \qquad 7.3$$

where

$$R = 1 + \frac{\rho_b}{\phi}\cdot K_d \qquad 7.4$$

and K_d is the distribution coefficient. As described in Chapter 5, equation 7.4 represents linear sorption.

The analytical solution to equation 7.1 is

$$C(x,t) = \frac{1}{2}\cdot C_o\cdot\left[\operatorname{erfc}\left[\frac{x-\frac{v}{R}\cdot t}{2\cdot\sqrt{\frac{D}{R}\cdot t}}\right] + \exp\left(\frac{xv\cdot R}{D}\right)\cdot\operatorname{erfc}\left[\frac{x+\frac{v}{R}\cdot t}{2\cdot\sqrt{\frac{D}{R}\cdot t}}\right]\right] \qquad 7.5$$

For this case, the model parameters are as follows:

Cell length (Δx):	5 ft.
Cell width (Δy):	1 ft.
Cell depth (Δz):	1 ft.
Seepage velocity (ft/day):	0.25 ft/day
Dispersivity (ft.):	10 ft.
Retardation- R:	2
Length of simulation time (days):	2000 days

With a retardation factor (R) of two, half of the concentration will be sorbed onto the soil. The location where 50% of the contaminant has passed is equal to the seepage velocity

Reproduced with permission of the copyright owner. Further reproduction prohibited without permission.

divided by the retardation factor and multiplied by the simulation time. Here, the distance to the 50% mark is 250 ft. Again with the 50% mark known (x=250 ft.), the numerical results from MULTRAN and those from the analytical solution can be aligned at x=0. The results from this case and the previous case are depicted in Figure 7.3 (for comparison). There is a good correlation between MULTRAN and the analytical solution for this case.

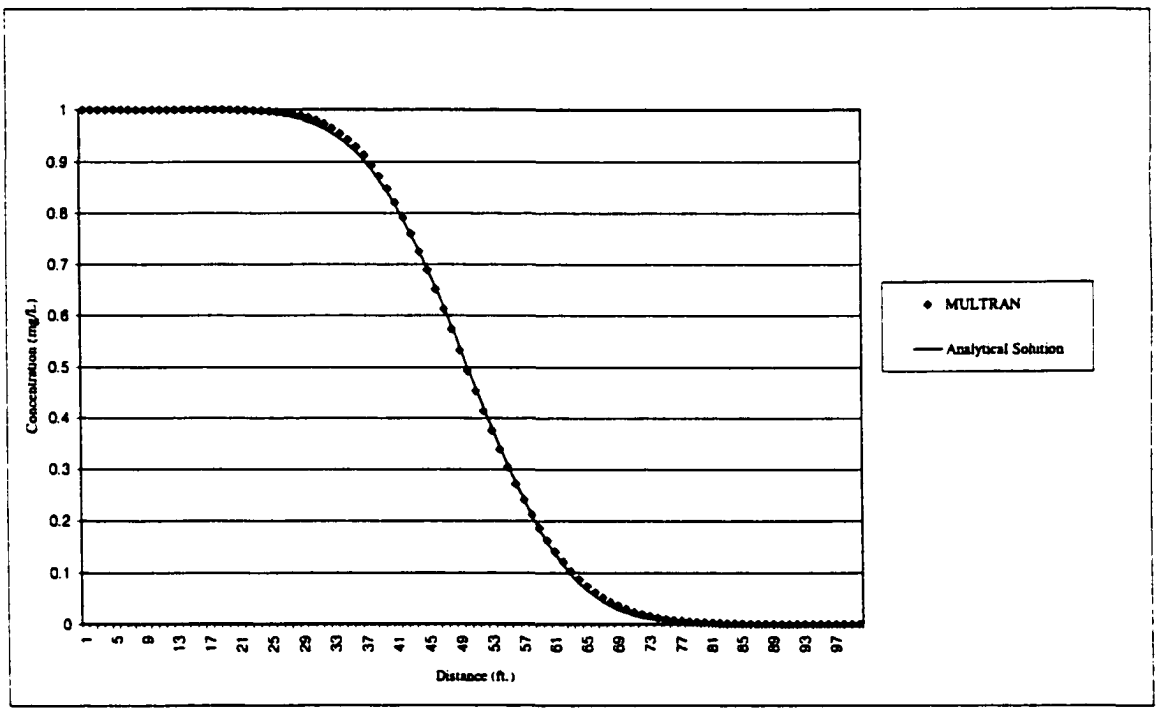

Figure 7.3. Comparison of MULTRAN and analytical solution for reactive contaminant transport in a semi-infinite column via sorption (R).

Case 3. Semi-infinite column with reactive contaminant transport via radioactive decay.

The boundary conditions for this case are the same as in Case 1. The partial differential equation is the transport equation in the x-direction including radioactive decay. Hence,

Reproduced with permission of the copyright owner. Further reproduction prohibited without permission.

$$D\cdot\frac{\delta^2\cdot C}{\delta x^2} - V\cdot\frac{\delta C}{\delta x} - \lambda C = \frac{\delta C}{\delta t} \qquad 7.6$$

where λ is the decay coefficient measured in T^{-1}. The analytical solution to equation 7.6 is

$$C(x,t) = \frac{1}{2}\cdot C_o\cdot\exp\left(\frac{vx}{2D}\right)\cdot\left[\exp(-x\beta)\cdot\operatorname{erfc}\left[\frac{\left(x-\sqrt{v^2+4\cdot\lambda D}\right)\cdot t}{2\cdot\sqrt{Dt}}\right] + \exp(x\beta)\cdot\operatorname{erfc}\left[\frac{\left(x+\sqrt{v^2+4\cdot\lambda D}\right)\cdot t}{2\cdot\sqrt{Dt}}\right]\right] \qquad 7.7$$

where β is defined as

$$\beta = \left(\frac{v^2}{4D^2} + \frac{\lambda}{D}\right)^{\frac{1}{2}} \qquad 7.8$$

For this case, the model parameters are as follows:

Cell length (Δx):	10 ft.
Cell width (Δy):	1 ft.
Cell depth (Δz):	1 ft.
Seepage velocity (ft/day):	0.25 ft/day
Dispersivity (ft.):	10 ft.
Decay coefficient:	0.0003465 $days^{-1}$
Length of simulation time (days):	2000 days

The location where 50% of the contaminant has passed is more difficult to determine here; therefore, the analytical and MULTRAN solutions are matched where C/Co = 50%. The results from this case are depicted in Figure 7.4. There is a very good correlation between MULTRAN and the analytical solution for this case.

Reproduced with permission of the copyright owner. Further reproduction prohibited without permission.

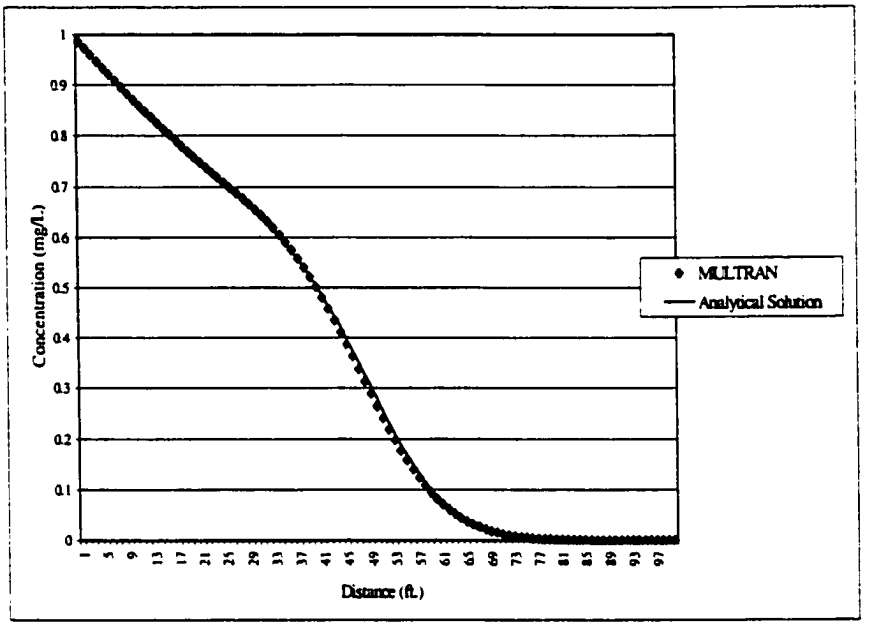

Figure 7.4. Comparison of MULTRAN and analytical solution for reactive contaminant transport in a semi-infinite column via radioactive decay.

Case 4. Semi-infinite column with reactive, multi-species transport via cation exchange.

Using the same boundary conditions as in Case 1, transport via cation exchange between two species is compared with the special analytical solution:

$$(C_1 + C_2) = \frac{1}{2} \cdot C_o \cdot \left(\operatorname{erfc}\left(\frac{x - vt}{2\sqrt{Dt}} \right) + \exp\left(\frac{xv}{D} \right) \cdot \operatorname{erfc}\left(\frac{x + vt}{2\sqrt{Dt}} \right) \right) \qquad 7.9$$

This analytical solution is considered special because whatever two species are simulated, they must be identical in nature; therefore, similar in molecular weight and valance. Equation 7.9 also requires that the equilibrium constant between the two species is equal

Reproduced with permission of the copyright owner. Further reproduction prohibited without permission.

to one. This translates into an equal number of adsorptions and desorptions by each species.

Hence, the following model parameters are set:

Cell length (Δx):	1 ft.
Cell width (Δy):	1 ft.
Cell depth (Δz):	1 ft.
Seepage velocity (ft/day):	1.2 ft/day
Dispersivity (ft.):	3 ft.
Length of simulation time (days):	2000 days
Initial Adsorbed Conc. of C_1:	1200 mg/L
Cation Exchange Capacity (CEC):	0.1
Molecular weight of $C_1$and C_2:	12.0
Valence of C_1 and C_2:	1.0

Figure 7.5 depicts the comparison of MULTRAN to the analytical solution. MULTRAN's results compare well with the analytical solution. Also from this case study, two further observations can be made as shown in Figures 7.6 and 7.7.

In Figure 7.6, one can see the dramatic increase in C_1 from its constant concentration input of 500 mg/L. In fact, concentrations reach as high as 673 mg/L. This anomaly is derived from dissolved C_2 replacing initially adsorbed C_1 on the media; thereby, releasing dissolved C_1 into the system. Also, the concentration curve for C_2 does not imitate the characteristic "S-shaped" curve most often encountered. This is due to C_2 being adsorbed onto the soil.

Reproduced with permission of the copyright owner. Further reproduction prohibited without permission.

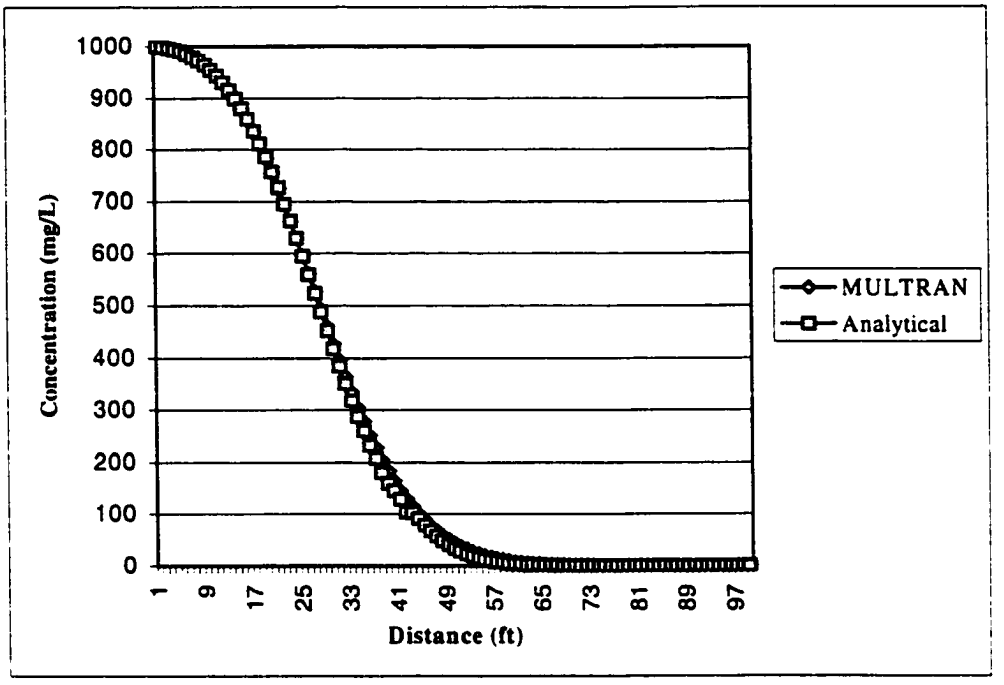

Figure 7.5. Comparison between MULTRAN and the analytical solution for multi-species transport

Figure 7.6 indicates the sorbed concentration of C_1 and C_2. Because the soil is initially at the cation exchange capacity of 0.1 (due to an initial adsorbed concentration of 1200 mg/L of C_1) and since the equilibrium constant is set to 1.0, the sorption concentration curves are symmetric. Hence, as mention previously, for every amount of one species' adsorption there must be an identical amount of desorption by the second species. (Note that the CEC for this case is calculated by converting the initial sorbed concentration, 1200 mg/L, into moles by dividing by C_1's molecular weight, 12, and by a factor of 1000 for conversion purposes.)

Reproduced with permission of the copyright owner. Further reproduction prohibited without permission.

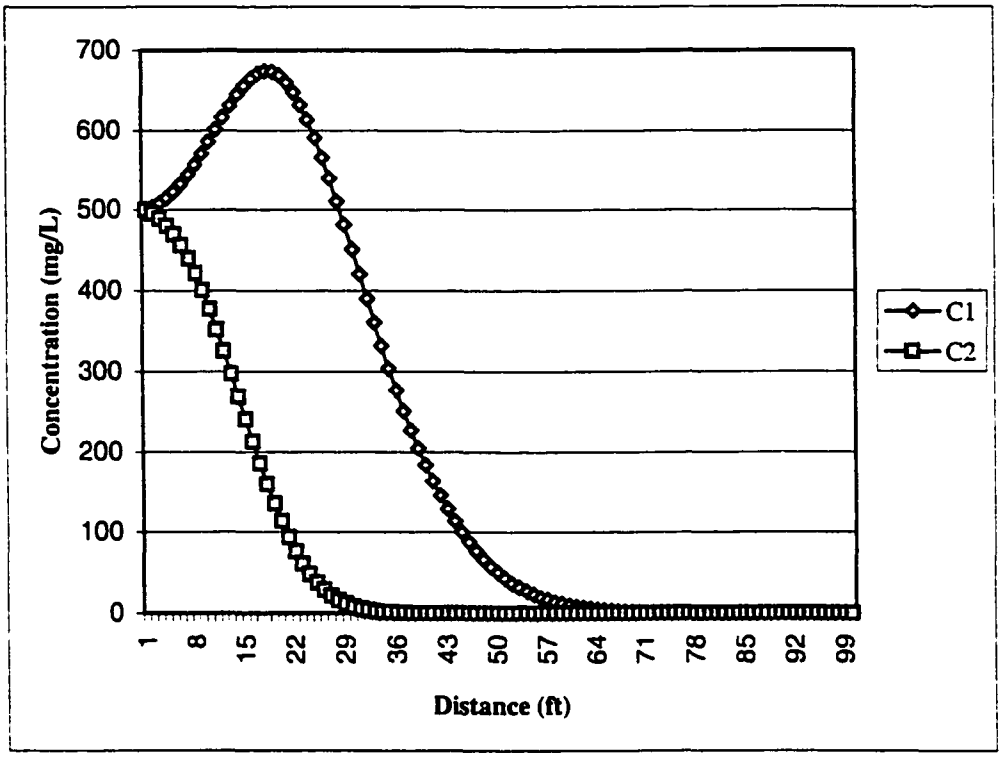

Figure 7.6. Dissolved concentration profile for C_1 and C_2.

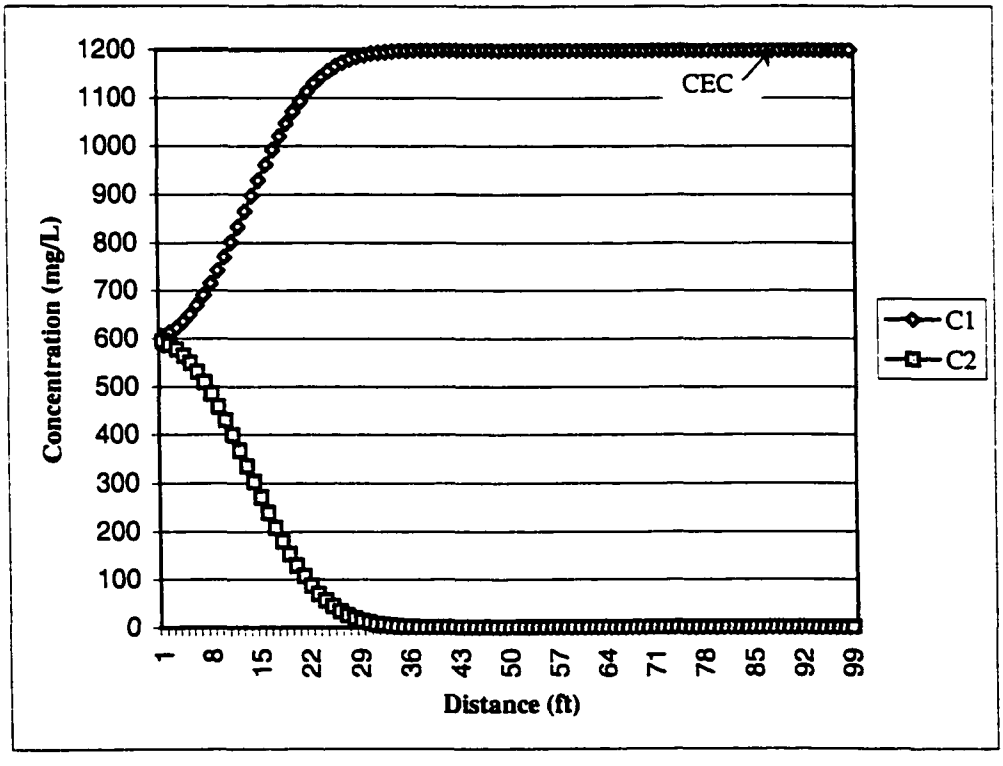

Figure 7.7. Adsorbed concentration profile of C_1 and C_2.

Reproduced with permission of the copyright owner. Further reproduction prohibited without permission.

Case 5. Two-dimensional, conservative contaminant transport with uniform flow: Comparing MULTRAN, the analytical solution, and MT3D.

The purpose of this case study is to verify MULTRAN's capability to model contaminant transport in two dimensions. To verify this, MULTRAN's results are compared with both the analytical solution and MT3D for a two-dimensional case involving uniform flow and contaminant input via a source well. Figure 7.8 depicts the model configuration. Other model parameters are as follows:

Cell length (Δx):	10 ft.
Cell width (Δy):	10 ft.
Cell depth (Δz):	10 ft.
Longitudinal dispersivity (ft.):	10 ft.
Transverse dispersivity (ft.):	5 ft.
Length of simulation time (days):	4 days
Porosity:	0.3

The analytical solution is derived from the instantaneous point source solution by converting to a form of the continuous line solution shown as

$$C(x,y,z,t)=\left[\sum_{i=1}^{N}\left[\frac{M_i}{4\cdot\phi\cdot B\cdot(t-t_i)\cdot\sqrt{D_L\cdot D_{TH}}}\cdot\exp\left[-\frac{\left[x-\upsilon\cdot(t-t_i)\right]^2}{4\cdot D_L\cdot(t-t_i)}-\frac{y^2}{4\cdot D_{TH}\cdot(t-t_i)}\right]\right]\right] \qquad 7.10$$

where: C: mass of solute per volume of solution (M/L^3)
M_i: constant mass of solute entering the system (M)
ϕ: aquifer porosity
B: aquifer thickness (L)
t: time at which concentration is to be calculated (D)
t_i: time at which excitation occurred (D)
D_L: longitudinal dispersion coefficient (L^2/D)
D_{TH}: transverse dispersion coefficient (L^2/D)
υ: seepage velocity (L/D)
x: x-coordinate where concentration is determined (L)
y: y-coordinate where concentration is determined (L)
N: number of steps to reach time, t.

Reproduced with permission of the copyright owner. Further reproduction prohibited without permission.

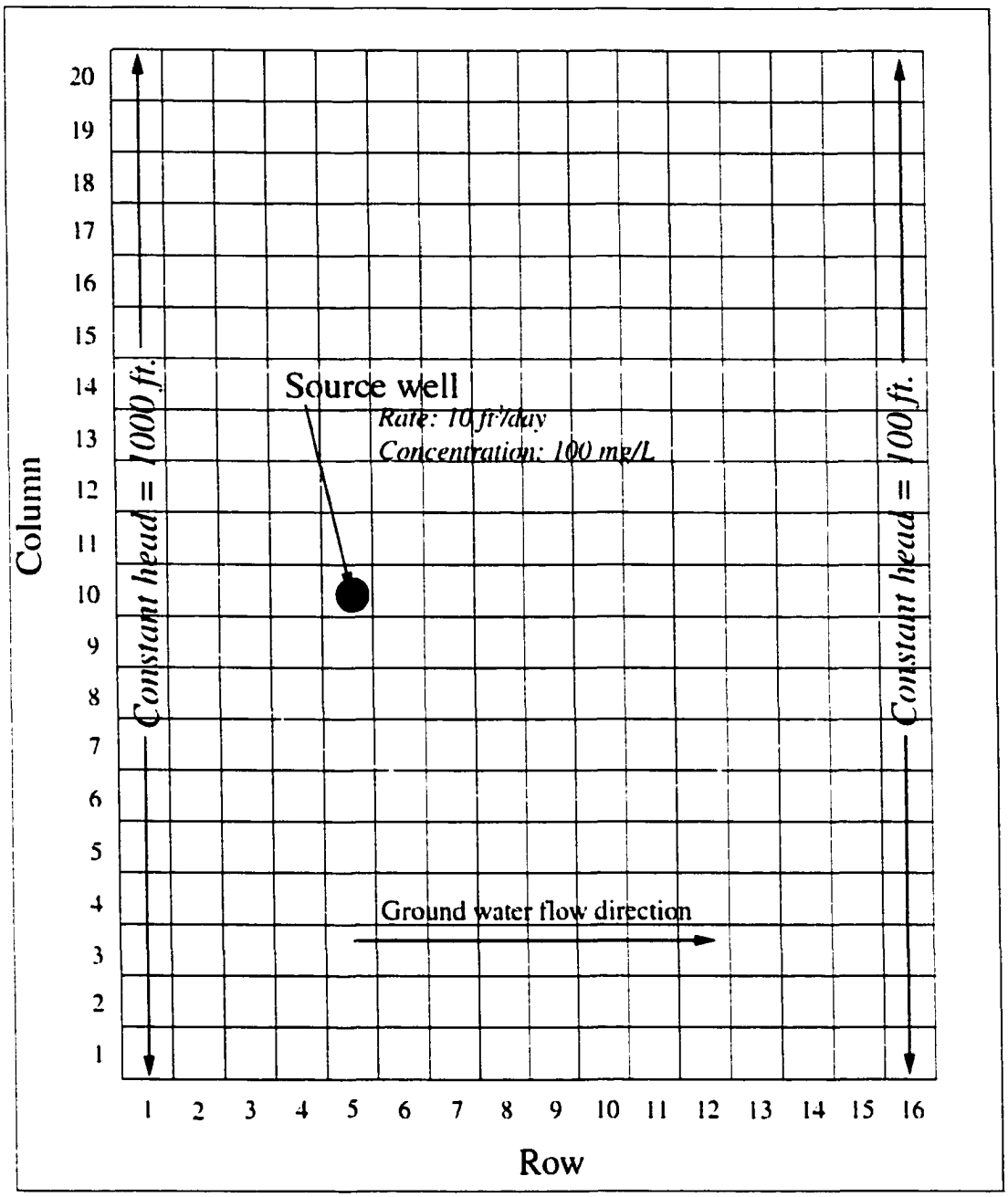

Figure 7.8. Model configuration for two-dimensional transport in uniform flow.

The constant mass, M_i, is determined from the product of the input concentration, the source well input rate, and the constant time step interval. The resulting concentration for each interval, i, is actually the instantaneous line solution determined at the midpoint of

Reproduced with permission of the copyright owner. Further reproduction prohibited without permission.

each excitation, t_i. Excitation occurs at the origin (x=y=0) of input which is the source well located at cell (10,5).

The time step determined by MULTRAN is 0.5 days. Therefore, the same time step is used in the analytical solution and MT3D. For MT3D, the hybrid method of characteristics, or HMOC option, is utilized with the other model parameters indicated in the input files in Appendix D. The time step for MT3D was initial determined by the model to be approximately 0.16 days; however, the results were typically shy of the analytical solution. To improve MT3D's results and to keep the time step consistent between the methods, the MT3D time step variable, DT0, is set to 0.5 days.

The results from MULTRAN, the analytical solution, and MT3D are shown in Figure 7.9. Concentration contours are drawn for 0.01, 0.02, 0.1, and 0.5 mg/L. MULTRAN closely matches the analytical solution both upstream and downstream from the well at each contour interval. MT3D also matches well except for slight over-estimations along the central longitudinal axis of each contour interval.

Reproduced with permission of the copyright owner. Further reproduction prohibited without permission.

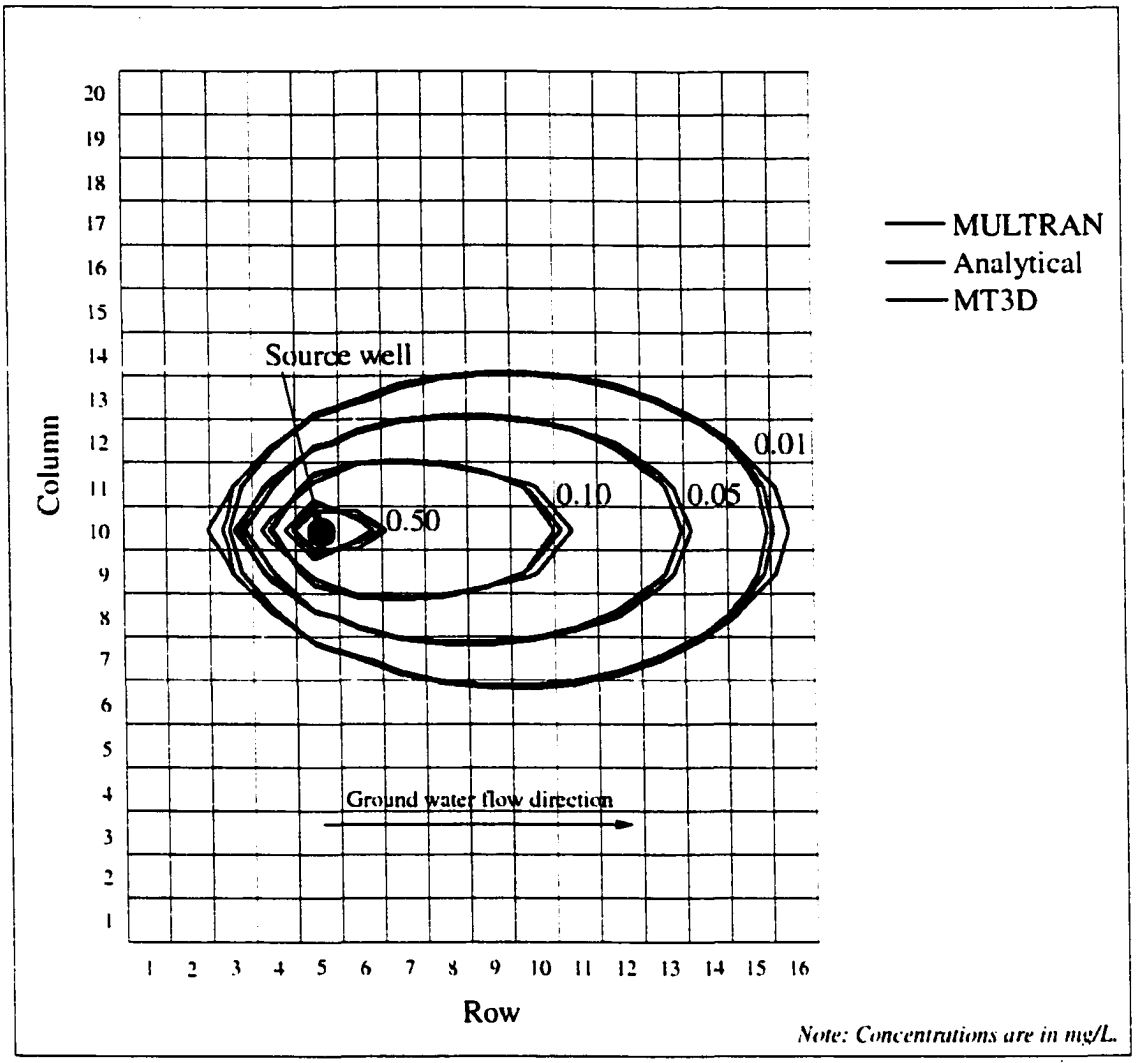

Figure 7.9. Contour plot of two-dimensional transport comparing MUTRAN with MT3D.

Reproduced with permission of the copyright owner. Further reproduction prohibited without permission.

Case 6. Two-dimensional, conservative contaminant transport in a heterogeneous aquifer.

For this case study, a two-dimensional, heterogeneous aquifer comprised of 20 rows and 16 columns is analyzed. A similar case study was conducted by Zheng (1996) using MT3D. The northern and southern boundaries of the aquifer system are set with constant head cells. The northern boundary has a constant head of 250 ft. and the southern boundary a varying constant head ranging from 12.0 ft. to 52.5 ft. (see Figure 7.10). The aquifer has a hydraulic conductivity of 1.0 ft/day everywhere in the system except in a small zone as shown in Figure 7.10. This small zone represents a hydraulic conductivity value of 0.001 ft/day. Contaminant with a concentration of 100 mg/L enters the aquifer via a northern well flowing at a rate of 50 ft^3/day. This well, as depicted in Figure 7.10, is located above the low conductivity zone. A second well located beneath the low conductivity zone, extracts water at 100 ft^3/day. Additional aquifer parameters are as follows:

Cell length (Δx):	10 ft.
Cell width (Δy):	10 ft.
Cell depth (Δz):	10 ft.
Longitudinal dispersivity (ft.):	10 ft.
Transverse dispersivity (ft.):	5 ft.
Length of simulation time (days):	70 days
Porosity:	0.3

From Figure 7.10, the general flow progresses southward from the source well, Well A, toward the area of low conductivity, continues clockwise around and then beneath the area of low conductivity, and beyond the sink well, Well B, toward the southwest corner of the aquifer system. With the flow vectors plotted, the general contaminant path is hence described.

Reproduced with permission of the copyright owner. Further reproduction prohibited without permission.

Simulating contaminant input by Well A for 70 days, the shape of the plume begins to imitate the general ground water flow pattern as indicated in Figure 7.10. The shape of the contaminant plume is shown in Figure 7.11. There are four specific regions of the aquifer system that are of interest. They are as follows:

1. Well A: Concentration values are high near the source well as would be expected. The approximate concentration at the source is 34 mg/L. This concentration value is less than the input water concentration of 100 mg/L because this finite difference cell is treated as a source cell, not a constant concentration cell. Over the 70-day period, approximately 1170 mg/L of contaminant enters through Well A.
2. Zone 1: A small amount of contaminant passes through the low conductivity zone.
3. Zone 2 (see Figure 7.11): Concentrations begin to increase as contaminant encounters the low conductivity area and advect and disperse to either side—thought mainly clockwise around the low conductivity area.
4. Well B: A slight contour indentation indicates the removal of contaminant by Well B.

This case study indicates MULTRAN's general ability to simulate contaminant transport in two dimensions.

Reproduced with permission of the copyright owner. Further reproduction prohibited without permission.

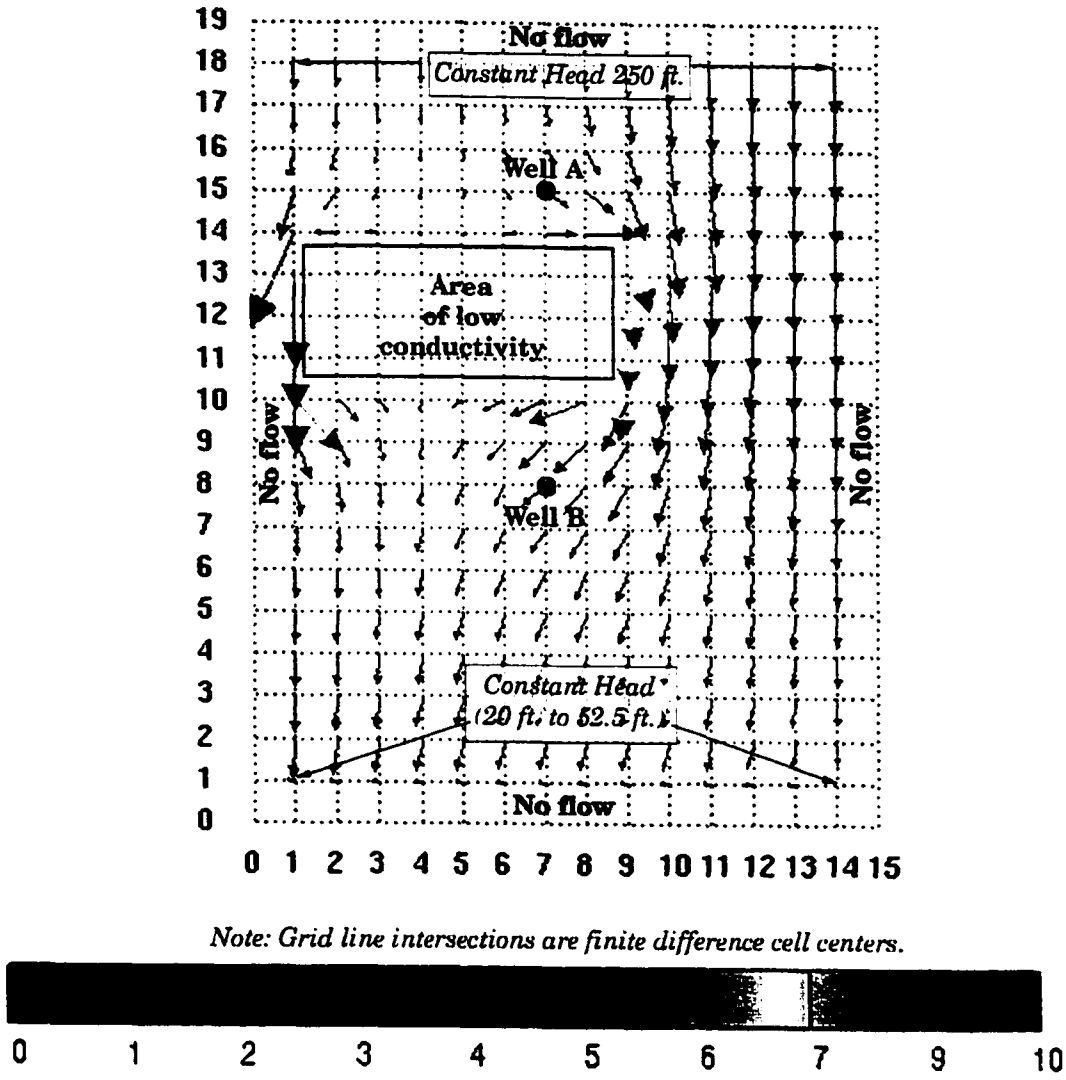

Figure 7.10. Two-dimensional field of velocity magnitude vectors for Case 6.

Reproduced with permission of the copyright owner. Further reproduction prohibited without permission.

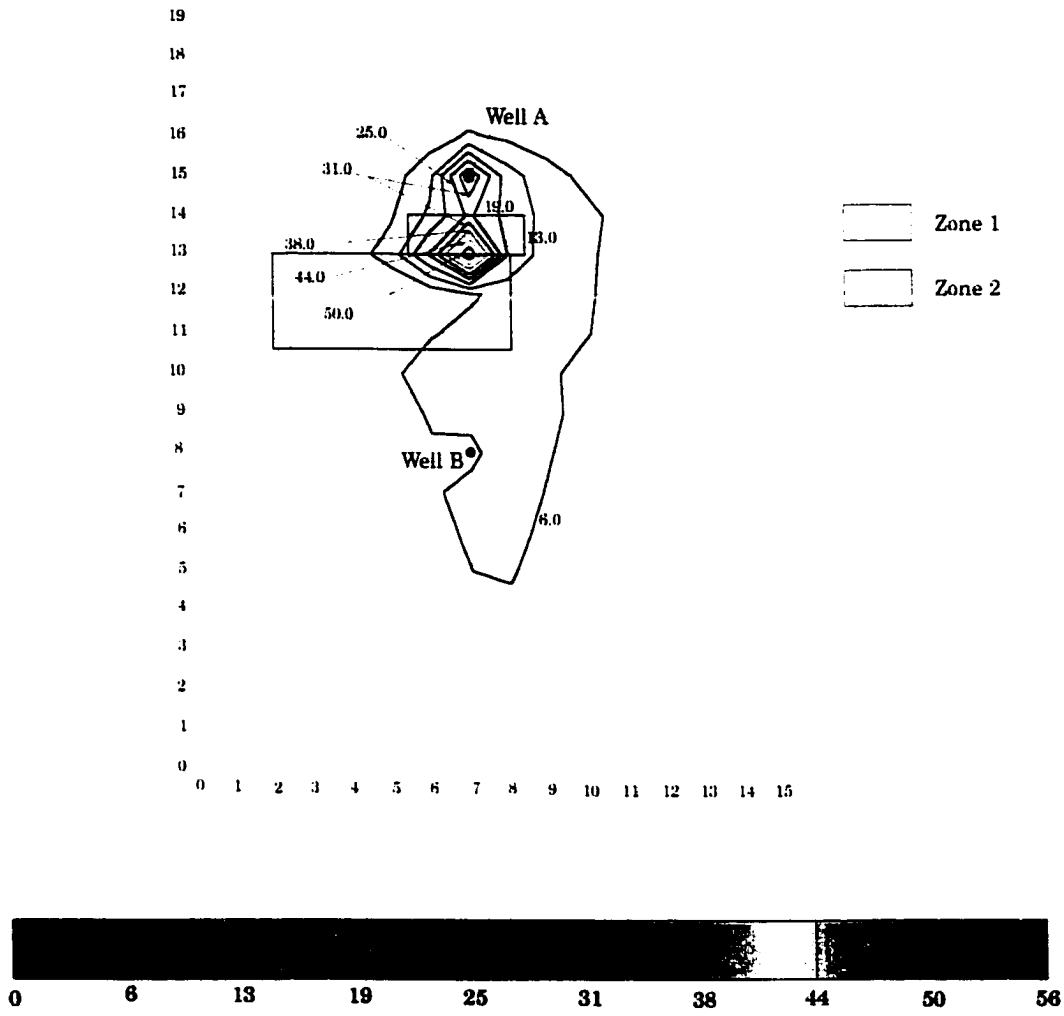

Figure 7.11. Contaminant contour plot for Case 6.

Reproduced with permission of the copyright owner. Further reproduction prohibited without permission.

Case 7. Three-dimensional, conservative contaminant transport: Comparing MULTAN and MT3D.

The purpose of this study is to verify MULTRAN's three-dimensional transport capability by comparing its results with the analytical solution. Results from using MT3D is also included for comparison. A three-dimensional model is developed with contaminant input from a source well. There are 31 rows, 50 columns and 5 layers. The source well is located in row 15, column 10, and layer 3. Ground water flow flows from the western boundary to the eastern boundary. The velocity variations caused by the source well is insignificant compared to the ground water velocity; thus, the flow is uniform. The well input rate is 10 ft^3/day with a concentration of 1000 mg/L. Other model parameters are as follows:

Cell length (Δx):	10 ft.
Cell width (Δy):	10 ft.
Cell depth (Δz):	5 ft.
Longitudinal dispersivity (ft.):	10 ft.
Transverse dispersivity (ft.):	5 ft.
Vertical dispersivity (ft.):	1 ft.
Length of simulation time (days):	20 days
Porosity:	0.3

To determine the analytical solution for a continuous source within a three-dimensional system, the instantaneous point source solution (equation 7.11)

$$C(x,y,z,t)=\frac{M_3}{8\cdot\phi\cdot\sqrt{\pi^3\cdot t^3\cdot D_L\cdot D_{TH}\cdot D_{TV}}}\cdot\exp\left[-\frac{1}{4t}\cdot\left[\frac{(x-vt)^2}{D_L}+\frac{y^2}{D_{TH}}+\frac{z^2}{D_{TV}}\right]\right] \qquad 7.11$$

is integrated with respect to time (equation 7.12)

$$C(x,y,z,t)=\frac{M}{8\cdot\phi\cdot\sqrt{\pi^3\cdot D_L\cdot D_{TH}\cdot D_{TV}}}\cdot\int_0^t (t-\tau)^{-1.5}\cdot\exp\left[-\frac{(x-v\cdot(t-\tau))^2}{4\cdot D_L\cdot(t-\tau)}-\frac{1}{4\cdot(t-\tau)}\cdot\left(\frac{y^2}{D_{TH}}+\frac{z^2}{D_{TV}}\right)\right]d\tau \qquad 7.12$$

Reproduced with permission of the copyright owner. Further reproduction prohibited without permission.

to arrive at the following analytical solution, as shown by Hunt (1983):

$$C(x,y,z,t)=\frac{M\cdot\exp\left(\frac{x\cdot v}{2\cdot D_L}\right)}{8\cdot\phi\cdot\sqrt{D_{TH}\cdot D_{TV}}\cdot R}\cdot\left(\exp\left(\frac{-a\cdot R}{\sqrt{D_L}}\right)\cdot\operatorname{erfc}\left(\frac{R}{2\cdot\sqrt{D_L\cdot t}}-a\cdot\sqrt{t}\right)+\exp\left(\frac{a\cdot R}{\sqrt{D_L}}\right)\cdot\operatorname{erfc}\left(\frac{R}{2\cdot\sqrt{D_L\cdot t}}+a\cdot\sqrt{t}\right)\right) \quad 7.13$$

where

$$R=\sqrt{x^2+\frac{D_L}{D_{TH}}\cdot y^2+\frac{D_L}{D_{TV}}\cdot z^2} \quad 7.14$$

$$a=\sqrt{\frac{v^2}{4\cdot D_L}} \quad 7.15$$

The mass in equation 7.13 is the mass flux entering the system that has the units (M/T). The vertical dispersion coefficient is termed D_{TV} in equation 7.13. The other terms have previously been defined in Case 7.

The results of this case study are shown in Figure 7.12. Only layers 2-4 are shown here. MULTRAN clearly matches the analytical solution with good accuracy within each layer shown. MT3D's results are included to show MULTRAN's capability to match MT3D in three-dimensional analyses. In conclusion of this case study, MULTRAN is capable of producing reliable results in three-dimensional systems.

Reproduced with permission of the copyright owner. Further reproduction prohibited without permission.

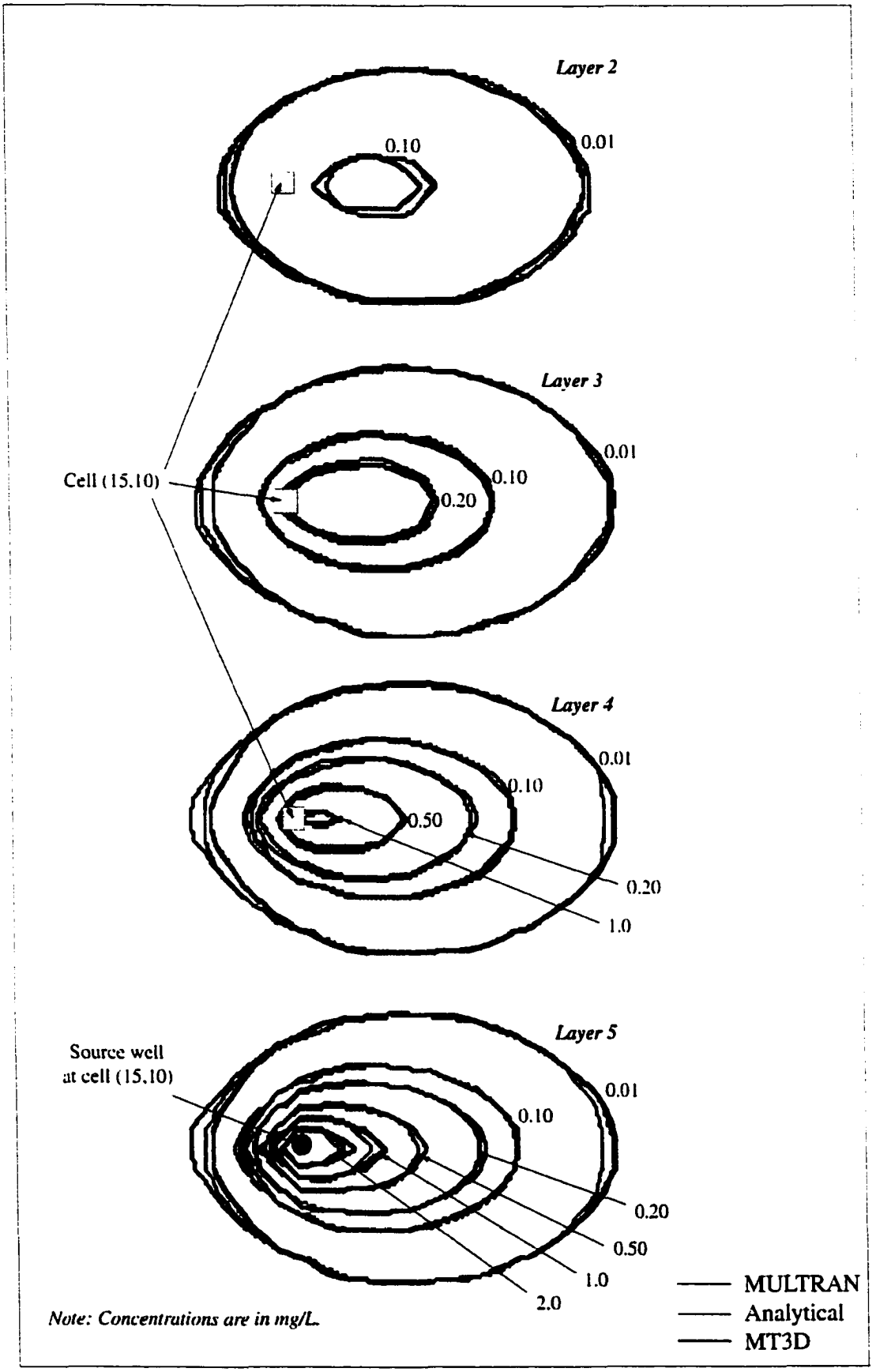

Figure 7.12. Comparison of MULTRAN, analytical solution, and MT3D for a three dimensional case.

Reproduced with permission of the copyright owner. Further reproduction prohibited without permission.

Case 8: Site analysis of contaminant cleanup using natural ground water flushing or an injection of a competing cation to compare cleanup times. MT3D results are included.

The purpose of this case study is to portray the power of MULTRAN as a multi-species contaminant transport model. Single species models can only allow the flushing of contaminants from a system using water exclusive of any reactive qualities. To illustrate this point more clearly, a case site is proposed consisting of an injection well, extraction well and two chemical components, C_1 and C_2, that describe the natural ground water chemistry and the contaminant, respectively.

Before the contaminant, C_2, is injected into the ground water system, the ground water is assumed to have a dissolved phase concentration of 50 mg/L including all of the exchange sites filled to the CEC of 0.0217, or 500 mg/L of C_1. The model is transient with two designated stress periods. For the first stress period, reactive C_2 at a concentration of 10000 mg/L is injected into the aquifer via a source well at a rate of 100 ft^3/d. After three days of injecting C_2 into the aquifer, a cleanup process will begin to remove C_2 from the aquifer; hence, the beginning of the second stress period.

The second stress period spans 500 days. An extraction well directly downstream from the source well pumps at a rate of 100 ft^3/d. The source well continues to pump at its previous rate, but under two scenarios. The first scenario is to attempt cleanup by flushing C_2 from the system with natural ground water. The second scenario involves increasing the amount of C_1 already present in the ground water regime to 10000 mg/L. Again, the ground water already contains 50 mg/L of dissolved C_1 that is not a harmful component.

With the idea of the case study understood, the model is developed. The model consists of 20 rows by 16 columns and one layer. Each cell is a ten foot cube. The

Reproduced with permission of the copyright owner. Further reproduction prohibited without permission.

source well is located at cell (10,4) and the extraction well at cell (10,13). The eastern and western boundaries are designated as constant head cells. Ground water flow is from west to east. The longitudinal and transverse dispersivity values are 10 ft. and 5 ft., respectively.

The chemical components, C_1 and C_2, are also given certain physical parameters which is required by MULTRAN for multi-species transport. Because MT3D is a single-species transport model, only the input concentration of C_2 is required along with information pertaining to the chosen isotherm. For MULTRAN, the following parameters for C_1 and C_2 are supplied:

Molecular weight of C_1:	23.0
Molecular weight of C_2:	24.0
Valance of C_1:	1.0
Valence of C_2:	1.0
Equilibrium constant:	4.0

To determine the equilibrium constant for MT3D, MULTRAN's results of the dissolved and adsorbed concentrations for the first stress period are plotted. The resulting equilibrium constant is 50 cm^3/gm: similar to units of the bulk density, ρ_b, which is 2.65 gm/cm^3. The isotherm is linear. The input data files for this case study are in Appendix D.

For this case study, three simulations are conducted. The first simulation involves flushing C_2 from the system using the natural ground water. The second involves flushing C_2 from the system using a high concentration of C_1 to compete for exchange sites to which C_2 has adsorbed. Both of these simulations are conducted using MULTRAN. The last case is to use MT3D in a similar way as in the first simulation.

Reproduced with permission of the copyright owner. Further reproduction prohibited without permission.

In Figure 7.13, the dissolved and sorbed concentrations for each pre-described simulation are depicted. In reference to the first simulation, the cleanup of the aquifer is an arduous process since a majority of C_2 is adsorbed to the soil and is difficult to remove from the matrix. The dissolved concentration drops rapidly as cleanup begins with the curve growing more asymptotic as time progresses. Cleanup of the aquifer is reached when the concentration of C_2, dissolved and adsorbed, is reduced to an acceptable level. For this case, concentrations of C_2 need to drop below 20 mg/L. After 500 days of flushing with natural ground water, the dissolved phase concentration of C_2 is approximately 9.4 mg/L. This value is below the required minimum. However, the adsorbed phase concentration is approximately 350 mg/L. Though sorbed C_2 may not currently cause any environmental/health problems, continual desorption of C_2 after flushing may increase the dissolved amounts of C_2 to above the minimum 20 mg/L requirement.

For the second simulation, the dissolved concentration of C_2 reaches a higher level at the beginning of cleanup (3900 mg/L) than in the first simulation (3600 mg/L). This higher dissolved concentration amount is due to the fact that the additional amount of C_1 is competing for exchange sites; thereby, releasing more C_2 into the dissolved phase for removal by the extraction well. Hence, this is affirmed by the lower amount of adsorbed C_2 than in the first simulation (see Figure 7.13). At the end of the second stress period, the dissolved and adsorbed C_2 concentrations are approximately 0.23 mg/L and 12.4 mg/L, respectively. Both of these levels are below the required minimum.

Reproduced with permission of the copyright owner. Further reproduction prohibited without permission.

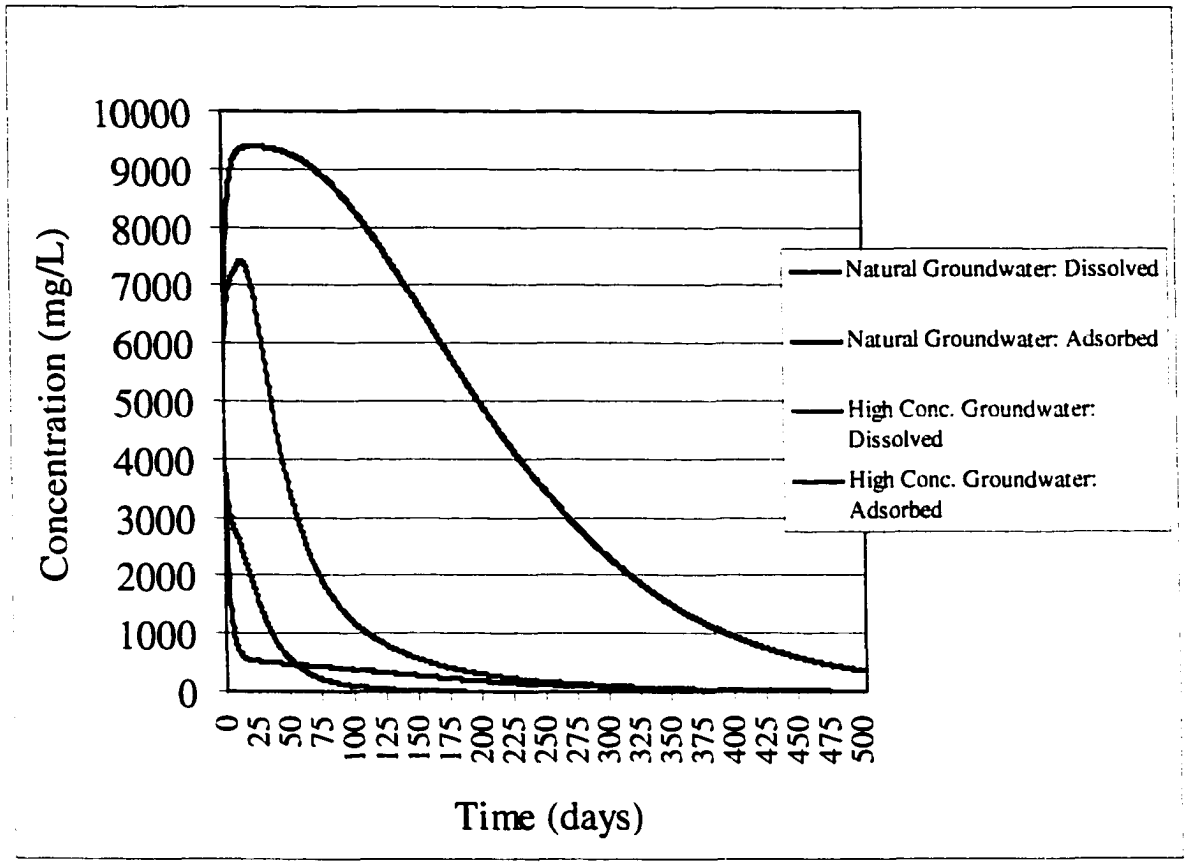

Figure 7.13. Concentration amounts for dissolved and adsorbed C_2 for the two, pre-defined simulations during the cleanup stage (Stress period 2).

Based upon this minimum concentration, the aquifer is actually clean by day 455 with the dissolved and adsorbed concentrations at approximately 0.4 mg/L and 19.9 mg/L, respectively.

The last simulation involves modeling the system using MT3D. Problems were encountered using MT3D for this particular problem. The choice of the advection scheme (MMOC using the Euler algorithm) resulted in a reasonably shaped curve. The other schemes and algorithms resulted in oscillations. The results from this scenario are not shown or discussed due to their possible erroneous nature.

Reproduced with permission of the copyright owner. Further reproduction prohibited without permission.

A second graph is made of the mass of C_2 removed at the extraction well located downstream from the source well (see Figure 7.14). The amount of mass removed in the first simulation follows a pattern of first slowly increasing, then peaking, and finally dropping to toward zero. The slow increase is due to the lag time of the added dissolved amount of C_2 near the source well to reach the extraction well. As more of C_2 desorbs from the soil matrix, the mass extracted by the well increases to a point where the mass of C_2 peaks during removal. The decrease in mass removed is indicative of lesser amounts of sorbed mass to be released and finishing cleanup.

As for the second simulation, the added C_1 to the flushing process releases a large amount of C_2 into the dissolved phase for removal by the extraction well. Cleanup is achieved more quickly using a competing component for exchange sites. The use of a multi-species model aids consultant's estimates of cleanup time and resulting contaminant concentrations since competing species for exchange sites give markedly different results than just flushing with natural ground water. This case study not only this depicts this process, but also indicates the capability of MULTRAN as a multi-species modeling tool.

Reproduced with permission of the copyright owner. Further reproduction prohibited without permission.

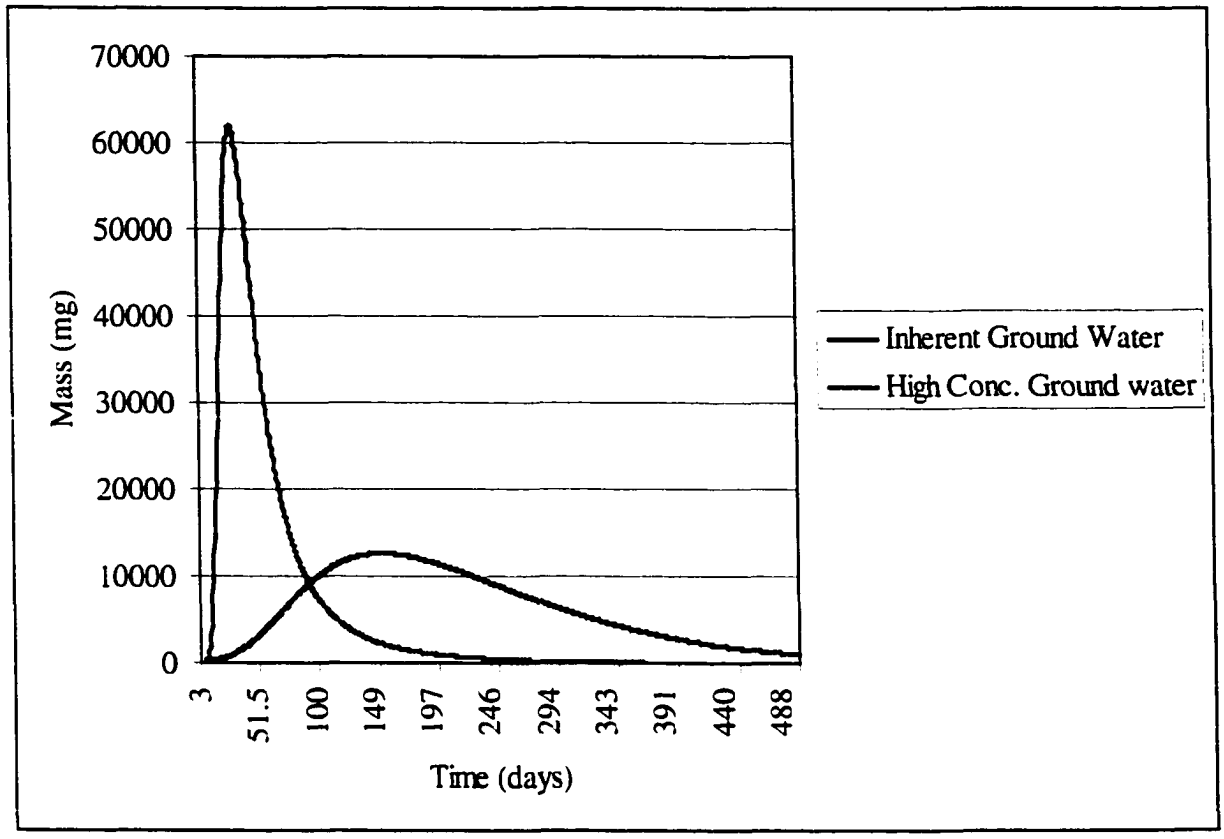

Figure 7.14. Mass of C_2 removed by the extraction well during the cleanup phase for the first and second simulation.

Reproduced with permission of the copyright owner. Further reproduction prohibited without permission.

Chapter 8

Conclusion and Recommendations

Ground water contamination will continue to occur since nothing is perfectly sealed or always environmentally safe. To return ground water systems to their previous state before contamination, remediation is necessary. Tools to aid agencies and environmental contractors to determine contaminant migration and its fate are available in many different forms such as analytical solutions, numerical models, and laboratory experiments.

Analytical models can provide a quick analysis of contaminant migration, yet are restricted to a particular set of conditions. Laboratory experiments are helpful in acquiring pertinent field data; however, little information on contaminant migration can be provided through these analyses. Numerical models bridge the inability or limited nature of analytical models and utilize the data acquired through laboratory experiments.

As there are a number of tools to study ground water contamination, so there are a number of numerical models for analyzing contaminant migration and its fate. Popular contaminant transport models, such as MT3D, are used widely for single species transport. However, ground water chemistry and/or multiple species can sometimes affect the transport of contaminants. Though models exist that can handle multi-species transport, an easy to understand model that also connects to the extremely popular ground water model, MODFLOW, does not exist.

Therefore, the multi-species, three-dimensional, contaminant transport model, MULTRAN, is developed to fill this need. MULTRAN is a finite difference model that can simulate the stress packages associated with MODFLOW, capable of handling single

Reproduced with permission of the copyright owner. Further reproduction prohibited without permission.

species transport akin to MT3D, and handle multi-species transport. MULTRAN requires eight input files, three of which are previously needed or created by running MODFLOW.

Verification of MULTRAN's numerical code and contaminant transport modeling capability is conducted for one-, two-, and three-dimensional systems. In all cases, MULTRAN matches the analytical solutions well. Including MT3D's results in these solutions, which also match the analytical solutions, shows MULTRAN's ability to model single species transport similar to that of MT3D. Though single species transport is possible with MULTRAN, the main thrust of this study is the modeling of multi-species transport.

To show this multi-species capability and its significance in contaminant transport, an example case study involving remediation of a contaminated site is conducted. Clearly, the adding of a competing species that can be used to drive off contaminants from the soil matrix will aid and expedite the cleanup process. MULTRAN's multi-species capability indicates this procedure to be true.

Therefore, MULTRAN allows modelers a greater freedom in modeling contaminated ground water systems due to MULTRAN's multi-species capability. Yet with most models, recommendations are necessary to better the model's ability to solve the often, complex ground water contamination problems or to meet other needs of the modeler. Following is a list of recommendations for MULTRAN:

1. Use MULTRAN in the field to estimate contaminant migration and its fate so to continually validate MULTRAN's capability.

Reproduced with permission of the copyright owner. Further reproduction prohibited without permission.

2. Port MULTRAN to Microsoft's® Visual Basic program so MULTRAN may be more accessible to modelers.
3. Possibly change MULTRAN from having to account for numerical dispersion due to the space and time derivative to adjusting the advection and time partial differentials to second order accuracy.
4. Provide descriptions on how to include additional stresses added to MODFLOW into MULTRAN's coding.

Reproduced with permission of the copyright owner. Further reproduction prohibited without permission.

References

Afifi, S. A Three-Dimensional Finite-Element Model for Reactive Multicomponent-multispecies Subsurface Transport, Dissertation Colorado State University, 1994.

Appelo, C. A., 1994. Some Calculations on Multicomponent Transport with Cation Exchange in Aquifers, Ground Water, Vol. 32, No. 6, pp. 968-975.

Bajracharya, K. and Barry, D. A., 1995. Analysis of One-dimensional Multispecies Transport Experiments in Laboratory Soil Columns, Environmental International, Vol. 21, No. 5, pp. 687-691.

Barry, D. A., Miller, C. T., Culligan, P. J., *et al.*, 1997. Analysis of Split Operator Methods for Nonlinear and Multispecies Groundwater Chemical Transport Models, Mathematics and Computers in Simulation, Vol. 43, No. 3/6, pp. 331-341.

Bear, J. Hydraulics of Groundwater. McGraw- Hill Inc., 1979.

Bear, J. and Bachmat, Y., 1967. A Generalized Theory on Hydrodynamic Dispersion in Porous Media, International Association of Scientific Hydrology, Symposium of Haifa, pp. 7-16.

Bjerg, P. L., Ammentorp, H. C., and Christensen, T. H., 1993. Model Simulations of a Field Experiment on Cation Exchange-affected Multicomponent Solute Transport in a Sandy Aquifer, Journal of Contaminant Hydrology, Vol. 12, No. 4, pp. 291-311.

Borkovec, M., Burgisser, C. S., Miroslav, C., *et al.*, 1996. Quantitative Description of Multi-component Reactive Transport in Porous Media: An Empirical Approach, Transport in Porous Media, Vol. 25, No. 2, pp. 193-204.

Brussino, G. and Sonnad, V., 1989. A Comparison of Direct and Preconditioned Iterative Techniques for Sparse, Unsymmetric Systems of Linear Equations, International Journal for Numerical Methods in Engineering, Vol. 28, No. 4, pp. 801-815.

Bryant, S. L., Schechter, R. S., and Lake, L. W., 1986. Interactions of Precipitation/Dissolution Waves and Ion Exchange in Flow Through Permeable Media, AIChE Journal, Vol. 32, No. 5, pp. 751-764.

Cederberg, G. A., Street, R. L., and Leckie, J. O., 1985. A Groundwater Mass Transport and Equilibrium Chemistry Model for Multicomponent Systems, Water Resources Research, Vol. 21, No. 8, pp. 1095-1104.

Reproduced with permission of the copyright owner. Further reproduction prohibited without permission.

Cernik, M., Barmettler, K., Grolimund, D., *et al.*, 1994. Cation Transport in Natural Porous Media on Laboratory Scale: Multicomponent Effects, Journal of Contaminant Hydrology, Vol. 16, pp. 319-337.

Chen, Y.-M., Koniges, A. E., and Anderson, D. V., 1989. ILUBCG2-11: Solution of 11-banded Nonsymmetric Linear Equation Systems by a Preconditioned Biconjugate Gradient Routine, Computer Physics Communications, Vol. 55, No. 3, pp. 359-365.

Chrysikopoulos, C. V., Kitanidis, PP. K., and Roberts, PP. V., 1990. Analysis of One-Dimensional Solute Transport Through Porous Media with Spatially Variable Retardation Factor, Water Resources Research, Vol. 26, No. 3, pp. 437-446.

Clement, T. P., Sun, Y., Hooker, B. S., *et al.*, 1998. Modeling Multispecies Reactive Transport in Ground Water, Ground Water Modeling and Remediation, Vol. 18, No. 2, pp. 79-92.

Edwards, A. L., 1972. TRUMP: A Computer Program for Transient and Steady State Temperature Distributions in Multi-dimensional Systems, Rep. 14754, Rev. 3, Livermore, California, Lawrence Livermore National Laboratory.

Engesgaard, PP. and Christensen, Th. H., 1988. A review of Chemical Solute Transport Models, Nordic Hydrology, Vol. 19, pp. 183-216.

Falta, R. W., *et al*, 1995. T2VOC User's Guide.

Garcia-Delgado, R. A. and Koussis, A. D., 1997. Ground-Water Solute Transport with Hydrogeochemical Reactions, Ground Water, Vol. 35, No. 2, pp. 243-249.

Gelhar, L. and Collins, M., 1971. General Analysis of Longitudinal Dispersion in Nonuniform Flow, Water Resources Research, Vol. 7, No. 6, pp.1511-1521.

Gomis, V., Boluda, N., and Ruiz, F., 1996. Application of a Model for Simulating Transport of Reactive Multispecies Components to the Study of the Hydrochemistry of Salt Water Intrusions, Journal of Contaminant Hydrology, Vol. 22, No. ½, pp. 67-81.

Harris, D. C. Quantitative Chemical Analysis, W. H. Freeman and Company, New York, New York, 1995, pp. 701-703.

Hernand, S. C. and Melancon, S. M. Vadose Zone Modeling of Organic Pollutants, Lewis Publishers, Inc., Chelsea, Michigan, 1986.

Reproduced with permission of the copyright owner. Further reproduction prohibited without permission.

Hu, Q. and Brusseau, M. L., 1995. Dispersive-diffusive Transport of Non-sorbed Solute in Multicomponent Solutions, Journal of Contaminant Hydrology, Vol. 19, No. 4, pp. 261-267.

Hunt, B. Mathematical Analysis of Groundwater Resources. Butterworth and Co. Ltd, 1983.

Javandel, I., Doughty, C. and Tsang, C. Ground Water Transport: Handbook of Mathematical Models. American Geophysical Union, 1984.

Jennings, A. A. and Kirkner, D. J., 1984. Instantaneous Equilibrium Approximation Analysis, Journal of Hydraulic Engineering, Vol. 110, No. 12, pp. 1700-1701.

Kaushik, S. and Hagelstein, P. L., 1992. The Application of the Preconditioned Biconjugate Gradient Algorithm to NLTE Rate Matrix Equations, Journal of Computational Physics, Vol. 101, No. 2, pp. 360-367.

Kipp, K. L., 1987. HST3D: A Computer Code for Simulation of Heat and Solute Transport in Transport in Three-Dimensional Ground-water Flow Systems, Water Resources Investigations Report 86-4095.

Kobus, H. E. and Kinzelbach, W. Contaminant Transport in Groundwater, A. A. Balkema Publishers, Brookfield, Vermont, 1989.

Korsakova, N. K., 1996. Numerical Modeling of Reactive and Nonreactive Solute Transport in Porous Medium, Water Resources, Vol. 23, No. 6, p. 623.

Leij, F. J., Dane, J. H., and van Genuchten, M. Th., 1991. Mathematical Analysis of One-Dimensional Solute Transport in a Layered Soil Profile, Soil Science of America Journal, Vol. 55, No. 4, pp. 944-953.

Lewis, F. M., Voss, C. I., and Rubin, J., 1987. Solute Transport with Equilibrium Aqueous Complexation and Either Sorption or Ion Exchange: Simulation Methodology and Applications, Journal of Hydrology, Vol. 90, No. ???, pp. 81-115.

Lui, C. W. and Narasimhan, T. N., 1989. Redox-controlled Multiple-species Reactive Chemical Transport: 1. Model Development, Water Resources Research, Vol. 25, No. 5, pp. 869-882.

Mansell, R. S., Bond, W. J., Bloom, S. A., 1993. Simulating Cation Transport During Water Flow in Soil; Two Approaches, Soil Science Society of America Journal, Vol. 57, No. 1, pp. 3-9.

Reproduced with permission of the copyright owner. Further reproduction prohibited without permission.

Mikic, Z. and Morse, E. C., 1985. The Use of a Preconditioned Bi-Conjugate Gradient Method for Hybrid Plasma Stability Analysis, Journal of Computational Physics, Vol. 61, No. (**looked?**), pp. 154-185.

Moldrup, P., Yamaguchi, T., Hanson, J. A., and Rolston, D. E., 1992. An Accurate and Numerically Stable Model for One-Dimensional Solute Transport in Soils, Soil Science, Vol. 153, No. 4, pp. 261.

Morel, F. and Morgan, J., 1972. A Numerical Method for Computing Equilibria in Aqueous Chemical Systems, Environmental Science and Technology, Vol. 6, No. 1., pp. 58-66.

Narasimhan, T. N., White, A. F., and Tokunaga, T., 1986. Groundwater Contamination from an Inactive Uranium Mill Tailings Pile, 2, Application of a Dynamic Mixing Model, Water Resources Research, Vol. 22, No. 13, pp. 1820-1834.

Ogata, A, 1970. Theory of Dispersion in a Granular Media, Geological Survey Professional Paper 411-I.

Ong, S. K, Culver, T. B., Lion, L. W., and Shoemaker, C. A., 1992. Effects of Soil Moisture and Physical-Chemical Properties of Organic Pollutants on Vapor-phase Transport in the Vadose Zone, Journal of Contaminant Hydrology, Vol. 11, No. 314, pp. 273-290.

Orzol, L. L., McGrath, T. S., 1993. Summary of Modifications of the U. S. Geological Survey Modular, Finite-Difference, Ground-Water Flow Model to Read and Write Geographic Information System Files, Water Resources Bulletin, Vol. 29, No. 5, pp. 843-846.

Parkhurst, D. L., Thortensen, D. C., and Plummer, L. N., 1980. PHREEQE- A Computer Program for Geochemical Calculation, U. S. Geological Survey Water Resource Investigation, pp. 80-96.

Pfingsten, W., 1995. Efficient Modeling of Reactive Transport Phenomena by a Multispecies Random Walk Coupled to Chemical Equilibrium, Nuclear Technology, Vol. 116, No. 2, pp. 208-221.

Pini, G. and Zilli, G., 1989. Preconditioned Iterative Algorithms for Large Sparse Unsymmetric Problems, Numerical Methods for Partial Differential Equations, Vol. 5, No. 2, pp. 107-120.

Plato, PP. R., 1993. SHYDG.FOR—Hydrograph Package for MODFLOW, Ground Water, Vol. 31, No. 6, pp. 1025-1028.

Reproduced with permission of the copyright owner. Further reproduction prohibited without permission.

Reardon, E. H., 1981. K_d's—Can They be Used to Describe Reversible Ion Sorption Reactions in Contaminant Migration?, Ground Water, Vol. 19, No. 3, pp. 279-286.

Reardon, E. J., Dance, J. T., and Lolcama, J. L., 1983. Field Determination of Cation Exchange Properties of Calcareous Sand, Ground Water, Vol. 21, No. 4, pp. 421-428.

Richards, C. J., Roaza, H., and Roaza, R. M., 1993. Integrating Geographic Information Sytems and MODFLOW for Ground Water Resources Assessments, Water Resources Bulletin, Vol. 29, No. 5, pp. 847-853.

Sabadell, G. P., 1989. Modeling of Volatile Organic Transport in Soils, Dissertation Colorado State University.

San Juan, C. and Kolm, K. E., 1996. Conceptualization, Characterization and Numerical Modeling of the Jackson Hole alluvial aquifer using ARC/INFO and MODFLOW, Engineering Geology, Vol. 42, No. 2-3, pp. 119-137.

Shapiro, M., Fedou, R., Thovert, J.-F., *et al.*, 1996. Coupled Transport and Dispersion of Multi-component Reactive Solutes in Rectilinear Flows, Chemical Engineering Science, Vol. 51, No. 22, pp. 5017-5041.

Shen, H. and Nikolaidis, N. P., 1997. A Direct Substitution Method for Multicomponent Solute Transport in Ground Water, Ground Water, Vol. 35, No. 1, pp. 67-78.

Shultz, H. D. and Reardon, E. J., 1983. A Combined Mixing Cell/Analytical Model to Describe Two-dimensional Reactive Solute Transport for Unidirectional Groundwater Flow, Water Resources Research, Vol. 19, No. 2, pp. 493-502.

Sonneveld, P., 1989. CGS, A fast Lanczos-type Solver for Nonsymmetric Linear Systems, SIAM Journal on Scientific and Statistical Computing, Vol. 10, No. 1, pp. 36-52.

Sonntag, R. E. and Van Wylen, G. J. Fundamentals of Statistical Thermodynamics, Krieger Publishing Company, Malabar, Florida, pp. 239-243, 1966.

Sparks, D. L. Soil Physical Chemistry. CRC Press, Boca Raton, FL., 1986, pp. 148-150.

Sposito, G. Chemical equilibria and kinetics in soils. Oxford University Press, 1994.

Srivastava, R. and Yeh, J. T-C., 1992. A Three-dimesional Numerical Model for Water Flow and Transport of Chemically Reactive Solute Through Porous Media Under

Reproduced with permission of the copyright owner. Further reproduction prohibited without permission.

Variably Saturated Conditions, Advances in Water Resources, Vol. 15, No. 5, pp. 275-287.

Travis, C. C. and Etnier, E. L., 1981. A Survey of Sorption Relationships for Reactive Solutes in Soil, Journal of Environmental Quality, Vol. 10, No. 1, pp. 8-17.

USGS, 1984. SUTRA: Saturated-Unsaturated Transport: A Finite-element Simulation Model for Saturated-Unsaturated, Fluid-Density-Dependent Ground-Water Flow with Energy Transport or Chemically-Reactive Single-Species Solute Transport, USGS Water-Resources Investigations Report 84-4369.

Valocchi, A. J., 1984. Describing the Transport of Ion-Exchanging Contaminants Using an Effective K_d Approach, Water Resources Research, Vol. 20, No. 4, pp. 499-503.

Valocchi, A. J., Roberts, P. V., Parks, G. A., *et al.*, 1981. Simulation of the Transport of Ion-exchanging Solutes Using Laboratory-determined Chemical Parameter Values, Ground Water, Vol. 19, No. 6, pp. 600-607.

van der Heijde, PP. K. M. and Elnawawy, O. A., 1993. Compilation of Ground-water Models, EPA/600/R-93/118.

Walsh, M. P., Bryant, S. L., Schechter, R. S., and Lake, L. W., 1984. Precipitation and Dissolution of Solids Attending Flow Through Porous Media, AIChE Journal, Vol. 30, No. 2, pp. 317-327.

Walter, A. L., Frind, E. O., Blowes, D. W., *et al.*, 1994. Modeling of Multicomponent Reactive Transport in Groundwater: 1. Model Development and Evaluation, Water Resources Research, Vol. 30, No. 11, pp. 3137-3148.

Westall, J. C., Zachary, J. L., and Morel, F. M. M., 1976. MINEQL: A Computer Program for the Calculation of Chemical Equilibrium Composition of Aqueous System, Technical Note 18, pp. 91.

Wilson, J., A. M. ASCE and Miller, P., 1978. Two-dimensional Plume in Uniform Ground-water Flow, Journal of the Hydraulics Division, Vol. 4, pp. 503-514.

Wolfsberg, A. V. and Freyberg, D. L., 1994. Efficient Simulation of Single Species and Multispecies Transport in Groundwater with Local Adaptive Grid Refinement, Water Resources Research, Vol. 30, No. 11, pp. 2979-2991.

Yeh, G. T. and Tripathi, V. S., 1991. A Model for Simulating Transport of Reactive Multispecies Components: Model Development and Demonstration, Water Resources Research, Vol. 27, No. 12, pp. 3075-3094.

Reproduced with permission of the copyright owner. Further reproduction prohibited without permission.

Yeh, G. T. and Tripathi, V. S., 1989. A Critical Evaluation of Recent Developments in Hydrogeochemical Transport Models of Reactive Multichemical Components, Water Resources Research, Vol. 25, No. 1, pp. 93-108.

Zheng, C. and Neville, C., 1996. A Modular Three-Dimensional Transport Model for Simulation of Advection, Dispersion and Chemical Reactions of Contaminants in Groundwater Systems.

Zilli, G., 1992. Iterative Methods for Solving Sparse Linear Systems with a Parallel Preconditioner, International Journal of Computer Mathematics, Vol. 44, No. ¼, pp. 111-119.

Zimmerman, R. W. and Bodvarsson, G. S., 1989. An Approximate Solution for One-Dimensional Adsorption in Unsaturated Porous Media, Water Resources Research, Vol. 25, No. 6, pp. 1422-1428.

Zimmie, T. F. and Riggs, C. O., 1981. Permeability and Groundwater Contaminant Transport, ASTM Special Technical Publication 746.

Zysset, A., Stauffer, F., and Dracos, T., 1994. Modeling of Chemically Reactive Groundwater Transport, Water Resources Research, Vol. 30, No. 7, pp. 2217-2228.

Reproduced with permission of the copyright owner. Further reproduction prohibited without permission.

Appendix A

Numerical dispersion enters into equation 5.49 through the velocity and time derivatives due to these partial derivative terms being of first order accuracy and the dispersion partial derivative terms being of second order accuracy. By not truncating the second order terms in the velocity and time derivatives, the second order term contribution to the calculation can be either added or subtracted from the dispersion coefficient as orchestrated by the difference scheme used.

For this model, the implicit in time and backward in space finite difference scheme is used. Because of this scheme, the contributing second order terms from the time and velocity terms are subtracted from the dispersion coefficient as is shown below. The numerical dispersion arising from the space derivative term is first analyzed. The example is for the transport equation in the x-dimension. The same analysis can be mirrored for the y- and z-dimensions.

Space:

The partial differential transport equation for flow in the x-direction is

$$\frac{\delta C}{\delta t} = D_L \cdot \frac{\delta^2 \cdot C}{\delta x^2} + D_{TY} \cdot \frac{\delta^2 \cdot C}{\delta y^2} + D_{TZ} \cdot \frac{\delta^2 \cdot C}{\delta z^2} - V \cdot \frac{\delta C}{\delta x} \qquad \text{A.1}$$

Expanding the velocity first order derivative term by upwinding, the resulting equation is

$$\frac{\delta C}{\delta t} = D_L \cdot \frac{\delta^2 \cdot C}{\delta x^2} + D_{TY} \cdot \frac{\delta^2 \cdot C}{\delta y^2} + D_{TZ} \cdot \frac{\delta^2 \cdot C}{\delta z^2} - V \cdot \left(\frac{C_i - C_{i-1}}{\Delta x} \right) \qquad \text{A.2}$$

An expression for the expanded term can be determined using the backward Taylor series as follows:

Reproduced with permission of the copyright owner. Further reproduction prohibited without permission.

$$\frac{C_i - C_{i-1}}{\Delta x} = \frac{\delta C}{\delta x} - \frac{\delta^2 \cdot C}{\delta x^2} \cdot \frac{\Delta x}{2} \qquad \text{A.3}$$

Replacing the expanded term in equation A.2 with the right hand side of equation A.3, the result is shown in equation A.4 with the second order velocity derivative now grouped with the longitudinal dispersion coefficient term.

$$\frac{\delta C}{\delta t} = \left(D_L + \frac{V \cdot \Delta x}{2}\right) \cdot \frac{\delta^2 \cdot C}{\delta x^2} + D_{TY} \cdot \frac{\delta^2 \cdot C}{\delta y^2} + D_{TZ} \cdot \frac{\delta^2 \cdot C}{\delta z^2} - V \cdot \frac{\delta C}{\delta x} \qquad \text{A.4}$$

Similarly, the equations for the y- and z-directions is shown in equations A.5 and A.6 with the second order velocity derivative grouped accordingly.

$$\frac{\delta C}{\delta t} = D_{TX} \cdot \frac{\delta^2 \cdot C}{\delta x^2} + \left(D_L + \frac{V \cdot \Delta y}{2}\right) \cdot \frac{\delta^2 \cdot C}{\delta y^2} + D_{TZ} \cdot \frac{\delta^2 \cdot C}{\delta z^2} - V \cdot \frac{\delta C}{\delta y} \qquad \text{A.5}$$

$$\frac{\delta C}{\delta t} = D_{TX} \cdot \frac{\delta^2 \cdot C}{\delta x^2} + D_{TY} \cdot \frac{\delta^2 \cdot C}{\delta y^2} + \left(D_L + \frac{V \cdot \Delta z}{2}\right) \cdot \frac{\delta^2 \cdot C}{\delta z^2} - V \cdot \frac{\delta C}{\delta z} \qquad \text{A.6}$$

Time:

The numerical dispersion contribution from the time derivative term is a little more tedious than the space term. Again, the partial derivative transport equation for flow in the x-direction (see equation A.1) is used. The derivation follows.

The time derivative term is expanded using the backward Taylor series.

$$\frac{(C_i)^t - (C_i)^{t+\Delta t}}{\Delta t} = \frac{\delta C}{\delta t} - \frac{\delta^2 \cdot C}{\delta t^2} \cdot \frac{\Delta t}{2} \qquad \text{A.7}$$

The second order derivative of concentration with respect to time appears in equation A.7. The next step in the derivation is to determine this second order term. The second order term can be separated into equation A.8.

Reproduced with permission of the copyright owner. Further reproduction prohibited without permission.

$$\frac{\delta^2 \cdot C}{\delta t^2} = \frac{\delta}{\delta t} \cdot \left(\frac{\delta C}{\delta t} \right) \qquad \text{A.8}$$

Knowing that the partial of concentration with respect to time equals that shown in equation A.1, the substitution of equation A.1 is made into equation A.8 resulting in

$$\begin{aligned}
\frac{\delta}{\delta t} \cdot \left(\frac{\delta C}{\delta t} \right) = & D_L \cdot \frac{\delta^2}{\delta x^2} \cdot \left(D_L \cdot \frac{\delta^2 \cdot C}{\delta x^2} + D_{TY} \cdot \frac{\delta^2 \cdot C}{\delta y^2} + D_{TZ} \cdot \frac{\delta^2 \cdot C}{\delta z^2} - V \cdot \frac{\delta C}{\delta x} \right) \\
+ & D_{TY} \cdot \frac{\delta^2}{\delta y^2} \cdot \left(D_L \cdot \frac{\delta^2 \cdot C}{\delta x^2} + D_{TY} \cdot \frac{\delta^2 \cdot C}{\delta y^2} + D_{TZ} \cdot \frac{\delta^2 \cdot C}{\delta z^2} - V \cdot \frac{\delta C}{\delta x} \right) \\
+ & D_{TZ} \cdot \frac{\delta^2}{\delta z^2} \cdot \left(D_L \cdot \frac{\delta^2 \cdot C}{\delta x^2} + D_{TY} \cdot \frac{\delta^2 \cdot C}{\delta y^2} + D_{TZ} \cdot \frac{\delta^2 \cdot C}{\delta z^2} - V \cdot \frac{\delta C}{\delta x} \right) \\
- & V \cdot \frac{\delta}{\delta x} \cdot \left(D_L \cdot \frac{\delta^2 \cdot C}{\delta x^2} + D_{TY} \cdot \frac{\delta^2 \cdot C}{\delta y^2} + D_{TZ} \cdot \frac{\delta^2 \cdot C}{\delta z^2} - V \cdot \frac{\delta C}{\delta x} \right)
\end{aligned} \qquad \text{A.9}$$

Performing the calculation indicated in equation A.9, the result is

$$\begin{aligned}
\frac{\delta}{\delta t} \cdot \left(\frac{\delta C}{\delta t} \right) = & (D_L)^2 \cdot \frac{\delta^4 \cdot C}{\delta x^4} + D_L \cdot D_{TY} \cdot \frac{\delta^4 \cdot C}{\delta x^2 \cdot \delta y^2} + D_L \cdot D_{TZ} \cdot \frac{\delta^4 \cdot C}{\delta x^2 \cdot \delta z^2} - D_L \cdot V \cdot \frac{\delta^3 \cdot C}{\delta x^3} \\
+ & D_L \cdot D_{TY} \cdot \frac{\delta^4 \cdot C}{\delta x^2 \cdot \delta y^2} + (D_{TY})^2 \cdot \frac{\delta^4 \cdot C}{\delta y^4} + D_{TY} \cdot D_{TZ} \cdot \frac{\delta^4 \cdot C}{\delta y^2 \cdot \delta z^2} - D_{TY} \cdot V \cdot \frac{\delta^3 \cdot C}{\delta y^2 \cdot \delta x} \\
+ & D_L \cdot D_{TZ} \cdot \frac{\delta^4 \cdot C}{\delta x^2 \cdot \delta z^2} + D_{TY} \cdot D_{TZ} \cdot \frac{\delta^4 \cdot C}{\delta y^2 \cdot \delta z^2} + (D_{TZ})^2 \cdot \frac{\delta^4 \cdot C}{\delta z^4} - D_{TZ} \cdot V \cdot \frac{\delta^3 \cdot C}{\delta z^2 \cdot \delta x} \\
- & V \cdot D_L \cdot \frac{\delta^3 \cdot C}{\delta x^3} - V \cdot D_{TY} \cdot \frac{\delta^3 \cdot C}{\delta y^2 \cdot \delta x} - V \cdot D_{TZ} \cdot \frac{\delta^3 \cdot C}{\delta z^2 \cdot \delta x} + V^2 \cdot \frac{\delta^2 \cdot C}{\delta x^2}
\end{aligned} \qquad \text{A.10}$$

Neglecting third and higher order terms, the second order derivative of concentration with respect to time equals

$$\frac{\delta^2 \cdot C}{\delta t^2} = V^2 \cdot \frac{\delta^2 \cdot C}{\delta x^2} \qquad \text{A.11}$$

Therefore substituting equation A.11 back into equation A.7 results in

Reproduced with permission of the copyright owner. Further reproduction prohibited without permission.

$$\frac{(C_i)^t - (C_i)^{t+\Delta t}}{\Delta t} = \frac{\delta C}{\delta t} - V^2 \cdot \frac{\delta^2 \cdot C}{\delta x^2} \cdot \frac{\Delta t}{2} \qquad \text{A.12}$$

Substituting equation A.7 into equation A.1 results in the added numerical dispersion term within the second order derivative for the longitudinal dispersion coefficient.

$$\frac{\delta C}{\delta t} = \left(D_L + \frac{V^2 \cdot \Delta t}{2}\right) \cdot \frac{\delta^2 \cdot C}{\delta x^2} + D_{TY} \cdot \frac{\delta^2 \cdot C}{\delta y^2} + D_{TZ} \cdot \frac{\delta^2 \cdot C}{\delta z^2} - V \cdot \frac{\delta C}{\delta x} \qquad \text{A.13}$$

Again, the equations for the y- and z-directions are simply a copycat of equation A.13. as indicated in equations A.14 and A.15.

$$\frac{\delta C}{\delta t} = D_{TX} \cdot \frac{\delta^2 \cdot C}{\delta x^2} + \left(D_L + \frac{V^2 \cdot \Delta t}{2}\right) \cdot \frac{\delta^2 \cdot C}{\delta y^2} + D_{TZ} \cdot \frac{\delta^2 \cdot C}{\delta z^2} - V \cdot \frac{\delta C}{\delta y} \qquad \text{A.14}$$

$$\frac{\delta C}{\delta t} = D_{TX} \cdot \frac{\delta^2 \cdot C}{\delta x^2} + D_{TY} \cdot \frac{\delta^2 \cdot C}{\delta y^2} + \left(D_L + \frac{V^2 \cdot \Delta t}{2}\right) \cdot \frac{\delta^2 \cdot C}{\delta z^2} - V \cdot \frac{\delta C}{\delta z} \qquad \text{A.15}$$

Combine space and time:

The second order terms from the space and time derivatives can be combined into the following three equations for the x-, y- and z-directions, respectively:

$$\frac{\delta C}{\delta t} = \left(D_L + \frac{V \cdot \Delta x}{2} + \frac{V^2 \cdot \Delta t}{2}\right) \cdot \frac{\delta^2 \cdot C}{\delta x^2} + D_{TY} \cdot \frac{\delta^2 \cdot C}{\delta y^2} + D_{TZ} \cdot \frac{\delta^2 \cdot C}{\delta z^2} - V \cdot \frac{\delta C}{\delta x} \qquad \text{A.16}$$

$$\frac{\delta C}{\delta t} = D_{TX} \cdot \frac{\delta^2 \cdot C}{\delta x^2} + \left(D_L + \frac{V \cdot \Delta y}{2} + \frac{V^2 \cdot \Delta t}{2}\right) \cdot \frac{\delta^2 \cdot C}{\delta y^2} + D_{TZ} \cdot \frac{\delta^2 \cdot C}{\delta z^2} - V \cdot \frac{\delta C}{\delta y} \qquad \text{A.17}$$

$$\frac{\delta C}{\delta t} = D_{TX} \cdot \frac{\delta^2 \cdot C}{\delta x^2} + D_{TY} \cdot \frac{\delta^2 \cdot C}{\delta y^2} + \left(D_L + \frac{V \cdot \Delta z}{2} + \frac{V^2 \cdot \Delta t}{2}\right) \cdot \frac{\delta^2 \cdot C}{\delta z^2} - V \cdot \frac{\delta C}{\delta z} \qquad \text{A.18}$$

Since the terms are added contributions to the original longitudinal dispersion terms, these values must be subtracted from only the actual longitudinal dispersion terms in

Reproduced with permission of the copyright owner. Further reproduction prohibited without permission.

order to account for numerical dispersion affects. Therefore, the dispersion coefficient equations in Chapter 5 (se equations 5.39 to 5.44), can be rewritten respectively as

$$D_{xx}=\left[\alpha_L - 0.5\cdot(|v|\cdot\Delta t+\Delta x)\right]\cdot\frac{(v_x)^2}{|v|}+\alpha_{TH}\cdot\frac{(v_y)^2}{|v|}+\alpha_{TV}\cdot\frac{(v_z)^2}{|v|}+D_{dif} \quad \text{A.19}$$

$$D_{yy}=\alpha_{TH}\cdot\frac{(v_x)^2}{|v|}+\left[\alpha_L - 0.5\cdot(|v|\cdot\Delta t+\Delta x)\right]\cdot\frac{(v_y)^2}{|v|}+\alpha_{TV}\cdot\frac{(v_z)^2}{|v|}+D_{dif} \quad \text{A.20}$$

$$D_{zz}=\alpha_{TV}\cdot\frac{(v_x)^2}{|v|}+\alpha_{TV}\cdot\frac{(v_y)^2}{|v|}+\left[\alpha_L - 0.5\cdot(|v|\cdot\Delta t+\Delta x)\right]\cdot\frac{(v_z)^2}{|v|}+D_{dif} \quad \text{A.21}$$

$$D_{xy}=D_{yx}=\left[\left[\alpha_L - 0.5\cdot\left(|v|\cdot\Delta t+\frac{\Delta x+\Delta y}{2}\right)\right]-\alpha_{TH}\right]\cdot\frac{v_x\cdot v_y}{|v|} \quad \text{A.22}$$

$$D_{xz}=D_{zx}=\left[\left[\alpha_L - 0.5\cdot\left(|v|\cdot\Delta t+\frac{\Delta x+\Delta z}{2}\right)\right]-\alpha_{TV}\right]\cdot\frac{v_x\cdot v_z}{|v|} \quad \text{A.23}$$

$$D_{yz}=D_{zy}=\left[\left[\alpha_L - 0.5\cdot\left(|v|\cdot\Delta t+\frac{\Delta y+\Delta z}{2}\right)\right]-\alpha_{TV}\right]\cdot\frac{v_y\cdot v_z}{|v|} \quad \text{A.24}$$

In equations A.19 through A.24, numerical dispersion is represented as a dispersivity value by dividing the numerical dispersion by the velocity magnitude. As indicated in the aforementioned equations, the numerical dispersion is subtracted from each longitudinal dispersivity value. The effects of numerical dispersion on a solution can be seen in Case 1 in Chapter 7.

Reproduced with permission of the copyright owner. Further reproduction prohibited without permission.

Appendix B

To expand equation 5.32, a Taylor series expansion is performed on each derivative term. The result of this expansion is shown in Chapter 5 as equation 5.49. With the advective-transport equation written as a ordinary differential equation, equation 5.49 can be separated into individual equations that represent the concentrations for each of the 19 contributing cells (see Figure 5.9) indicated by the concentration subscripts in equation 5.49. Below are the individual equations for each of the 19 cells. The process of deriving these equations aids in the coding process by indicating which values contribute to a cell's concentration and an insight into reducing the number of repetitious calculations. Note that j, i, and k represent the row, column and layer, respectively.

$C_{j,i,k}$:

$$C_{j,i,k} = \left(\frac{D_{xx_{j,i+1,k}} + D_{xx_{j,i,k}}}{2}\right)\cdot\frac{-1}{.5\cdot\Delta x_{j,i+1,k} + .5\cdot\Delta x_{j,i,k}}\cdot\frac{1}{\Delta x_{j,i,k}} - \frac{D_{xx_{j,i,k}} + D_{xx_{j,i-1,k}}}{2}\cdot\frac{1}{.5\cdot\Delta x_{j,i,k} + .5\cdot\Delta x_{j,i-1,k}}\cdot\frac{1}{\Delta x_{j,i,k}}$$
$$+ \left(\frac{D_{yy_{j+1,i,k}} + D_{yy_{j,i,k}}}{2}\right)\cdot\frac{-1}{.5\cdot\Delta y_{j+1,i,k} + .5\cdot\Delta y_{j,i,k}}\cdot\frac{1}{\Delta y_{j,i,k}} - \left(\frac{D_{yy_{j,i,k}} + D_{yy_{j-1,i,k}}}{2}\right)\cdot\frac{1}{.5\cdot\Delta y_{j,i,k} + .5\cdot\Delta y_{j-1,i,k}}\cdot\frac{1}{\Delta y_{j,i,k}}$$
$$+ \left(\frac{D_{zz_{j,i,k+1}} + D_{zz_{j,i,k}}}{2}\right)\cdot\frac{-1}{.5\cdot\Delta z_{j,i,k+1} + .5\cdot\Delta z_{j,i,k}}\cdot\frac{1}{\Delta z_{j,i,k}} - \left(\frac{D_{zz_{j,i,k}} + D_{zz_{j,i,k-1}}}{2}\right)\cdot\frac{1}{.5\cdot\Delta z_{j,i,k} + .5\cdot\Delta z_{j,i,k-1}}\cdot\frac{1}{\Delta z_{j,i,k}}$$
$$- \left(\frac{q_{x_{j,i,k}} + q_{x_{j,i-1,k}}}{2\cdot\theta}\right)\cdot\frac{1}{\Delta x_{j,i,k}}$$
$$- \left(\frac{q_{y_{j,i,k}} + q_{y_{j-1,i,k}}}{2\cdot\theta}\right)\cdot\frac{1}{\Delta y_{i,j,k}}$$
$$- \left(\frac{q_{z_{j,i,k}} + q_{z_{j,i,k-1}}}{2\cdot\theta}\right)\cdot\frac{1}{\Delta z_{i,j,k}}$$

$C_{j,i+1,k}$:

$$C_{j,i+1,k} = \left(\frac{D_{xx_{j,i+1,k}} + D_{xx_{j,i,k}}}{2}\right)\cdot\frac{1}{.5\cdot\Delta x_{j,i+1,k} + .5\cdot\Delta x_{j,i,k}}\cdot\frac{1}{\Delta x_{j,i,k}}$$

Reproduced with permission of the copyright owner. Further reproduction prohibited without permission.

$$+\left(\frac{D_{yx_{j+1,i,k}}+D_{yx_{j,i,k}}}{2}\right)\cdot\frac{1}{2}\cdot\frac{1}{.5\cdot\Delta x_{j,i+1,k}+\Delta x_{j,i,k}+.5\cdot\Delta x_{j,i-1,k}}\cdot\frac{1}{\Delta y_{j,i,k}}$$

$$+\left(\frac{D_{yx_{j,i,k}}+D_{yx_{j-1,i,k}}}{2}\right)\cdot\frac{1}{2}\cdot\frac{-1}{.5\cdot\Delta x_{j,i+1,k}+\Delta x_{j,i,k}+.5\cdot\Delta x_{j,i-1,k}}\cdot\frac{1}{\Delta y_{j,i,k}}$$

$$+\left(\frac{D_{zx_{j,i,k+1}}+D_{zx_{j,i,k}}}{2}\right)\cdot\frac{1}{2}\cdot\frac{1}{.5\cdot\Delta x_{j,i+1,k}+\Delta x_{j,i,k}+.5\cdot\Delta x_{j,i-1,k}}\cdot\frac{1}{\Delta z_{j,i,k}}$$

$$+\left(\frac{D_{zx_{j,i,k}}+D_{zx_{j,i,k-1}}}{2}\right)\cdot\frac{1}{2}\cdot\frac{-1}{.5\cdot\Delta x_{j,i+1,k}+\Delta x_{j,i,k}+.5\cdot\Delta x_{j,i-1,k}}\cdot\frac{1}{\Delta z_{j,i,k}}$$

$C_{j,i-1,k}$:

$$C_{j,i-1,k}=\left(\frac{D_{xx_{j,i,k}}+D_{xx_{j,i-1,k}}}{2}\right)\cdot\frac{1}{.5\cdot\Delta x_{j,i,k}+.5\cdot\Delta x_{j,i-1,k}}\cdot\frac{1}{\Delta x_{j,i,k}}$$

$$+\left(\frac{D_{yx_{j+1,i,k}}+D_{yx_{j,i,k}}}{2}\right)\cdot\frac{1}{2}\cdot\frac{-1}{.5\cdot\Delta x_{j,i+1,k}+\Delta x_{j,i,k}+.5\cdot\Delta x_{j,i-1,k}}\cdot\frac{1}{\Delta y_{j,i,k}}$$

$$+\left(\frac{D_{yx_{j,i,k}}+D_{yx_{j-1,i,k}}}{2}\right)\cdot\frac{1}{2}\cdot\frac{1}{.5\cdot\Delta x_{j,i+1,k}+\Delta x_{j,i,k}+.5\cdot\Delta x_{j,i-1,k}}\cdot\frac{1}{\Delta y_{j,i,k}}$$

$$+\left(\frac{D_{zx_{j,i,k+1}}+D_{zx_{j,i,k}}}{2}\right)\cdot\frac{1}{2}\cdot\frac{-1}{.5\cdot\Delta x_{j,i+1,k}+\Delta x_{j,i,k}+.5\cdot\Delta x_{j,i-1,k}}\cdot\frac{1}{\Delta z_{j,i,k}}$$

$$+\left(\frac{D_{zx_{j,i,k}}+D_{zx_{j,i,k-1}}}{2}\right)\cdot\frac{1}{2}\cdot\frac{1}{.5\cdot\Delta x_{j,i-1,k}+\Delta x_{j,i,k}+.5\cdot\Delta x_{j,i-1,k}}\cdot\frac{1}{\Delta z_{j,i,k}}$$

$$+\left(\frac{q_{x_{j,i-1,k}}-q_{x_{j,i-2,k}}}{2\cdot\theta}\right)\cdot\frac{1}{\Delta x_{j,i-1,k}}$$

$C_{j+1,i+1,k}$:

$$C_{j+1,i+1,k}=\left(\frac{D_{xy_{j,i+1,k}}+D_{xy_{j,i,k}}}{2}\right)\cdot\frac{1}{2}\cdot\frac{1}{.5\cdot\Delta y_{j+1,i+1,k}+\Delta y_{j,i+1,k}+.5\cdot\Delta y_{j-1,i+1,k}}\cdot\frac{1}{\Delta x_{j,i,k}}$$

$$+\left(\frac{D_{yx_{j+1,i,k}}+D_{yx_{j,i,k}}}{2}\right)\cdot\frac{1}{2}\cdot\frac{1}{.5\cdot\Delta x_{j+1,i+1,k}+\Delta x_{j+1,i,k}+.5\cdot\Delta x_{j+1,i-1,k}}\cdot\frac{1}{\Delta y_{j,i,k}}$$

$C_{j-1,i+1,k}$:

$$C_{j-1,i+1,k}=\left(\frac{D_{xy_{j,i+1,k}}+D_{xy_{j,i,k}}}{2}\right)\cdot\frac{1}{2}\cdot\frac{-1}{.5\cdot\Delta y_{j+1,i+1,k}+\Delta y_{j,i+1,k}+.5\cdot\Delta y_{j-i,i+1,k}}\cdot\frac{1}{\Delta x_{j,i,k}}$$

$$+\left(\frac{D_{yx_{j,i,k}}+D_{yx_{j-1,i,k}}}{2}\right)\cdot\frac{1}{2}\cdot\frac{-1}{.5\cdot\Delta x_{j-1,i+1,k}+\Delta x_{j-1,i,k}+.5\cdot\Delta x_{j-1,i-1,k}}\cdot\frac{1}{\Delta y_{j,i,k}}$$

Reproduced with permission of the copyright owner. Further reproduction prohibited without permission.

$C_{j+1,i,k}$:

$$C_{j+1,i,k} = \left(\frac{D_{xy_{j,i+1,k}} + D_{xy_{j,i,k}}}{2}\right)\cdot\frac{1}{2}\cdot\frac{1}{.5\cdot\Delta y_{j+1,i,k} + \Delta y_{j,i,k} + .5\cdot\Delta y_{j-1,i,k}}\cdot\frac{1}{\Delta x_{j,i,k}}$$

$$+ \left(\frac{D_{xy_{j,i,k}} + D_{xy_{j,i-1,k}}}{2}\right)\cdot\frac{1}{2}\cdot\frac{-1}{.5\cdot\Delta y_{j+1,i,k} + \Delta y_{j,i,k} + .5\cdot\Delta y_{j-1,i,k}}\cdot\frac{1}{\Delta x_{j,i,k}}$$

$$+ \left(\frac{D_{yy_{j+1,i,k}} + D_{yy_{j,i,k}}}{2}\right)\cdot\frac{1}{.5\cdot\Delta y_{j+1,i,k} + .5\cdot\Delta y_{j,i,k}}\cdot\frac{1}{\Delta y_{j,i,k}}$$

$$+ \left(\frac{D_{zy_{j,i,k+1}} + D_{zy_{j,i,k}}}{2}\right)\cdot\frac{1}{2}\cdot\frac{1}{.5\cdot\Delta y_{j+1,i,k} + \Delta y_{j,i,k} + .5\cdot\Delta y_{j-1,i,k}}\cdot\frac{1}{\Delta z_{j,i,k}}$$

$$+ \left(\frac{D_{zy_{j,i,k}} + D_{zy_{j,i,k-1}}}{2}\right)\cdot\frac{1}{2}\cdot\frac{-1}{.5\cdot\Delta y_{j+1,i,k} + \Delta y_{j,i,k} + .5\cdot\Delta y_{j-1,i,k}}\cdot\frac{1}{\Delta z_{j,i,k}}$$

$C_{j-1,i,k}$:

$$C_{j-1,i,k} = \left(\frac{D_{xy_{j,i+1,k}} - D_{xy_{j,i,k}}}{2}\right)\cdot\frac{1}{2}\cdot\frac{-1}{.5\cdot\Delta y_{j+1,i,k} + \Delta y_{j,i,k} + .5\cdot\Delta y_{j-1,i,k}}\cdot\frac{1}{\Delta x_{j,i,k}}$$

$$+ \left(\frac{D_{xy_{j,i,k}} + D_{xy_{j,i-1,k}}}{2}\right)\cdot\frac{1}{2}\cdot\frac{1}{.5\cdot\Delta y_{j+1,j,k} + \Delta y_{j,i,k} + .5\cdot\Delta y_{j-1,i,k}}\cdot\frac{1}{\Delta x_{j,i,k}}$$

$$+ \left(\frac{D_{zy_{j,i,k+1}} + D_{zy_{j,i,k}}}{2}\right)\cdot\frac{1}{2}\cdot\frac{-1}{.5\cdot\Delta y_{j+1,i,k} + \Delta y_{j,i,k} + .5\cdot\Delta y_{j-1,i,k}}\cdot\frac{1}{\Delta z_{j,i,k}}$$

$$+ \left(\frac{D_{zy_{j,i,k}} + D_{zy_{j,i,k-1}}}{2}\right)\cdot\frac{1}{2}\cdot\frac{1}{.5\cdot\Delta y_{j+1,i,k} + \Delta y_{j,i,k} + .5\cdot\Delta y_{j-1,i,k}}\cdot\frac{1}{\Delta z_{j,i,k}}$$

$$+ \left(\frac{D_{yy_{j,i,k}} + D_{yy_{j-1,i,k}}}{2}\right)\cdot\frac{1}{.5\cdot\Delta y_{j,i,k} + .5\cdot\Delta y_{j-1,i,k}}\cdot\frac{1}{\Delta y_{j,i,k}}$$

$$+ \left(\frac{q_{y_{j-1,i,k}} + q_{y_{j-2,i,k}}}{2\cdot\theta}\right)\cdot\frac{1}{\Delta y_{j-1,i,k}}$$

$C_{j+1,i-1,k}$:

$$C_{j+1,i-1,k} = -\left(\frac{D_{xy_{j,i,k}} + D_{xy_{j,i-1,k}}}{2}\right)\cdot\frac{1}{2}\cdot\frac{-1}{.5\cdot\Delta y_{j+1,i-1,k} + \Delta y_{j,i-1,k} + .5\cdot\Delta y_{j-1,i-1,k}}\cdot\frac{1}{\Delta x_{j,i,k}}$$

$$+ \left(\frac{D_{yx_{j+1,i,k}} + D_{yx_{j,i,k}}}{2}\right)\cdot\frac{1}{2}\cdot\frac{-1}{.5\cdot\Delta x_{j+1,i+1,k} + \Delta x_{j+1,i,k} + .5\cdot\Delta x_{j+1,i-1,k}}\cdot\frac{1}{\Delta y_{j,i,k}}$$

Reproduced with permission of the copyright owner. Further reproduction prohibited without permission.

$C_{j-1,i-1,k}$:

$$C_{j-1,i-1,k} = \left(\frac{D_{xy_{j,i,k}} + D_{xy_{j,i-1,k}}}{2}\right) \cdot \frac{1}{2} \cdot \frac{1}{.5\cdot\Delta y_{j+1,i-1,k} + \Delta y_{j,i-1,k} + .5\cdot\Delta y_{j-1,i-1,k}} \cdot \frac{1}{\Delta x_{j,i,k}}$$

$$+ \left(\frac{D_{yx_{j,i,k}} + D_{yx_{j-1,i,k}}}{2}\right) \cdot \frac{1}{2} \cdot \frac{1}{.5\cdot\Delta x_{j-1,i+1,k} + \Delta x_{j-1,i,k} + .5\cdot\Delta x_{j-1,i-1,k}} \cdot \frac{1}{\Delta y_{j,i,k}}$$

$C_{j,i+1,k+1}$:

$$C_{j,i+1,k+1} = \left(\frac{D_{xz_{j,i+1,k}} + D_{j,i,k}}{2}\right) \cdot \frac{1}{2} \cdot \frac{1}{.5\cdot\Delta z_{j,i+1,k+1} + \Delta z_{j,i+1,k} + .5\cdot\Delta z_{j,i+1,k-1}} \cdot \frac{1}{\Delta x_{j,i,k}}$$

$$+ \left(\frac{D_{zx_{j,i,k+1}} + D_{zx_{j,i,k}}}{2}\right) \cdot \frac{1}{2} \cdot \frac{1}{.5\cdot\Delta x_{j,i+1,k+1} + \Delta x_{j,i,k+1} + .5\cdot\Delta x_{j,i-1,k+1}} \cdot \frac{1}{\Delta z_{j,i,k}}$$

$C_{j,i+1,k-1}$:

$$C_{j,i+1,k-1} = \left(\frac{D_{xz_{j,i+1,k}} + D_{xz_{j,i,k}}}{2}\right) \cdot \frac{1}{2} \cdot \frac{-1}{.5\cdot\Delta z_{j,i+1,k+1} + \Delta z_{j,i+1,k} + .5\cdot\Delta z_{j,i+1,k-1}} \cdot \frac{1}{\Delta x_{j,i,k}}$$

$$+ \left(\frac{D_{zx_{j,i,k}} + D_{zx_{j,i,k-1}}}{2}\right) \cdot \frac{1}{2} \cdot \frac{-1}{.5\cdot\Delta x_{j,i+1,k-1} + \Delta x_{j,i,k-1} + .5\cdot\Delta x_{j,i-1,k-1}} \cdot \frac{1}{\Delta z_{j,i,k}}$$

$C_{j,i,k+1}$:

$$C_{j,i,k+1} = \left(\frac{D_{xz_{j,i+1,k}} + D_{xz_{j,i,k}}}{2}\right) \cdot \frac{1}{2} \cdot \frac{1}{.5\cdot\Delta z_{j,i,k+1} + \Delta z_{j,i,k} + .5\cdot\Delta z_{j,i,k-1}} \cdot \frac{1}{\Delta x_{j,i,k}}$$

$$+ \left(\frac{D_{xz_{j,i,k}} + D_{xz_{j,i-1,k}}}{2}\right) \cdot \frac{1}{2} \cdot \frac{-1}{.5\cdot\Delta z_{j,i,k+1} + \Delta z_{j,i,k} + .5\cdot\Delta z_{j,i,k-1}} \cdot \frac{1}{\Delta x_{j,i,k}}$$

$$+ \left(\frac{D_{yz_{j+1,i,k}} + D_{yz_{j,i,k}}}{2}\right) \cdot \frac{1}{2} \cdot \frac{1}{.5\cdot\Delta z_{j,i,k+1} + \Delta z_{j,i,k} + .5\cdot\Delta z_{j,i,k-1}} \cdot \frac{1}{\Delta y_{j,i,k}}$$

$$+ \left(\frac{D_{yz_{j,i,k}} + D_{yz_{j-1,i,k}}}{2}\right) \cdot \frac{1}{2} \cdot \frac{-1}{.5\cdot\Delta z_{j,i,k+1} + \Delta z_{j,i,k} + .5\cdot\Delta z_{j,i,k-1}} \cdot \frac{1}{\Delta y_{j,i,k}}$$

$$+ \left(\frac{D_{zz_{j,i,k+1}} + D_{zz_{j,i,k}}}{2}\right) \cdot \frac{1}{.5\cdot\Delta z_{j,i,k+1} + .5\cdot\Delta z_{j,i,k}} \cdot \frac{1}{\Delta z_{j,i,k}}$$

$C_{j,i,k-1}$:

$$C_{j,i,k-1} = \left(\frac{D_{xz_{j,i+1,k}} + D_{xz_{j,i,k}}}{2}\right) \cdot \frac{1}{2} \cdot \frac{-1}{.5\cdot\Delta z_{j,i,k+1} + \Delta z_{j,i,k} + .5\cdot\Delta z_{j,i,k-1}} \cdot \frac{1}{\Delta x_{j,i,k}}$$

$$+ \left(\frac{D_{xz_{j,i,k}} + D_{xz_{j,i-1,k}}}{2}\right) \cdot \frac{1}{2} \cdot \frac{1}{.5\cdot\Delta z_{j,i,k+1} + \Delta z_{j,i,k} + .5\cdot\Delta z_{j,i,k-1}} \cdot \frac{1}{\Delta x_{j,i,k}}$$

Reproduced with permission of the copyright owner. Further reproduction prohibited without permission.

$$+\left(\frac{D_{yz_{j+1,i,k}}+D_{yz_{j,i,k}}}{2}\right)\cdot\frac{1}{2}\cdot\frac{-1}{.5\cdot\Delta z_{j,i,k+1}+\Delta z_{j,i,k}+.5\cdot\Delta z_{j,i,k-1}}\cdot\frac{1}{\Delta y_{j,i,k}}$$

$$+\left(\frac{D_{yz_{j,i,k}}+D_{yz_{j-1,i,k}}}{2}\right)\cdot\frac{1}{2}\cdot\frac{1}{.5\cdot\Delta z_{j,i,k+1}+\Delta z_{j,i,k}+.5\cdot\Delta z_{j,i,k-1}}\cdot\frac{1}{\Delta y_{j,i,k}}$$

$$+\left(\frac{D_{zz_{j,i,k}}+D_{zz_{j,i,k-1}}}{2}\right)\cdot\frac{1}{.5\cdot\Delta z_{j,i,k}+.5\cdot\Delta z_{j,i,k-1}}\cdot\frac{1}{\Delta z_{j,i,k}}$$

$$+\left(\frac{q_{z_{j,i,k-1}}+q_{z_{j,i,k-2}}}{2\cdot\theta}\right)\cdot\frac{1}{\Delta z_{i,j,k-1}}$$

$C_{j,i-1,k+1}$:

$$C_{j,i-1,k+1}=\left(\frac{D_{xz_{j,i,k}}+D_{xz_{j,i-1,k}}}{2}\right)\cdot\frac{1}{2}\cdot\frac{-1}{.5\cdot\Delta z_{j,i-1,k+1}+\Delta z_{j,i-1,k}+.5\cdot\Delta z_{j,i-1,k-1}}\cdot\frac{1}{\Delta x_{j,i,k}}$$

$$+\left(\frac{D_{zx_{j,i,k+1}}+D_{zx_{j,i,k}}}{2}\right)\cdot\frac{1}{2}\cdot\frac{-1}{.5\cdot\Delta x_{j,i+1,k+1}+\Delta x_{j,i,k+1}+.5\cdot\Delta x_{j,i-1,k+1}}\cdot\frac{1}{\Delta z_{j,i,k}}$$

$C_{j,i-1,k-1}$:

$$C_{j,i-1,k-1}=\left(\frac{D_{xz_{j,i,k}}+D_{xz_{j,i-1,k}}}{2}\right)\cdot\frac{1}{2}\cdot\frac{-1}{.5\cdot\Delta z_{j,i-1,k+1}+\Delta z_{j,i-1,k}+.5\cdot\Delta z_{j,i-1,k-1}}\cdot\frac{1}{\Delta x_{j,i,k}}$$

$$+\left(\frac{D_{zx_{j,i,k}}+D_{zx_{j,i,k-1}}}{2}\right)\cdot\frac{1}{2}\cdot\frac{-1}{.5\cdot\Delta x_{j,i+1,k-1}+\Delta x_{j,i,k-1}+.5\cdot\Delta x_{j,i-1,k-1}}\cdot\frac{1}{\Delta z_{j,i,k}}$$

$C_{j+1,i,k+1}$:

$$C_{j+1,i,k+1}=\left(\frac{D_{yz_{j+1,i,k}}+D_{yz_{j,i,k}}}{2}\right)\cdot\frac{1}{2}\cdot\frac{1}{.5\cdot\Delta z_{j+1,i,k+1}+\Delta z_{j+1,i,k}+.5\cdot\Delta z_{j+1,i,k-1}}\cdot\frac{1}{\Delta y_{j,i,k}}$$

$$+\left(\frac{D_{zy_{j,i,k+1}}+D_{zy_{j,i,k}}}{2}\right)\cdot\frac{1}{2}\cdot\frac{1}{.5\cdot\Delta y_{j+1,i,k+1}+\Delta y_{j,i,k+1}+.5\cdot\Delta y_{j-1,i,k+1}}\cdot\frac{1}{\Delta z_{j,i,k}}$$

$C_{j+1,i,k-1}$:

$$C_{j+1,i,k-1}=\left(\frac{D_{yz_{j+1,i,k}}+D_{yz_{j,i,k}}}{2}\right)\cdot\frac{1}{2}\cdot\frac{-1}{.5\cdot\Delta z_{j+1,i,k+1}+\Delta z_{j+1,i,k}+.5\cdot\Delta z_{j+1,i,k-1}}\cdot\frac{1}{\Delta y_{j,i,k}}$$

$$+\left(\frac{D_{zy_{j,i,k}}+D_{zy_{j,i,k-1}}}{2}\right)\cdot\frac{1}{2}\cdot\frac{-1}{.5\cdot\Delta y_{j+1,i,k-1}+\Delta y_{j,i,k-1}+.5\cdot\Delta y_{j-1,i,k-1}}\cdot\frac{1}{\Delta z_{j,i,k}}$$

Reproduced with permission of the copyright owner. Further reproduction prohibited without permission.

$C_{j-1,i,k+1}$:

$$C_{j-1,i,k+1} = \left(\frac{D_{yz_{j,i,k}} + D_{yz_{j-1,i,k}}}{2}\right) \cdot \frac{1}{2} \cdot \frac{-1}{.5 \cdot \Delta z_{j-1,i,k+1} + \Delta z_{j-1,i,k} + .5 \cdot \Delta z_{j-1,i,k-1}} \cdot \frac{1}{\Delta y_{j,i,k}}$$

$$+ \left(\frac{D_{zy_{j,i,k+1}} + D_{zy_{j,i,k}}}{2}\right) \cdot \frac{1}{2} \cdot \frac{-1}{.5 \cdot \Delta y_{j+1,i,k+1} + \Delta y_{j,i,k+1} + .5 \cdot \Delta y_{j-1,i,k+1}} \cdot \frac{1}{\Delta z_{j,i,k}}$$

$C_{j-1,i,k-1}$:

$$C_{j-1,i,k-1} = \left(\frac{D_{yz_{j,i,k}} + D_{yz_{j-1,i,k}}}{2}\right) \cdot \frac{1}{2} \cdot \frac{1}{.5 \cdot \Delta z_{j-1,i,k+1} + \Delta z_{j-1,i,k} + .5 \cdot \Delta z_{j-1,i,k-1}} \cdot \frac{1}{\Delta y_{j,i,k}}$$

$$+ \left(\frac{D_{zy_{j,i,k}} + D_{zy_{j,i,k-1}}}{2}\right) \cdot \frac{1}{2} \cdot \frac{1}{.5 \cdot \Delta y_{j+1,i,k-1} + \Delta y_{j,i,k-1} + .5 \cdot \Delta y_{j-1,i,k-1}} \cdot \frac{1}{\Delta z_{j,i,k}}$$

The total number of calculations in the above 19 equations is approximately 800. By finding similar calculations between the equations, the total number of calculations can be reduced to approximately 165. This approximate 400 % reduction saves computer simulation time, especially for large problems involving many cells.

Reproduced with permission of the copyright owner. Further reproduction prohibited without permission.

Appendix C

Input File Descriptions

- **CHM**
- **CON**
- **DIS**
- **global.file**
- **OUT**
- **SSM**

Reproduced with permission of the copyright owner. Further reproduction prohibited without permission.

CHM FILE

Description

The chemical parameters for each species and component are read from this file by MULTRAN. These chemical parameters include the number of aqueous and cation exchange species being simulated, molecular weight of each component, stoichiometric and selectivity coefficients, equilibrium constants, hydrogen condition, and the cation exchange capacity. This file is empty for single species transport.

Data Format

1. TITLE
   (4A20)

2. TITLE
   (4A20)

3. NSPECIES NCATEXH
   (INT) (INT)

For each component (NCOMP):

4. CP_NAM MOLWT ID_HYD
   (A15) (F14.6) (I5)

For each species (NSPECIES):

5. SP_NAM
   (4A20)

6. AC EQKLOG
   (REAL) (REAL)

If NCATEXH is greater than zero, read the remainder of the file.

7. CEC
   (REAL)

For each cation exchange species (NCATEXH):

8. CAT_NAM
   (4A20)

9. AZ RKEQ IDAQ IDAZ VALNC
   (REAL) (REAL) (INT) (INT) (REAL)

Reproduced with permission of the copyright owner. Further reproduction prohibited without permission.

TITLE: description of problem

NSPECIES: number of aqueous species.

NCATEXH: number of cation exchange species.

CP_NAM: name of chemical component.

MOLWT: molecular weight of chemical component.

ID_HYD: This is a flag which indicates whether or not a component contains hydrogen.

The flag is as follows:

ID_HYD=0: the component does not contain hydrogen
ID_HYD=1: the component does contain hydrogen

SP_NAM: name of the chemical species.

AC: This term is a two-dimensional array that contains the stoichiometric coefficients for each chemical species as they relate to each chemical component. The array is dimensioned as AC(NSPECIES,NCOMP). Therefore, if there are 4 species and 3 components, then there will be 4 lines of input with 3 stoichiometric coefficient values on each line (see example below).

EQKLOG: equilibrium constant.

CEC: cation exchange capacity in units of Molar. Therefore, if C_1 fills all of the exchange sites at the beginning of the simulation at a concentration of 500 mg/L, then divide the concentration by 1000 and the component's molecular weight to arrive in the proper units of Molar. If for the above case the molecular weight of C_1 is 23.0, then the CEC value is approximately 0.02174 M.

CAT_NAM: name of the cation exchange species.

Reproduced with permission of the copyright owner. Further reproduction prohibited without permission.

AZ: This is the stoichiometric coefficient for how the cation exchange species relates to the chemical components. Like the term, AC, above, AZ is a two dimensional array of the form AZ(NCATEXH,NCOMP).

RKEQZ: selectivity coefficient.

IDAQ: IDAQ is an integer specifying the aqueous species number. This number is based on the species listing within this input file. For example, assume four species are specified in the respective order: C_1, C_2, C_3, and C_4. Next, assume that C_3 is listed again as a cation exchange species. IDAQ for the C_3 list would be 3. If C_4 is listed also, then IDAQ for C_4 is 4.

IDAZ: This is an integer specifying the replaced cation that is based on the listing in the cation exchange species listing. Therefore, if C_4 from above is listed first in this section of the input file and it replaces C_2 that is listed third in this listing, then IDAQ equals 4 and IDAZ equals 3.

VALNC: valance of the cation species.

Example

```
CHM file.
Reactions involving two components and two chemical species
2  2                                    ___NSPECIES,NCATEXH
Sodium          22.98968       0       ___CP_NAM,MOLWT,ID_HYD for component 1
Magnesium        24.3050       0       ___CP_NAM,MOLWT,ID_HYD for component 2
Na+                                    ___SP_NAM for species 1
1.  0.           0.                    ___AC,EQKLOG for species 1
Mg++                                   ___SP_NAM for species 2
0.  1.           0.                    ___AC,EQKLOG for species 2
0.0217391304                           ___cation exchange capacity (CEC)
Mg(adsorbed)                           ___CAT_NAM for cation exchange species (CES) 1
0.  1.    2.0    2    2   2.          ___AZ,RKEQ,IDAQ,IDAZ,VALNC for CES 1
Na(replaced)                           ___CAT_NAM for CES 2
1.  0.    0.0    1    0   1.          ___AZ,RKEQ,IDAQ,IDAZ,VALNC for CES 2
```


Reproduced with permission of the copyright owner. Further reproduction prohibited without permission.

CON FILE

Description

The CON file contains the constant concentration cell data for each component. The user provides this information for each stress period. The purpose for specifying constant concentrations for each stress period is so concentration changes can be applied over time. This can be the case with landfill leachate that can vary in concentration from past filled cells to newly constructed cells.

For each stress period, the number of constant concentration cells followed by those cells' information (row, column, layer, and concentration) is provided for each component modeled. If there are no constant concentration cells for a component, a zero is placed in the NCONC field (see Data Format).

Data Format

For each stress period:
For each component:

1. NCONC
   (INT)

2. JROW (INT) ICOL (INT) KLAY (INT) CONCNST (REAL)

NCONC: The number of constant concentration cells (free format) within stress period for the particular component. A zero is placed in this field for components without constant concentration cells.

JROW: The row location within the finite difference grid.

ICOL: The column location within the finite difference grid.

KLAY: The layer location within the finite difference grid.

CONCNST: The constant concentration cell value.

Reproduced with permission of the copyright owner. Further reproduction prohibited without permission.

Example

(for 2 components, 2 stress periods, 1 layer)

```
2                    .....NCONC for component 1, stress period 1
2 1 1 100.0          .....JROW,ICOL,KLAY,CONCNST for component 1, stress period 1
3 10 1 50.0          .....JROW,ICOL,KLAY,CONCNST for component 1, stress period 1
5                    .....NCONC for component 2, stress period 1
2 1 1 100.0          .....JROW,ICOL,KLAY,CONCNST for component 2, stress period 1
3 10 1 50.0          .....JROW,ICOL,KLAY,CONCNST for component 2, stress period 1
4 10 1 75.0          .....JROW,ICOL,KLAY,CONCNST for component 2, stress period 1
5 5 1 200.0          .....JROW,ICOL,KLAY,CONCNST for component 2, stress period 1
5 10 1 100.0         .....JROW,ICOL,KLAY,CONCNST for component 2, stress period 1
0                    .....NCONC for component 1, stress period 2
5                    .....NCONC for component 2, stress period 2
2 1 1 100.0          .....JROW,ICOL,KLAY,CONCNST for component 2, stress period 2
3 10 1 50.0          .....JROW,ICOL,KLAY,CONCNST for component 2, stress period 2
4 10 1 75.0          .....JROW,ICOL,KLAY,CONCNST for component 2, stress period 2
5 5 1 250.0          .....JROW,ICOL,KLAY,CONCNST for component 2, stress period 2
5 10 1 90.0          .....JROW,ICOL,KLAY,CONCNST for component 2, stress period 2
```


Reproduced with permission of the copyright owner. Further reproduction prohibited without permission.

DIS FILE

Description

The transport parameters for each component and each layer are read from this file by MULTRAN. These transport parameters include the number of chemical components being simulated, porosity, hydraulic conductivity, the longitudinal, horizontal, and transverse dispersivity coefficients, diffusion, radioactive decay and biodegradation values, and the initial and sorbed concentrations for each component. For single species transport, the initial sorbed concentration values are substituted with sorption isotherm information. Three isotherm options are provided for estimated sorption: linear, Freundlich, and Langmuir.

In reference to the dispersion coefficients, the horizontal dispersivity typically ranges from a tenth of the longitudinal to equaling the longitudinal dispersivity. The transverse dispersivity is usually a tenth of the transverse. Concentration units specified in this file are in mg/L.

Data Format

1.	NCOMP			
	(INT)			

For each layer (NLAY):

2.	AL	ATH	ATV	DIFSION
	(REAL)	(REAL)	(REAL)	(REAL)

For each component (NCOMP):

3.	LAMCOD	LAMDA1	LAMDA2
	(REAL)	(REAL)	(REAL)

For dissolved concentrations for each component for each layer:

5.	IUNIT	VALUE	FORM
	(I10)	(F10.1)	(A10)

For NCOMP greater than one:

Reproduced with permission of the copyright owner. Further reproduction prohibited without permission.

Sorbed concentrations for each component for each layer:

6.	IUNIT	VALUE	FORM
	(I10)	(F10.1)	(A10)

For NCOMP equal one:

Sorption isotherm:

7.	IISO
	(INT)

8.	RHOB	KISO
	(REAL)	(REAL)

For IISO = 2:

9.	AEXPO
	(REAL)

For IISO = 3:

10.	BMAX
	(REAL)

For each layer:

Hydraulic conductivity:

11.	IUNIT	VALUE	FORM
	(I10)	(F10.1)	(A10)

Porosity:

12.	IUNIT	VALUE	FORM
	(I10)	(F10.1)	(A10)

NCOMP: The number of chemical components (free format).

AL: The longitudinal dispersivity coefficient (L).

ATH: The horizontal transverse dispersivity coefficient (L).

ATV: The vertical transverse dispersivity coefficient (L).

DIFSION: Measure of diffusion (L^2/T).

LAMCOD: A flag indicating the following three possible options:

(1) LAMCOD=0: No radioactive decay or biodegradation is to be simulated.
(2) LAMCOD=1: Radioactive decay is to be simulated.
(3) LAMCOD=2: Biodegradation is to be simulated.

LAMDA1: The dimensionless radioactive decay constant (LAMCOD=1) or biodegradation constant (LAMCOD=2).

Reproduced with permission of the copyright owner. Further reproduction prohibited without permission.

LAMDA2: The second biodegradation constant when LAMCOD=2. For LAMCOD=1, this term may be set to zero. This term is also dimensionless.

IUNIT: IUNIT = 0, variable is constant throughout system.
IUNIT = DIS code, variable is read within file following input line.
IUNIT = (other), variable is read from external file.

VALUE: Variable multiplier.

FORM: The data format listing. The form must be within parentheses.

IISO: IISO = 1, use linear sorption isotherm.
IISO = 2, use Freundlich sorption isotherm.
IISO = 3, use Langmuir sorption isotherm.

RHOB: porous media bulk density (M/L^3).

KISO: If IISO = 1, KISO is the distribution coefficient (L^3/M).
If IISO = 2, KISO is the Freundlich constant (L^3/M).
If IISO = 3, KISO is Langmuir constant (L^3/M).

AEXPO: Freundlich exponent (dimensionless).

BMAX: Maximum limit of sorbed solute on media (M/M).

Reproduced with permission of the copyright owner. Further reproduction prohibited without permission.

Example

(for 2 components, 2 layers)

```
2                                          .....number of components: NCOMP
3.0  1.0 0.1  0.0                    .....Layer 1: AL,ATH,ATV,DIFSION
3.5  1.2 0.0  0.0                    .....Layer 2: AL,ATH,ATV,DIFSION
0  0.  0.                            .....Component 1: LAMCOD, LAMDA1, LAMDA2
0  0.  0.                            .....Component 2: LAMCOD, LAMDA1, LAMDA2
    44    100.0 (12f4.1)             .....initial dissolved concentrations (44 is the DIS code, IDIS)
1.0 1.0 1.0 1.0 1.0 1.0 1.0 1.0 1.0 1.0 1.0 1.0
1.0 1.0 1.0 1.0 1.0 1.0 1.0 1.0 1.0 1.0 1.0 1.0
1.0 1.0 1.0 1.0 1.0 1.0 1.0 1.0 1.0 1.0 1.0 1.0
1.0 1.0 1.0 1.0 1.0 1.0 1.0 1.0 1.0 1.0 1.0 1.0
1.0 1.0 1.0 1.0 1.0 1.0 1.0 1.0 1.0 1.0 1.0 1.0 .....end component 1, Layer 1
2.0 2.0 2.0 2.0 2.0 2.0 2.0 2.0 2.0 2.0 2.0 2.0
2.0 2.0 2.0 2.0 2.0 2.0 2.0 2.0 2.0 2.0 2.0 2.0
2.0 2.0 2.0 2.0 1.5 1.5 1.5 2.0 2.0 2.0 2.0 2.0
2.0 2.0 2.0 2.0 2.0 2.0 2.0 2.0 2.0 2.0 2.0 2.0
2.0 2.0 2.0 2.0 2.0 2.0 2.0 2.0 2.0 2.0 2.0 2.0 .....end component 2, Layer 1
     0      0.0                     .....initial dissolved concentrations, component 1, Layer 2
     0      0.0                     .....initial dissolved concentrations, component 2, Layer 2
    57    100.0 (12f5.2)            .....initial sorbed concentrations, component 1, Layer 1
     0      0.0                     .....initial sorbed concentrations, component 2, Layer 1
     0      0.0                     .....initial sorbed concentrations, component 1, Layer 2
     0      0.0                     .....initial sorbed concentrations, component 2, Layer 2
    66      1.0 (12f7.1)            .....hydraulic conductivity, Layer 1
    67      1.0 (12f7.1)            .....hydraulic conductivity, Layer 2
    68     0.01 (12f4.1)            .....porosity, Layer 1
    69     0.01 (12f4.1)            .....porosity, Layer 2
```


Reproduced with permission of the copyright owner. Further reproduction prohibited without permission.

GLOBAL.FILE

Description

The global.file contains a list of all the external files used by MULTRAN. In the least, eight files are required as discussed in Chapter 6. The eight files are as follows; (1) MODFLOW BAS file, (2) MODFLOW BCF file, (3) MODFLOW LKMT file, (4) transport parameters and constant cell concentration file, (5) initial concentrations file, (6) chemical data file, (7) sink/source listing file, and (8) timing and maximum iteration listing.

For MULTRAN to recognize these files, three-character code text is supplied within the listing of these files in the global.file. Corresponding to the above listing, the code text is as follows: BAS, BCF, LKM, DIS, CON, CHM, SSM, and OUT. The files can be listed in any order as long as each entry follows the FORTRAN format (A3, A3, I7, A20). Both formatted and unformatted files are supported. Unformatted files require negative unit numbers.

Data Format

For each file:

	IEOF	CODE	GUNIT	GFILE
1.	(A3)	(A3)	(I7)	(A20)

IEOF: This field remains a blank three-character text until the last line of the global.file. At the last line of the global.file, the IEOF field is set to "EOF" specifying the end of the file.

CODE: For the required MULTRAN files mentioned in the description, the code text is placed in this field. Otherwise the field remains a blank three-character text.

Reproduced with permission of the copyright owner. Further reproduction prohibited without permission.

GUNIT: The user defined unit numbers are placed in this field (right justified). A negative GUNIT indicates a binary, or unformatted file.

GFILE: The name of the file. Depending upon the computer system, this parameter may be case sensitive.

Example

```
BAS      20  modflow.bas
BCF      30  modflow.bcf
CHM      40  multran.chm
DIS      44  dispersion
CON      45  ini_conc
LKM     -60  modflow.lkm
SSM      70  sink_source
OUT      21  time
         57  sorbed_conc1
         66  hydr_cond1
         67  hydr_cond2
         68  porosity1
         69  porosity2
EOF
```


Reproduced with permission of the copyright owner. Further reproduction prohibited without permission.

OUT FILE

Description

The input parameters into the OUT file are very simple, as there are only four. These parameters are the matrix symmetry flag, the iteration convergence criteria, maximum iteration limit, and the total simulation time. Below is a more in depth description of these parameters with an example input file. The format of this file is free format.

Data Format

1.	ISYM	TOL	ITMAX	TRNTIME
	(INTEGER)	(REAL)	(REAL)	(REAL)

ISYM: This parameter is a flag that specifies whether the matrix of transport equations is symmetric or asymmetric by:

ISYM=1: symmetric
ISYM=0: asymmetric.

If almost every case, ISYM will be zero. Only in a very ideal, one-dimensional case could ISYM possibly equal 1.

TOL: The tolerance criterion for convergence within the bi-preconjugate gradient squared iterative solver (BPCG).

ITMAX: The maximum limit of iterations allowed for the bi-preconjugate gradient squared iterative solver. The BPCG typically takes at most 10 to 20 iterations to converge.

TRNTIME: This parameter need only be specified when the ground water solution is steady state as indicated in MODFLOW with the ISS term in the BCF file. For steady state ground water solutions, TRNTIME is the length of time for the

Reproduced with permission of the copyright owner. Further reproduction prohibited without permission.

transport simulation. The units of TRNTIME is (T) with the unit, whether day, month, or year, needing to be the same as the time units used in MODFLOW.

Example

(for a steady state ground water solution)

0 .001 800 4.0

Reproduced with permission of the copyright owner. Further reproduction prohibited without permission.

SSM FILE

Description

The SSM file allows the user to specify concentrations that enter into the system during different time intervals via the following sources: (1) constant heads, (2) wells, (3) rivers, (4) recharge, (5) streams, (6) general head boundaries, and as a special case for a sink, (7) evapotranspiration (see Chapters 5 and 6). Whether or not if these sources are simulated is determined within the MODFLOW BAS file which MULTRAN reads.

The stresses are read by MULTRAN in the following order:

(1) Constant head
(2) Well
(3) Drain
(4) Recharge
(5) Evapotranspiration
(6) River
(7) Stream
(8) General head boundary.

Data Format

For each MODFLOW stress period:

For each component and for each stress flagged in the MODFLOW BAS file:

1. NCNH
   (INTEGER)

2. NROW (INTEGER) NCOL (INTEGER) NLAY (INTEGER) VALUE (REAL)

NCNH: The number of values to be read for the following stress. If a stress is active, but no contaminants enter through the source, then NCNH=0. *Note: Constant head cells are usually present in most MODFLOW models.*

Reproduced with permission of the copyright owner. Further reproduction prohibited without permission.

NROW, NCOL, NLAY: The row, column and layer location of the stress, respectively. These values need to correspond to the locations specified in the MODFLOW addition package files.

VALUE: The concentration value in mg/L.

Example

(For 2 MODFLOW stress periods, wells are active, 2 components)

```
0                       constant head, component 1, stress period 1
0                       constant head, component 2, stress period 1
1                       well, component 1, stress period 1
10 6  1  100.0          .....row, column, layer, concentration
0                       well, component 2, stress period 1
0                       constant head, component 1, stress period 2
0                       constant head, component 2, stress period 2
0                       well, component 1, stress period 2
1                       well, component 2, stress period 2
5  9  1  250.0          .....row, column, layer, concentration
```


Reproduced with permission of the copyright owner. Further reproduction prohibited without permission.

Appendix D

Following are the input files for each of the Case studies described in Chapter 7.

Case 1. Conservative, single species, semi-infinite column compared with analytical solution and MT3D.

- case1.bas
- case1.bcf
- case1.dis
- case1.ssm
- case1.conc
- case1.chm
- case1.out
- global.file
  - ibnd_1d
  - head_1d

case1.bas

```
Case 1.  Conservative, single species, semi-infinite column
compared with analytical solution and MT3D.
         1       1       100         1         4
 11 00 00 00 00 00 00 00 19 00 00 22 00 00 00 00 00 00 00 00 00 32
         0         0
        40         1 (20I3)
   -9999.0
        50        .1 (20f4.1)
        1.         1       1.0
```

case1.bcf

```
         1         0
 0
         0       1.0
         0       10.
         0        1.
         0       10.
         0       0.0
```

case1.dis

```
1
10. .0 .0 0.0
0 0. 0.
         0       0.0
  0
         0       10.
         0    0.2525
```

case1.ssm

```
0
```


Reproduced with permission of the copyright owner. Further reproduction prohibited without permission.

case2.conc

```
1
1 1 1 1.
```

case2.chm

(empty)

case2.out

```
0 .001 800 2000.
```

global.file

```
   BAS      30 case1.bas
   LKM     -42 case1.bih.mt3d
   BCF      80 case1.bcf
   CHM      70 namg.inp
   DIS      75 case1.dis2
   SSM      78 case1.ssm
   CON      33 case1.conc2
   OUT      90 case1.iout
            40 case1.ibnd
            50 case1.head
EOF
```

head_1d

```
70. 10. 10. 10. 10. 10. 10. 10. 10. 10. 10. 10. 10. 10. 10. 10. 10. 10. 10. 10.
10. 10. 10. 10. 10. 10. 10. 10. 10. 10. 10. 10. 10. 10. 10. 10. 10. 10. 10. 10.
10. 10. 10. 10. 10. 10. 10. 10. 10. 10. 10. 10. 10. 10. 10. 10. 10. 10. 10. 10.
10. 10. 10. 10. 10. 10. 10. 10. 10. 10. 10. 10. 10. 10. 10. 10. 10. 10. 10. 10.
10. 10. 10. 10. 10. 10. 10. 10. 10. 10. 10. 10. 10. 10. 10. 10. 10. 10. 10. 10.
```

ibnd_1d

```
 -1  1  1  1  1  1  1  1  1  1  1  1  1  1  1  1  1  1  1  1
  1  1  1  1  1  1  1  1  1  1  1  1  1  1  1  1  1  1  1  1
  1  1  1  1  1  1  1  1  1  1  1  1  1  1  1  1  1  1  1  1
  1  1  1  1  1  1  1  1  1  1  1  1  1  1  1  1  1  1  1  1
  1  1  1  1  1  1  1  1  1  1  1  1  1  1  1  1  1  1  1 -1
```

Case 2. Reactive via sorption, single species, semi-infinite column compared with analytical solution.

- case2.bas
- case2.bcf
- case2.dis
- case2.ssm-- same as Case 1
- case2.conc-- same as Case 1
- case2.chm-- same as Case 1
- case2.out-- same as Case 1
- global.file-- same as Case 1
  - head_1d
  - ibnd_1d-- same as Case 1

Reproduced with permission of the copyright owner. Further reproduction prohibited without permission.

case2.bas

Case 2. Reactive via sorption, single species, semi-infinite column

```
compared with analytical solution.
         1       1        100         1         4
 11 00 00 00 00 00 00 00 19 00 00 22 00 00 00 00 00 00 00 00 00 32
         0          0
        40          1 (20I3)
   -9999.0
        50      1000. (20f6.1)
        1.          1       1.0
```

case1.bcf

```
         1          0
 0
         0        1.0
         0         5.
         0         1.
         0         1.
         0        0.0
```

case2.dis

```
1
10. 0. 0. 0.0
0 0. 0.
         0        0.0
  1
  .808   1.
         0         1.
         0      0.808
```

head_1d

```
10.0  10.0  10.0  10.0  10.0  10.0  10.0  10.0  10.0  10.0  10.0  10.0  10.0  10.0  10.0  10.0  10.0  10.0  10.0  10.0
10.0  10.0  10.0  10.0  10.0  10.0  10.0  10.0  10.0  10.0  10.0  10.0  10.0  10.0  10.0  10.0  10.0  10.0  10.0  10.0
10.0  10.0  10.0  10.0  10.0  10.0  10.0  10.0  10.0  10.0  10.0  10.0  10.0  10.0  10.0  10.0  10.0  10.0  10.0  10.0
10.0  10.0  10.0  10.0  10.0  10.0  10.0  10.0  10.0  10.0  10.0  10.0  10.0  10.0  10.0  10.0  10.0  10.0  10.0  10.0
10.0  10.0  10.0  10.0  10.0  10.0  10.0  10.0  10.0  10.0  10.0  10.0  10.0  10.0  10.0  10.0  10.0  10.0  10.0  9.62
```


Reproduced with permission of the copyright owner. Further reproduction prohibited without permission.

Case 3. Reactive via radioactive decay, single species, semi-infinite column compared with analytical solution.

- case3.bas
- case3.bcf
- case3.dis
- case3.ssm-- same as Case 1
- case3.conc-- same as Case 1
- case3.chm-- same as Case 1
- case3.out-- same as Case 1
- global.file-- same as Case 1
  - head_1d
  - ibnd_1d-- same as Case 1

case3.bas

```
Case 3. Reactive via radioactive decay, single species, semi-infinite
column compared with analytical solution.
         1       1       100         1         4
 11 00 00 00 00 00 00 00 19 00 00 22 00 00 00 00 00 00 00 00 00 32
         0         0
        40         1 (20I3)
   -9999.0
        50     1000. (20f6.1)
        1.         1       1.0
```

case1.bcf

```
         1         0
 0
         0       1.0
         0       10.
         0        1.
         0        1.
         0       0.0
```

case3.dis

```
1
10. 0. 0. 0.0
1 0.0003465 0.
         0       0.0
  0
         0        1.
         0      .404
```

head_1d

```
10.0 10.0 10.0 10.0 10.0 10.0 10.0 10.0 10.0 10.0 10.0 10.0 10.0 10.0 10.0 10.0 10.0 10.0 10.0 10.0
10.0 10.0 10.0 10.0 10.0 10.0 10.0 10.0 10.0 10.0 10.0 10.0 10.0 10.0 10.0 10.0 10.0 10.0 10.0 10.0
10.0 10.0 10.0 10.0 10.0 10.0 10.0 10.0 10.0 10.0 10.0 10.0 10.0 10.0 10.0 10.0 10.0 10.0 10.0 10.0
10.0 10.0 10.0 10.0 10.0 10.0 10.0 10.0 10.0 10.0 10.0 10.0 10.0 10.0 10.0 10.0 10.0 10.0 10.0 10.0
10.0 10.0 10.0 10.0 10.0 10.0 10.0 10.0 10.0 10.0 10.0 10.0 10.0 10.0 10.0 10.0 10.0 10.0 10.0 9.90
```

Case 4. Reactive via cation exchange, multi-species, semi-infinite column compared with analytical solution.

Reproduced with permission of the copyright owner. Further reproduction prohibited without permission.

- case4.bas
- case4.bcf
- case4.dis
- case4.ssm-- same as Case 1
- case4.conc
- case4.chm
- case4.out
- global.file-- same as Case 1
  - head_1d
  - ibnd_1d-- same as Case 1

case4.bas

```
Case 4.  Reactive via cation exchange, multi-species,
semi-infinite column compared with analytical solution.
         1       1       100         1         4
 11 00 00 00 00 00 00 00 19 00 00 22 00 00 00 00 00 00 00 00 00 32
         0         0
        40         1 (20I3)
   -9999.0
        50       10. (20f6.1)
        1.         1       1.0
```

case4.bcf

```
         1         0
 0
         0       1.0
         0        1.
         0        1.
         0        1.
         0       0.0
```

case4.dis

```
2
3. 0. 0. 0.0
0 0. 0.
0 0. 0.
         0       0.0
         0       0.0
         0    1200.0
         0       0.0
         0        1.
         0     .3885
```

case4.conc

```
1
1 1 1 500.
1
1 1 1 500.
```

case4.chm

```
*****         EXAMPLE  1                *****
```


Reproduced with permission of the copyright owner. Further reproduction prohibited without permission.

```
      *********   DATA SET  (I)   (FREE FORMAT)     *********
2  2

      *********   DATA SET  (II)  (A15,E12.4)   ******
C1             12.       0
C2             12.       0

      *********   DATA SET  (III) (A80,/,FREE FORMAT)  *******
 C1
1  0          0
 C2
0  1          0
     **********   DATA SET  (IV)   CEC was 0.6701********
0.1
 C2
0  1    1.00  2    2   1
 C1
1  0    0    1    0   1
```

case4.out

```
0 .001 800 20.
```

head 1d

```
10.0 10.0 10.0 10.0 10.0 10.0 10.0 10.0 10.0 10.0 10.0 10.0 10.0 10.0 10.0 10.0 10.0 10.0 10.0 10.0
10.0 10.0 10.0 10.0 10.0 10.0 10.0 10.0 10.0 10.0 10.0 10.0 10.0 10.0 10.0 10.0 10.0 10.0 10.0 10.0
10.0 10.0 10.0 10.0 10.0 10.0 10.0 10.0 10.0 10.0 10.0 10.0 10.0 10.0 10.0 10.0 10.0 10.0 10.0 10.0
10.0 10.0 10.0 10.0 10.0 10.0 10.0 10.0 10.0 10.0 10.0 10.0 10.0 10.0 10.0 10.0 10.0 10.0 10.0 10.0
10.0 10.0 10.0 10.0 10.0 10.0 10.0 10.0 10.0 10.0 10.0 10.0 10.0 10.0 10.0 10.0 10.0 10.0 10.0 5.00
```

Case 5. Conservative transport compared to the analytical solution and MT3D.

- case5.bas
- case5.bcf
- case5.dis
- case5.ssm
- case5.conc
- case5.chm-- same as Case 1
- case5.out
- global.file
  - head
  - ibnd
- ADV.INP(MT3D)
- BTN.INP(MT3D)
- DSP.INP(MT3D)
- SSM.INP(MT3D)
- RUN.FIL(MT3D)

case5.bas

```
Case 5.  Conservative transport compared to the analytical solution
and MT3D.
         1       20         16         1         4
 11 12 00 00 00 00 00 00 19 00 00 22 00 00 00 00 00 00 00 00 00 32
         0          0
        40          1 (16I3)
   -9999.0
        50        1.0 (16f7.1)
```


Reproduced with permission of the copyright owner. Further reproduction prohibited without permission.

```
        1.          1        1.0
```

case5.bcf

```
         1          0
 0
         0        1.0
         0        10.
         0        10.
         0        10.
```

case5.dis

```
1
10.  5. 0. 0.0
0 0. 0.
         0        0.0
  0
         0         1.
         0         .3
```

case5.ssm

```
0
1
10 5 1 100.
```

case5.conc

```
0
```

case5.out

```
0 .001 800 4.
```

global.file

```
   BAS      30 case1.bas
   LKM     -42 case1.bih.mt3d
   BCF      80 case1.bcf
   CHM      70 namg.inp
   DIS      75 case1.dis2
   SSM      78 case1.ssm
   CON      33 case1.conc2
   OUT      90 case1.iout
            40 ibnd
            50 head
EOF
```

head

```
1000.  0.0  0.0  0.0  0.0  0.0  0.0  0.0  0.0  0.0  0.0  0.0  0.0  0.0  0.0 100.0
1000.  0.0  0.0  0.0  0.0  0.0  0.0  0.0  0.0  0.0  0.0  0.0  0.0  0.0  0.0 100.0
1000.  0.0  0.0  0.0  0.0  0.0  0.0  0.0  0.0  0.0  0.0  0.0  0.0  0.0  0.0 100.0
1000.  0.0  0.0  0.0  0.0  0.0  0.0  0.0  0.0  0.0  0.0  0.0  0.0  0.0  0.0 100.0
1000.  0.0  0.0  0.0  0.0  0.0  0.0  0.0  0.0  0.0  0.0  0.0  0.0  0.0  0.0 100.0
1000.  0.0  0.0  0.0  0.0  0.0  0.0  0.0  0.0  0.0  0.0  0.0  0.0  0.0  0.0 100.0
1000.  0.0  0.0  0.0  0.0  0.0  0.0  0.0  0.0  0.0  0.0  0.0  0.0  0.0  0.0 100.0
1000.  0.0  0.0  0.0  0.0  0.0  0.0  0.0  0.0  0.0  0.0  0.0  0.0  0.0  0.0 100.0
1000.  0.0  0.0  0.0  0.0  0.0  0.0  0.0  0.0  0.0  0.0  0.0  0.0  0.0  0.0 100.0
1000.  0.0  0.0  0.0  0.0  0.0  0.0  0.0  0.0  0.0  0.0  0.0  0.0  0.0  0.0 100.0
1000.  0.0  0.0  0.0  0.0  0.0  0.0  0.0  0.0  0.0  0.0  0.0  0.0  0.0  0.0 100.0
```


Reproduced with permission of the copyright owner. Further reproduction prohibited without permission.

```
1000.  0.0  0.0  0.0  0.0  0.0  0.0  0.0  0.0  0.0  0.0  0.0  0.0  0.0  0.0 100.0
1000.  0.0  0.0  0.0  0.0  0.0  0.0  0.0  0.0  0.0  0.0  0.0  0.0  0.0  0.0 100.0
1000.  0.0  0.0  0.0  0.0  0.0  0.0  0.0  0.0  0.0  0.0  0.0  0.0  0.0  0.0 100.0
1000.  0.0  0.0  0.0  0.0  0.0  0.0  0.0  0.0  0.0  0.0  0.0  0.0  0.0  0.0 100.0
1000.  0.0  0.0  0.0  0.0  0.0  0.0  0.0  0.0  0.0  0.0  0.0  0.0  0.0  0.0 100.0
1000.  0.0  0.0  0.0  0.0  0.0  0.0  0.0  0.0  0.0  0.0  0.0  0.0  0.0  0.0 100.0
1000.  0.0  0.0  0.0  0.0  0.0  0.0  0.0  0.0  0.0  0.0  0.0  0.0  0.0  0.0 100.0
1000.  0.0  0.0  0.0  0.0  0.0  0.0  0.0  0.0  0.0  0.0  0.0  0.0  0.0  0.0 100.0
1000.  0.0  0.0  0.0  0.0  0.0  0.0  0.0  0.0  0.0  0.0  0.0  0.0  0.0  0.0 100.0
```

ibnd

```
 -1  1  1  1  1  1  1  1  1  1  1  1  1  1  1 -1
 -1  1  1  1  1  1  1  1  1  1  1  1  1  1  1 -1
 -1  1  1  1  1  1  1  1  1  1  1  1  1  1  1 -1
 -1  1  1  1  1  1  1  1  1  1  1  1  1  1  1 -1
 -1  1  1  1  1  1  1  1  1  1  1  1  1  1  1 -1
 -1  1  1  1  1  1  1  1  1  1  1  1  1  1  1 -1
 -1  1  1  1  1  1  1  1  1  1  1  1  1  1  1 -1
 -1  1  1  1  1  1  1  1  1  1  1  1  1  1  1 -1
 -1  1  1  1  1  1  1  1  1  1  1  1  1  1  1 -1
 -1  1  1  1  1  1  1  1  1  1  1  1  1  1  1 -1
 -1  1  1  1  1  1  1  1  1  1  1  1  1  1  1 -1
 -1  1  1  1  1  1  1  1  1  1  1  1  1  1  1 -1
 -1  1  1  1  1  1  1  1  1  1  1  1  1  1  1 -1
 -1  1  1  1  1  1  1  1  1  1  1  1  1  1  1 -1
 -1  1  1  1  1  1  1  1  1  1  1  1  1  1  1 -1
 -1  1  1  1  1  1  1  1  1  1  1  1  1  1  1 -1
 -1  1  1  1  1  1  1  1  1  1  1  1  1  1  1 -1
 -1  1  1  1  1  1  1  1  1  1  1  1  1  1  1 -1
 -1  1  1  1  1  1  1  1  1  1  1  1  1  1  1 -1
 -1  1  1  1  1  1  1  1  1  1  1  1  1  1  1 -1
```

ADV.INP(MT3D)

```
       3      0.5     8000                                              MIXELM,PERCEL,MXPART
       1       .5                                                       ITRACK,WD
  1.E-5         1        0        9        0       16      1.0          DCEPS,NPLANE,NPL,NPH,NPMIN,NPMAX,SSMULT
       1        1        9                                              INTERP,NLSINK,NPSINK
    .001                                                                DCHMOC
```

BTN.INP(MT3D)

```
CASE 5. 2D TEST PROBLEM
UNIFORM FLOW FIELD WITH CONTINUOUS SOURCE
         1         20         16          1                 !NLAY,NROW,NCOL,NPER
 DAY FT    MG                                               !TUNIT,LUNIT,MUNIT
T T T F                                                     !TRNOP
 0                                                          !LAYCON
         0       10.                                        !DELR
         0       10.                                        !DELC
         0       10.                                        !HTOP
         0       10.                                        !DZ
         0       .30                                        !PRSITY
         0         1                                        !ICBUND-LAY1
         0        0.                                        !SCONC-LAY1
   -999.00                                                  !CINACT
         4         2          5          4          T       !IFMTCN,IFMTNP,IFMTRF,IFMTDP,SAVUCN
         0                                                  !NPRS
         0                                                  !NOBS
         T
      4.00         1         1.                             !PERLEN,NSTP,TSMULT
     0.025      1000                                        !DT0 MXSTRN
```

DSP.INP(MT3D)

```
      0        10.        AL
      0         .5        TRPT
      0         .0        TRPV
      0          0        DMCOEF
```


Reproduced with permission of the copyright owner. Further reproduction prohibited without permission.

SSM.INP(MT3D)

```
T F F F F F
       100
         1
         1        10         5       100.         2
```

RUN.FIL(MT3D)

```
case5.out
BTN.INP
ADV.INP
DSP.INP
SSM.INP
case5.bih.mt3d
N
```

Case 6. Conservative transport in a heterogeneous aquifer example case.

- case6.bas
- case6.bcf
- case6.dis
- case6.ssm
- case6.conc-- same as Case 5
- case6.chm-- same as Case 1
- case6.out
- global.file
  - head
  - ibnd
  - case6.K

case6.bas

```
Case 6.  Conservative transport in a heterogeneous aquifer
example case.
         1      20         16          1          4
 11 12 00 00 00 00 00 00 19 00 00 22 00 00 00 00 00 00 00 00 00 32
         0          0
        40          1 (16I3)
   -9999.0
        50        1.0 (16f7.1)
      365.          1       1.0
```

case6.bcf

```
         1          0
 0
         0        1.0
         0        10.
         0        10.
        60      10.0(16f6.1)
```


Reproduced with permission of the copyright owner. Further reproduction prohibited without permission.

case6.dis

```
1
10.  5. 0. 0.0
0 0. 0.
          0        0.0
  0
         60         1.(16f6.1)
          0         .3
```

case6.ssm

```
0
1
5 8 1 100.
```

case6.out

```
0 .001 800 70.
```

global.file

```
   BAS      30 test.bas
   LKM     -42 test.bih.mt3d
   BCF      80 test.bcf
   CHM      70 namg.inp
   DIS      75 test.dis
   SSM      78 test.ssm
   CON      33 test.conc
   OUT      90 chit.iout
            40 ibnd
            50 head
            60 test_K
EOF
```

head

```
250.0 250.0 250.0 250.0 250.0 250.0 250.0 250.0 250.0 250.0 250.0 250.0 250.0 250.0 250.0 250.0
250.0 250.0 250.0 250.0 250.0 250.0 250.0 250.0 250.0 250.0 250.0 250.0 250.0 250.0 250.0 250.0
250.0 250.0 250.0 250.0 250.0 250.0 250.0 250.0 250.0 250.0 250.0 250.0 250.0 250.0 250.0 250.0
250.0 250.0 250.0 250.0 250.0 250.0 250.0 250.0 250.0 250.0 250.0 250.0 250.0 250.0 250.0 250.0
250.0 250.0 250.0 250.0 250.0 250.0 250.0 250.0 250.0 250.0 250.0 250.0 250.0 250.0 250.0 250.0
250.0 250.0 250.0 250.0 250.0 250.0 250.0 250.0 250.0 250.0 250.0 250.0 250.0 250.0 250.0 250.0
250.0 250.0 250.0 250.0 250.0 250.0 250.0 250.0 250.0 250.0 250.0 250.0 250.0 250.0 250.0 250.0
250.0 250.0 250.0 250.0 250.0 250.0 250.0 250.0 250.0 250.0 250.0 250.0 250.0 250.0 250.0 250.0
250.0 250.0 250.0 250.0 250.0 250.0 250.0 250.0 250.0 250.0 250.0 250.0 250.0 250.0 250.0 250.0
250.0 250.0 250.0 250.0 250.0 250.0 250.0 250.0 250.0 250.0 250.0 250.0 250.0 250.0 250.0 250.0
250.0 250.0 250.0 250.0 250.0 250.0 250.0 250.0 250.0 250.0 250.0 250.0 250.0 250.0 250.0 250.0
250.0 250.0 250.0 250.0 250.0 250.0 250.0 250.0 250.0 250.0 250.0 250.0 250.0 250.0 250.0 250.0
250.0 250.0 250.0 250.0 250.0 250.0 250.0 250.0 250.0 250.0 250.0 250.0 250.0 250.0 250.0 250.0
250.0 250.0 250.0 250.0 250.0 250.0 250.0 250.0 250.0 250.0 250.0 250.0 250.0 250.0 250.0 250.0
250.0 250.0 250.0 250.0 250.0 250.0 250.0 250.0 250.0 250.0 250.0 250.0 250.0 250.0 250.0 250.0
250.0 250.0 250.0 250.0 250.0 250.0 250.0 250.0 250.0 250.0 250.0 250.0 250.0 250.0 250.0 250.0
250.0 250.0 250.0 250.0 250.0 250.0 250.0 250.0 250.0 250.0 250.0 250.0 250.0 250.0 250.0 250.0
250.0 250.0 250.0 250.0 250.0 250.0 250.0 250.0 250.0 250.0 250.0 250.0 250.0 250.0 250.0 250.0
17.50 20.00 22.50 25.00 27.50 30.00 32.50 35.00 37.50 40.00 42.50 45.00 47.50 50.00 52.50 55.00
250.0 250.0 250.0 250.0 250.0 250.0 250.0 250.0 250.0 250.0 250.0 250.0 250.0 250.0 250.0 250.0
```

.

ibnd

```
 0  0  0  0  0  0  0  0  0  0  0  0  0  0  0  0
 0 -1 -1 -1 -1 -1 -1 -1 -1 -1 -1 -1 -1 -1 -1  0
 0  1  1  1  1  1  1  1  1  1  1  1  1  1  1  0
 0  1  1  1  1  1  1  1  1  1  1  1  1  1  1  0
 0  1  1  1  1  1  1  1  1  1  1  1  1  1  1  0
 0  1  1  1  1  1  1  1  1  1  1  1  1  1  1  0
 0  1  1  1  1  1  1  1  1  1  1  1  1  1  1  0
 0  1  1  1  1  1  1  1  1  1  1  1  1  1  1  0
 0  1  1  1  1  1  1  1  1  1  1  1  1  1  1  0
 0  1  1  1  1  1  1  1  1  1  1  1  1  1  1  0
```


Reproduced with permission of the copyright owner. Further reproduction prohibited without permission.

```
0  1  1  1  1  1  1  1  1  1  1  1  1  1  1  0
0  1  1  1  1  1  1  1  1  1  1  1  1  1  1  0
0  1  1  1  1  1  1  1  1  1  1  1  1  1  1  0
0  1  1  1  1  1  1  1  1  1  1  1  1  1  1  0
0  1  1  1  1  1  1  1  1  1  1  1  1  1  1  0
0  1  1  1  1  1  1  1  1  1  1  1  1  1  1  0
0  1  1  1  1  1  1  1  1  1  1  1  1  1  1  0
0  1  1  1  1  1  1  1  1  1  1  1  1  1  1  0
0 -1 -1 -1 -1 -1 -1 -1 -1 -1 -1 -1 -1 -1 -1  0
0  0  0  0  0  0  0  0  0  0  0  0  0  0  0  0
```

case6.K

```
1.0   1.0   1.0   1.0   1.0   1.0   1.0   1.0   1.0   1.0   1.0   1.0   1.0   1.0   1.0   1.0
1.0   1.0   1.0   1.0   1.0   1.0   1.0   1.0   1.0   1.0   1.0   1.0   1.0   1.0   1.0   1.0
1.0   1.0   1.0   1.0   1.0   1.0   1.0   1.0   1.0   1.0   1.0   1.0   1.0   1.0   1.0   1.0
1.0   1.0   1.0   1.0   1.0   1.0   1.0   1.0   1.0   1.0   1.0   1.0   1.0   1.0   1.0   1.0
1.0   1.0   1.0   1.0   1.0   1.0   1.0   1.0   1.0   1.0   1.0   1.0   1.0   1.0   1.0   1.0
1.0   1.0   1.0   1.0   1.0   1.0   1.0   1.0   1.0   1.0   1.0   1.0   1.0   1.0   1.0   1.0
1.0   1.0   .001  .001  .001  .001  .001  .001  .001  1.0   1.0   1.0   1.0   1.0   1.0   1.0
1.0   1.0   .001  .001  .001  .001  .001  .001  .001  1.0   1.0   1.0   1.0   1.0   1.0   1.0
1.0   1.0   .001  .001  .001  .001  .001  .001  .001  1.0   1.0   1.0   1.0   1.0   1.0   1.0
1.0   1.0   1.0   1.0   1.0   1.0   1.0   1.0   1.0   1.0   1.0   1.0   1.0   1.0   1.0   1.0
1.0   1.0   1.0   1.0   1.0   1.0   1.0   1.0   1.0   1.0   1.0   1.0   1.0   1.0   1.0   1.0
1.0   1.0   1.0   1.0   1.0   1.0   1.0   1.0   1.0   1.0   1.0   1.0   1.0   1.0   1.0   1.0
1.0   1.0   1.0   1.0   1.0   1.0   1.0   1.0   1.0   1.0   1.0   1.0   1.0   1.0   1.0   1.0
1.0   1.0   1.0   1.0   1.0   1.0   1.0   1.0   1.0   1.0   1.0   1.0   1.0   1.0   1.0   1.0
1.0   1.0   1.0   1.0   1.0   1.0   1.0   1.0   1.0   1.0   1.0   1.0   1.0   1.0   1.0   1.0
1.0   1.0   1.0   1.0   1.0   1.0   1.0   1.0   1.0   1.0   1.0   1.0   1.0   1.0   1.0   1.0
1.0   1.0   1.0   1.0   1.0   1.0   1.0   1.0   1.0   1.0   1.0   1.0   1.0   1.0   1.0   1.0
1.0   1.0   1.0   1.0   1.0   1.0   1.0   1.0   1.0   1.0   1.0   1.0   1.0   1.0   1.0   1.0
1.0   1.0   1.0   1.0   1.0   1.0   1.0   1.0   1.0   1.0   1.0   1.0   1.0   1.0   1.0   1.0
1.0   1.0   1.0   1.0   1.0   1.0   1.0   1.0   1.0   1.0   1.0   1.0   1.0   1.0   1.0   1.0
```

Case 7. Conservative transport compared to the analytical solution and MT3D.

- case7.bas
- case7.bcf
- case7.dis
- case7.ssm
- case7.conc-- same as Case 5
- case7.chm-- same as Case 1
- case7.out
- global.file
  - head_3d1...head_3d9
  - ibnd_3d1...ibnd_3d9
- ADV.INP(MT3D)
- BTN.INP(MT3D)
- DSP.INP(MT3D)
- SSM.INP(MT3D)
- RUN.FIL(MT3D)

case7.bas

```
Case 7.  Conservative transport compared to the analytical solution
and MT3D.
         9         31         50          1         4
 11 12 00 00 00 00 00 00 19 00 00 22 00 00 00 00 00 00 00 00 00 32
```


Reproduced with permission of the copyright owner. Further reproduction prohibited without permission.

```
         0          0
        40          1 (10I4)
        41          1 (10I4)
        42          1 (10I4)
        43          1 (10I4)
        44          1 (10I4)
        45          1 (10I4)
        46          1 (10I4)
        47          1 (10I4)
        48          1 (10I4)
  -9999.0
        50        1.0 (10f7.1)
        51        1.0 (10f7.1)
        52        1.0 (10f7.1)
        53        1.0 (10f7.1)
        54        1.0 (10f7.1)
        55        1.0 (10f7.1)
        56        1.0 (10f7.1)
        57        1.0 (10f7.1)
        58        1.0 (10f7.1)
        1.          1        1.0
```

case7.bcf

```
         1          0
 0 0 0 0 0 0 0 0 0 0
         0        1.0
         0        10.
         0        10.
         0        50.
         0         .2
         0        50.
         0         .2
         0        50.
         0         .2
         0        50.
         0         .2
         0        50.
         0         .2
         0        50.
         0         .2
         0        50.
         0         .2
         0        50.
         0         .2
         0        50.
```

case7.dis

```
1
10. 5. 1. 0.0
10. 5. 1. 0.0
10. 5. 1. 0.0
10. 5. 1. 0.0
10. 5. 1. 0.0
10. 5. 1. 0.0
10. 5. 1. 0.0
10. 5. 1. 0.0
```


Reproduced with permission of the copyright owner. Further reproduction prohibited without permission.

```
10. 5. 1. 0.0
0 0. 0.
         0        0.0
  0
         0        10.
         0        10.
         0        10.
         0        10.
         0        10.
         0        10.
         0        10.
         0        10.
         0        10.
         0        10.
         0         .3
         0         .3
         0         .3
         0         .3
         0         .3
         0         .3
         0         .3
         0         .3
         0         .3
```

case7.ssm

```
0
1
15 10 5 1000.
```

case7.out

```
0 .001 800 20.
```

global.file

```
   BAS      30 test.bas
   LKM     -31 test.bih.mt3d
   BCF      80 test.bcf
   CHM      70 namg.inp
   DIS      75 test.dis
   SSM      78 test.ssm
   CON      33 test.conc
   OUT      90 chit.iout
             40 ibnd_3d1
             41 ibnd_3d2
             42 ibnd_3d3
             43 ibnd_3d4
             44 ibnd_3d5
             45 ibnd_3d6
             46 ibnd_3d7
             47 ibnd_3d8
             48 ibnd_3d9
             50 head_3d1
             51 head_3d2
             52 head_3d3
             53 head_3d4
             54 head_3d5
             55 head_3d6
```


Reproduced with permission of the copyright owner. Further reproduction prohibited without permission.

```
            56 head_3d7
            57 head_3d8
            58 head_3d9
EOF
```

head_3d1(same through head_3d9)

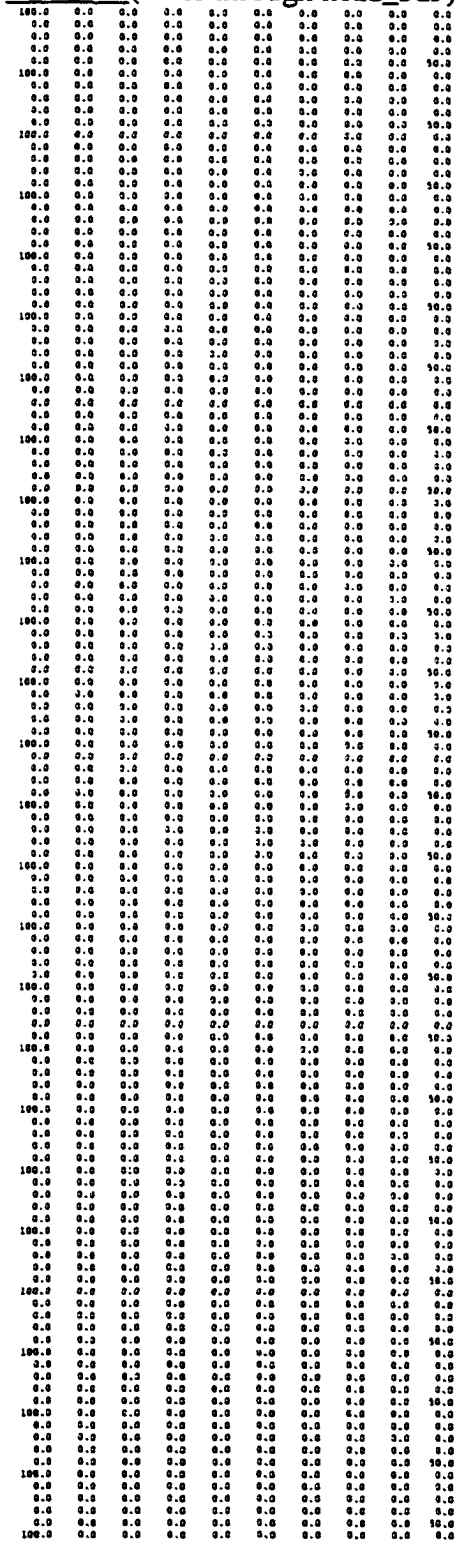

Reproduced with permission of the copyright owner. Further reproduction prohibited without permission.

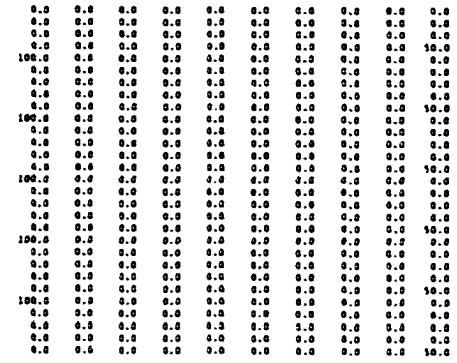

ibnd_3d11(same through ibnd_3d9)

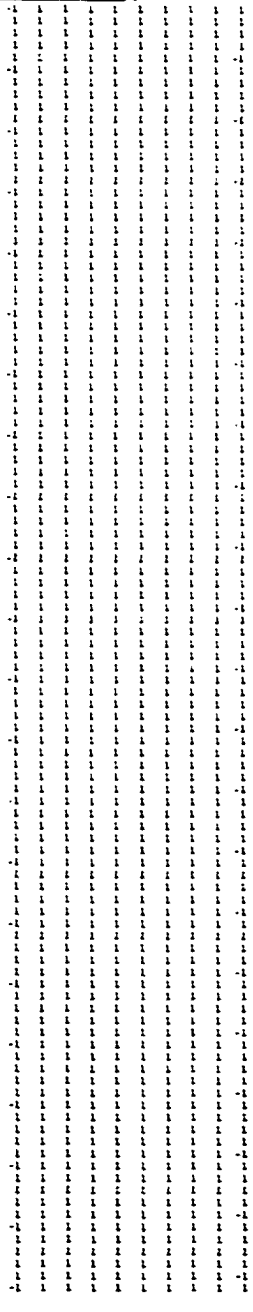

Reproduced with permission of the copyright owner. Further reproduction prohibited without permission.

```
 1  1  1  1  1  1  1  1  1  1
 1  1  1  1  1  1  1  1  1  1
 1  1  1  1  1  1  1  1  1  1
 1  1  1  1  1  1  1  1  1 -1
-1  1  1  1  1  1  1  1  1  1
 1  1  1  1  1  1  1  1  1  1
 1  1  1  1  1  1  1  1  1  1
 1  1  1  1  1  1  1  1  1  1
 1  1  1  1  1  1  1  1  1 -1
-1  1  1  1  1  1  1  1  1  1
 1  1  1  1  1  1  1  1  1  1
 1  1  1  1  1  1  1  1  1  1
 1  1  1  1  1  1  1  1  1  1
 1  1  1  1  1  1  1  1  1 -1
-1  1  1  1  1  1  1  1  1  1
 1  1  1  1  1  1  1  1  1  1
 1  1  1  1  1  1  1  1  1  1
 1  1  1  1  1  1  1  1  1  1
 1  1  1  1  1  1  1  1  1 -1
-1  1  1  1  1  1  1  1  1  1
 1  1  1  1  1  1  1  1  1  1
 1  1  1  1  1  1  1  1  1  1
 1  1  1  1  1  1  1  1  1  1
 1  1  1  1  1  1  1  1  1 -1
-1  1  1  1  1  1  1  1  1  1
 1  1  1  1  1  1  1  1  1  1
 1  1  1  1  1  1  1  1  1  1
 1  1  1  1  1  1  1  1  1  1
 1  1  1  1  1  1  1  1  1 -1
-1  1  1  1  1  1  1  1  1  1
 1  1  1  1  1  1  1  1  1  1
 1  1  1  1  1  1  1  1  1  1
 1  1  1  1  1  1  1  1  1  1
 1  1  1  1  1  1  1  1  1 -1
-1  1  1  1  1  1  1  1  1  1
 1  1  1  1  1  1  1  1  1  1
 1  1  1  1  1  1  1  1  1  1
 1  1  1  1  1  1  1  1  1  1
 1  1  1  1  1  1  1  1  1 -1
-1  1  1  1  1  1  1  1  1  1
 1  1  1  1  1  1  1  1  1  1
 1  1  1  1  1  1  1  1  1  1
 1  1  1  1  1  1  1  1  1  1
 1  1  1  1  1  1  1  1  1 -1
-1  1  1  1  1  1  1  1  1  1
 1  1  1  1  1  1  1  1  1  1
 1  1  1  1  1  1  1  1  1  1
 1  1  1  1  1  1  1  1  1  1
 1  1  1  1  1  1  1  1  1 -1
```

ADV.INP(MT3D)

```
        3       .50     20000                                          MIXELM,PERCEL,MXPART
        3       .5                                                     ITRACK,WD
   1.E-5        0         0        9        0       16       1.0      DCEPS,NPLANE,NPL,NPH,NPMIN,NPMAX,SSMULT
        1       1         9                                            INTERP,NLSINK,NPSINK
     .001                                                              DCHMOC
```

BTN.INP(MT3D)

```
CASE 7. 3D TEST PROBLEM
UNIFORM FLOW FIELD WITH CONTINUOUS SOURCE
         9         31         50          1                  !NLAY,NROW,NCOL,NPER
 DAY FT MG/L                                                 !TUNIT,LUNIT,MUNIT
T T T F                                                      !TRNOP
 0 0 0 0 0 0 0                                               !LAYCON
         0        10.                                        !DELR
         0        10.                                        !DELC
         0         5.                                        !HTOP
         0         5.                                        !DZ1
         0         5.                                        !DZ2
         0         5.                                        !DZ3
         0         5.                                        !DZ4
         0         5.                                        !DZ5
         0         5.                                        !DZ6
         0         5.                                        !DZ7
         0         5.                                        !DZ8
         0         5.                                        !DZ9
         0        .30                                        !PRSITY1
         0        .30                                        !PRSITY2
         0        .30                                        !PRSITY3
         0        .30                                        !PRSITY4
         0        .30                                        !PRSITY5
         0        .30                                        !PRSITY6
         0        .30                                        !PRSITY7
         0        .30                                        !PRSITY8
         0        .30                                        !PRSITY9
         0          1                                        !ICBUND-LAY1
         0          1                                        !ICBUND-LAY2
         0          1                                        !ICBUND-LAY3
         0          1                                        !ICBUND-LAY4
         0          1                                        !ICBUND-LAY5
         0          1                                        !ICBUND-LAY6
         0          1                                        !ICBUND-LAY7
         0          1                                        !ICBUND-LAY8
         0          1                                        !ICBUND-LAY9
         0         0.                                        !SCONC-LAY1
         0         0.                                        !SCONC-LAY2
         0         0.                                        !SCONC-LAY3
         0         0.                                        !SCONC-LAY4
         0         0.                                        !SCONC-LAY5
         0         0.                                        !SCONC-LAY6
```


Reproduced with permission of the copyright owner. Further reproduction prohibited without permission.

```
      0        0.                                  !SCONC-LAY7
      0        0.                                  !SCONC-LAY8
      0        0.                                  !SCONC-LAY9
-999.00                                            !CINACT
      4         2         5         4         T    !IFMTCN,IFMTNP,IFMTRF,IFMTDP,SAVUCN
      0                                            !NPRS
      0                                            !NOBS
      T                                            !CHKMAS
  20.00         1        1.                        !PERLEN,NSTP,TSMULT
  0.146      1000                                  !DT0 MXSTRN
```

DSP.INP(MT3D)

```
          0        10.        AL1
          0        10.        AL2
          0        10.        AL3
          0        10.        AL4
          0        10.        AL5
          0        10.        AL6
          0        10.        AL7
          0        10.        AL8
          0        10.        AL9
          0         .5        TRPT1
          0         .1        TRPV1
          0          0        DMCOEF1
```

SSM.INP(MT3D)

```
T F F F F F
      5000
         1
         5         15         10      1000.          2
```

RUN.FIL(MT3D)

```
case7.out
BTN.INP
ADV.INP
DSP.INP
SSM.INP
case7.bih.mt3d
N
```

Case 8. Transient, two-dimensional, multi-species, reactive transport sitr remediation including MT3D.

- case8.bas
- case8.bcf
- case8.dis
- case8.ssm (for inherent and high conc.)
- case8.conc-- same as Case 5
- case8.chm
- case8.out
- global.file
  - head
  - ibnd-- same as Case 5
- ADV.INP(MT3D)

Reproduced with permission of the copyright owner. Further reproduction prohibited without permission.

- BTN.INP(MT3D)
- DSP.INP(MT3D)
- SSM.INP(MT3D)
- RCT.INP(MT3D)
- RUN.FIL(MT3D)

case8.bas

```
Case 8.  Transient, two-dimensional, multi-species, reactive transport
site remediation including MT3D
         1      20         16          2          4
 11 12 00 00 00 00 00 00 19 00 00 22 00 00 00 00 00 00 00 00 00 32
          0          0
         40          1 (16I3)
   -9999.0
         50        1.0 (8f15.6)
         3.          1        1.0
       500.          1        1.0
```

case8.bcf

```
          0          0
 0
          0        1.0
          0        10.
          0        10.
          0       .001
          0        10.
```

case7.dis

```
2
10. 5. 0. 0.0
0 0. 0.
0 0. 0.
          0       50.0
          0        0.0
          0      500.0
          0        0.0
          0         1.
          0         .3
```

case7ssm (inherent.-- simulation 1)

```
20                              conc1:1
1 1 1 50.
2 1 1 50.
3 1 1 50.
4 1 1 50.
5 1 1 50.
6 1 1 50.
7 1 1 50.
8 1 1 50.
9 1 1 50.
10 1 1 50.
11 1 1 50.
12 1 1 50.
13 1 1 50.
14 1 1 50.
```


Reproduced with permission of the copyright owner. Further reproduction prohibited without permission.

```
15 1 1 50.
16 1 1 50.
17 1 1 50.
18 1 1 50.
19 1 1 50.
20 1 1 50.
0                                   ssm1:1
0                                   conc2:1
1                                   ssm2:2
10 4 1 10000.
20                                  conc1:2
1 1 1 50.
2 1 1 50.
3 1 1 50.
4 1 1 50.
5 1 1 50.
6 1 1 50.
7 1 1 50.
8 1 1 50.
9 1 1 50.
10 1 1 50.
11 1 1 50.
12 1 1 50.
13 1 1 50.
14 1 1 50.
15 1 1 50.
16 1 1 50.
17 1 1 50.
18 1 1 50.
19 1 1 50.
20 1 1 50.
1                                   ssm1:2
10 4 1 50.
0                                   conc2:2
0                                   ssm2:2
```

case7ssm (high conc.-- simulation 2)

```
20                                  conc1:1
1 1 1 50.
2 1 1 50.
3 1 1 50.
4 1 1 50.
5 1 1 50.
6 1 1 50.
7 1 1 50.
8 1 1 50.
9 1 1 50.
10 1 1 50.
11 1 1 50.
12 1 1 50.
13 1 1 50.
14 1 1 50.
15 1 1 50.
16 1 1 50.
17 1 1 50.
18 1 1 50.
19 1 1 50.
20 1 1 50.
0                                   ssm1:1
0                                   conc2:1
1                                   ssm2:2
10 4 1 10000.
20                                  conc1:2
1 1 1 50.
2 1 1 50.
3 1 1 50.
4 1 1 50.
5 1 1 50.
6 1 1 50.
7 1 1 50.
```


Reproduced with permission of the copyright owner. Further reproduction prohibited without permission.

```
8 1 1 50.
9 1 1 50.
10 1 1 50.
11 1 1 50.
12 1 1 50.
13 1 1 50.
14 1 1 50.
15 1 1 50.
16 1 1 50.
17 1 1 50.
18 1 1 50.
19 1 1 50.
20 1 1 50.
1                                   ssm1:2
10 4 1 10000.
0                                   conc2:2
0                                   ssm2:2
```

case7.chm

```
*****          EXAMPLE  1                  *****

       *********   DATA SET  (I)   (FREE FORMAT)     *********
2  2
       *********   DATA SET  (II)  (A15,E12.4)    ******
C1              22.98968       0
C2               24.3050       0

       *********   DATA SET  (III) (A80,/,FREE FORMAT)  *******
C1
1  0            0
C2
0  1            0

      **********   DATA SET  (IV)   CEC was 0.6701********
0.0217391304
 C2
0  1    2.0  2    2   1
 C1
1  0    0    1    0   1
```

case7.out

global.file

```
    BAS      30 test.bas
    LKM     -42 test.bih.mt3d
    BCF      80 test.bcf
    CHM      70 namg.inp
    DIS      75 test.dis
    SSM      78 test.ssm
    CON      33 test.conc
    OUT      90 chit.iout
             40 ibnd
             50 head.init
EOF
```

head

```
1000.000000   966.716492   933.424072   900.115479   866.786560   833.427012   800.070007   766.691345
 733.308716   699.930054   666.563049   633.211501   599.884583   566.575989   533.283508   500.000000
1000.000000   966.725464   933.440247   900.135803   866.807251   833.454529   800.081543   766.695435
 733.304688   699.918518   666.545593   633.192810   599.864258   566.559814   533.274597   500.000000
1000.000000   966.745117   933.475708   900.180115   866.852112   833.492188   800.106384   766.704041
 733.296021   699.893677   666.507874   633.147949   599.819946   566.524353   533.254944   500.000000
1000.000000   966.779236   933.537292   900.256897   866.928894   833.555786   800.147705   766.718323
 733.281799   699.852356   666.444336   633.071167   599.743164   566.462769   533.220825   500.000000
1000.000000   966.834473   933.637451   900.381226   867.050842   833.654236   800.210388   766.739685
 733.260376   699.789673   666.345825   632.949219   599.618835   566.362610   533.165588   500.000000
1000.000000   966.921265   933.796753   900.579651   867.239075   833.799866   800.299988   766.769714
 733.230408   699.700073   666.200195   632.760986   599.420610   566.203308   533.078796   500.000000
1000.000000   967.053711   934.048767   900.901611   867.525940   834.006226   800.420044   766.808716
```


Reproduced with permission of the copyright owner. Further reproduction prohibited without permission.

```
 733.191345    699.580078    665.993835    632.474182    599.098511    565.951294    532.946350    500.000000
1000.000000    967.264812    934.442932    901.452026    867.956787    834.279114    800.565125    766.853821
 733.146301    699.434998    665.721008    632.043274    598.548096    565.557129    532.755249    500.000000
1000.000000    967.482544    935.026184    902.506714    868.570129    834.588318    800.707520    766.895142
 733.104980    699.292603    665.411804    631.429993    597.493408    564.973938    532.517456    500.000000
1000.000000    967.659363    935.672424    904.978516    869.228699    834.796570    800.781372    766.914368
 733.085754    699.218689    665.203552    630.771423    595.021606    564.327637    532.340698    500.003000
1000.000000    967.482361    935.025757    902.506165    868.569580    834.587830    800.707153    766.895020
 733.105103    699.292969    665.412292    631.430542    597.493958    564.974304    532.517700    500.000000
1000.000000    967.264324    934.442017    901.450867    867.955566    834.278076    800.564392    766.853577
 733.146545    699.435730    665.722046    632.044556    598.549255    565.558044    532.755737    500.000000
1000.000000    967.052856    934.047180    900.899597    867.523865    834.004456    800.418823    766.808350
 733.191833    699.581299    665.995667    632.476257    599.100525    565.952881    532.947205    500.000000
1000.000000    966.919922    933.794312    900.576538    867.235840    833.797058    800.298096    766.769043
 733.231079    699.702087    666.202125    632.764343    599.423584    566.205750    533.080139    500.000000
1000.000000    966.832397    933.633667    900.376404    867.045837    833.649841    800.207458    766.738708
 733.261475    699.792725    666.350281    632.954346    599.623718    566.366455    533.167664    500.000000
1000.000000    966.776062    933.531494    900.249512    866.921204    833.549072    800.143188    766.716736
 733.283447    699.856995    666.451111    633.078979    599.750610    566.468567    533.223999    500.000000
1000.000000    966.740234    933.466858    900.168884    866.840454    833.482056    800.099548    766.701660
 733.298523    699.900635    666.518127    633.159729    599.831238    566.533203    533.259766    500.000000
1000.000000    966.718140    933.426880    900.118774    866.789551    833.439209    800.071228    766.691833
 733.308411    699.928955    666.561035    633.210632    599.881409    566.573181    533.281921    500.000000
1000.000000    966.705383    933.403809    900.089661    866.759827    833.413940    800.054443    766.685913
 733.314270    699.945801    666.586304    633.240356    599.910461    566.596313    533.294678    500.000000
1000.000000    966.699524    933.393188    900.076355    866.746094    833.402222    800.046631    766.683228
 733.317017    699.953613    666.597961    633.254089    599.923828    566.606873    533.300537    500.000000
```

ADV.INP(MT3D)

```
       2       0.5     10000                                    MIXELM,PERCEL,MXPART
       1        .5                                              ITRACK,WD
       1         1        16                                    INTERP,NLSINK,NPSINK
    .001                                                        DCHMOC
   1.E-5         1         0        16         0        16       1.0  DCEPS,NPLANE,NPL,NPH,NPMIN,NPMAX,SSMULT
```

BTN.INP(MT3D)

```
2D TEST PROBLEM
UNIFORM FLOW FIELD WITH CONTINUOUS SOURCE
         1        20        16         2                    !NLAY,NROW,NCOL,NPER
 DAY FT MG                                                   !TUNIT,LUNIT,MUNIT
T T T T                                                      !TRNOP
 0                                                           !LAYCON
         0       10.                                         !DELR
         0       10.                                         !DELC
         0       10.                                         !HTOP
         0       10.                                         !DZ
         0       .30                                         !PRSITY
         0         1                                         !ICBUND-LAY1
         0        0.                                         !SCONC-LAY1
   -999.00                                                   !CINACT
         4         0         0         0         F           !IFMTCN,IFMTNP,IFMTRF,IFMTDP,SAVUCN
         1                                                   !NPRS
        3.                                                         !TIMPRS
         1                                                   !NOBS
         1        10        13                                    !KOBS,IOBS,JOBS
         T                                                !CHKMAS
        3.         1        1.                                  !PERLEN,NSTP,TSMULT: stress period 1
     0.500     10000                                         !DT0 MXSTRN: stress period 1
      500.         1        1.                                  !PERLEN,NSTP,TSMULT: stress period 2
     0.500    100000                                         !DT0 MXSTRN: stress period 2
```

DSP.INP(MT3D)

```
         0       10.       AL
         0        .5       TRPT
         0        .0       TRPV
         0         0       DMCOEF
```

SSM.INP(MT3D)

```
T F F F F F
       200
         1
         1        10          4 283165.79          2
         0
```

RCT.INP(MT3D)

```
         1         0                 ISOTHM,IREACT
         0      2.65                 RHOB
```


Reproduced with permission of the copyright owner. Further reproduction prohibited without permission.

```
         0       50.0                SP1
         0        0.0                SP2
```

RUN.FIL(MT3D)

```
case8.out
BTN.INP
ADV.INP
DSP.INP
SSM.INP
RCT.INP
case8.bih.mt3d
N
```


Reproduced with permission of the copyright owner. Further reproduction prohibited without permission.